The Thesis committee for Brynjólfur Víðir Ólafsson
certifies that this is the approved version of the following thesis:

The Technical Potential of Renewable Natural Gas (RNG) in the United States, and the Economic Potential of Methanation-derived RNG in Texas

APPROVED BY

SUPERVISING COMMITTEE:

Michael E. Webber, Supervisor

Vaibhav Bahadur

The Technical Potential of Renewable Natural Gas (RNG) in the United States, and the Economic Potential of Methanation-derived RNG in Texas

by

Brynjólfur Víðir Ólafsson, B.Sc.

THESIS

Presented to the Faculty of the Graduate School of

The University of Texas at Austin

in Partial Fulfillment

of the Requirements

for the Degree of

MASTER OF SCIENCE IN ENGINEERING

The University of Texas at Austin

December 2014

Dedicated to my wife Kristine, whose support and encouragement has been unwaivering on my journey through graduate school, and to my children, Markús and Emilía, whose smiles, hugs, and laughter reminded me to keep going when things got tough.

Acknowledgments

I would like to thank my advisor, Dr. Michael E. Webber, for giving me the opportunity to work under his tutelage. Dr. Webber's guidance, patience, and support have helped grow intellectually, personally, and professionally during my time as a graduate student, and I will carry with me his vision of 'changing the way the world thinks about energy' as I transition into my professional career.

I would also like to express my appreciation to the other members of the Webber Energy Group, both past and present, for their support, friendship, and feedback. In particular, I am very grateful to Dr. Kelly Twomey Sanders for helping me organize my thoughts and develop a sense of direction for my research during my first few weeks in the group. I would also like to thank Dr. Jared Garrison for always being willing to answer my questions, explain difficult concepts, give me advice, and feed me with data. I would like to thank Jeffrey Phillips for lending me his skills as an illustrator and thus bringing to life the concepts discussed in this thesis. Finally, I would like to express my gratitude to Dr. Chioke Harris, Dr. Joshua Rhodes, and Dr. Todd Davidson for their honest feedback and guidance.

The data used in this thesis were primarily provided by the Energy Information Administration (EIA), Electric Reliability Council of Texas (ERCOT), and the Environmental Protection Agency (EPA). Additionally, I would like to acknowledge the contribution of Neil Hughes at the National Grid, for providing papers and data that proved to be very relevant to my research, and instrumental in the progression thereof.

Moving to the United States, attending graduate school, and experiencing the

rich culture of Austin and the surrounding areas has been an amazing adventure for me and my family. We have been afforded this opportunity through the support of the Fulbright Program and the American-Scandinavian Foundation, and for that I am deeply grateful. I would also like to express my gratitude to the Cynthia and George Mitchell Foundation for sponsoring my research, and the Department of Mechanical Engineering at the University of Texas at Austin, for giving me the opportunity to work as a teaching assistant before joining the Webber Energy Group.

Finally, I would like to thank my family: my wife Kristine, my kids, my parents, and my Heavenly Father, for their unceasing love, encouragement, and support.

The Technical Potential of Renewable Natural Gas (RNG) in the United States, and the Economic Potential of Methanation-derived RNG in Texas

Brynjólfur Víðir Ólafsson, M.S.E.
The University of Texas at Austin, 2014

Supervisor: Michael E. Webber

Renewable Natural Gas (RNG) is a low-carbon fuel source that is derived from the anaerobic digestion (AD) or thermal gasification (TG) of biomass, or produced using renewable electricity through the methanation of carbon dioxide. This thesis uses a thermodynamic balance to determine the total technical potential of RNG in the United States, as well as the future technical potential of methanation-derived RNG based on growth curves for renewable electricity. Furthermore, this work establishes an analytic decision-making framework for determining on a rolling basis, from an economic standpoint, whether to sell electricity directly to the grid, or produce and sell methanation-derived RNG. This framework is used to establish the economic potential of RNG, based on Texas wind resources. This work details the formulation of a model that determines which production option generates more marginal profit, based on fluctuating electricity and gas prices. The model also aggregates the total amount of electricity and RNG sold, assuming that the main objective is to maximize the marginal profit of integrated wind- and methanation facilities. This work concludes that the annual technical potential of methanation-derived RNG nationally was 1.03 Quads in 2011. The technical potential of biomass-derived RNG was 9.5

Quads. Thus, the total 2011 technical potential of RNG in the United States was 10.5 Quads, or equal to roughly 43% of the total US consumption of natural gas that year. Assuming a constant, 80% electrolyser efficiency, the technical potential of methanation-derived RNG is expected to rise at an average rate of 1.4% per year, following growth curves for renewable power, until the year 2040, when it will be 1.54 Quads. The 2011 economic potential of methanation-derived RNG in Texas was between 2.06×10^7 MMBTU and 3.19×10^7 MMBTU, or between 19.4% and 30.1% of the corresponding annual technical potential. Furthermore, the total marginal profit increase from introducing the option of producing and selling methanation-derived RNG was around $366 million, given a 'best case scenario' for the state of Texas.

Table of Contents

List of Tables

List of Figures

Chapter 1

Introduction

1.1 Motivation

Human interference with the climate system is the dominant cause for the climate change observed since the mid-20th century [9]. Climate change, which poses risks for various human and natural systems, is considered to be one of the most pressing environmental threats of our times [9, 10]. The atmospheric concentration of carbon dioxide (CO_2), which is the most significant anthropogenic greenhouse gas (GHG), was 395 ppm in 2013 [11]. By contrast, the pre-industrial value of carbon dioxide was only about 280 ppm [12]. This increase in atmospheric concentration of CO_2 is first and foremost a result of fossil fuel use [12], with fossil-derived CO_2 emissions representing 78% of the total Global Warming Potential-weighted emissions from all US emission sources [13]. In 2011, the United States consumed 79.8 quadrillion BTU of primary energy from fossil fuels, with roughly 33% of the total being consumed by the electric power generation sector [4]. Furthermore, 67% of the total primary energy consumed by the power sector came from fossil fuels [4].

Utilizing renewable, low-carbon energy sources can reduce the dependence on fossil fuels for electric generation, as well as the associated GHG-emissions. The utilization of renewable energy resources, such as wind and solar, has increased rapidly within the United States over the last decade [5]. These resources are domestic, clean, and do not require depletable fuel for electricity generation. However, due to the often remote location of wind and solar power plants, there is an inherent cost and

complexity associated with transferring generated electricity to population centers. Additionally, the generation from these energy sources is non-dispatchable, and their intermittent electric supply often does not align well with demand [14].

Using renewable resources to produce renewable natural gas (RNG) can mitigate the negative effects associated with an increased dependence on wind and solar resources for electric generation, and reduce GHG-emissions associated with the combustion of fossil fuels. Renewable natural gas (RNG) is a renewable alternative to traditional natural gas that is appealing because of its potential as a low-carbon fuel, and because it is a non-depleting energy source that would diversify the US fuel mix.

Many different terms are used to denote renewably produced natural gas. This work uses the term 'RNG' for pipeline quality natural gas that is produced using organic feedstocks or renewable electricity, and is fully interchangeable with natural gas. In addition to including natural gas produced through the anaerobic digestion (AD) and thermal gasification (TG) of biomass, this definition also encompasses natural gas produced through the electrolysis of water, where water is separated into oxygen and hydrogen, and the subsequent methanation of CO_2, where hydrogen (H_2) and CO_2 react to form methane. The methane product of this reaction is commonly referred to as synthetic natural gas (SNG), but if renewable electricity is used to drive the electrolysis process, the hydrogen product of that process is renewable, and the final methane product can be referred to as RNG. The term 'biogas', however, is used to denote lower quality natural gas that is produced during the initial step of the AD process. Biogas generally has a methane content of 54-70% [1], and it must be cleaned and upgraded before it can be classified as RNG.

By increasing the utilization of technologies such as AD and TG, the United States' vast biomass resources could be converted to RNG. This effort would diver-

sify the domestic energy supply portfolio, and increase the role of renewable energy resources [3]. Additionally, the utilization of biogas from agricultural manure, municipal solid waste (MSW), and other organic sources would decrease methane emissions. Methane (CH_4) is the second most prevalent anthropogenic greenhouse gas emitted in the United States, after carbon dioxide [15]. Over a period of 100 years, it has 21 times the global warming potential of CO_2 [15]. Thus, avoiding CH_4 emissions would have climate-related benefits [16].

When renewable electricity generation capacity exceeds either electric demand or transmission capabilities, surplus electricity can be utilized to produce RNG through methanation. In the case of a highly congested transmission grid, a co-located methanation plant can reduce curtailment of electricity production. Historically, electricity generation at wind farms in West Texas has been hampered by limited transmission capacity, relative to the actual production capacity of the power plants [17]. Foreign countries, such as Germany, Spain, and the Canadian province of Alberta have also experienced wind curtailments as a result of the rapid expansion of their renewable electric generation infrastructures [18]. In curtailment situations, electricity that would otherwise go unutilized can be used to produce RNG. Energy storage systems that convert surplus electricity into a storable medium can smooth the intermittent output of a renewable energy power plant and bring it into phase with customer demand [19]. This concept can be applied on either a diurnal or seasonal basis.

Finally, when the wholesale price of electricity is low compared to the price of natural gas, there is an economic incentive for using electricity to produce and sell RNG, rather than selling the electricity directly to the grid. This flexibility is a potentially attractive incentive in locations where negative price signals are common due to

wind production tax credits (PTC). An extreme example of the unusual market behavior resulting from government tax credits took place in Denmark and Germany on 25 December 2012 [20]. High generation capacity, coupled with low demand, caused negative electricity spot prices in both countries. The slightly lower German prices caused a net export of electricity to Denmark, while the bids of Danish producers had been curtailed to balance supply and demand. In situations such as this one, the option of utilizing electricity to produce RNG can potentially serve as a hedge against losses due to low electricity prices. Finally, CH_4 is a relatively energy-dense storage medium. Therefore, RNG is a proxy for a battery or other electricity storage devices.

1.2 Objectives, Scope, and Organization

The focus of this thesis is to expand the existing body of work on RNG, with a special focus on the technical and economic potential of RNG produced through electrolysis and methanation. Specifically, this work has two main objectives:

1. Quantify the total annual technical potential of biomass- and methanation-derived RNG in the United States.

2. Quantify the annual economic potential of methanation-derived RNG in Texas.

The first objective primarily expands on existing knowledge by including the technical potential of methanation-derived RNG as part of the total technical potential of RNG in the US. This expansion of scope is shown in Figure 1.1, which illustrates the three RNG production pathways considered in this work. The framework developed for this purpose is also used to determine the technical potential of

methanation-derived RNG within the state of Texas. Furthermore, the future technical potential of methanation-derived RNG is determined for the United States, based on EIA's projections for the growth in renewable power generation from 2015 to 2040.

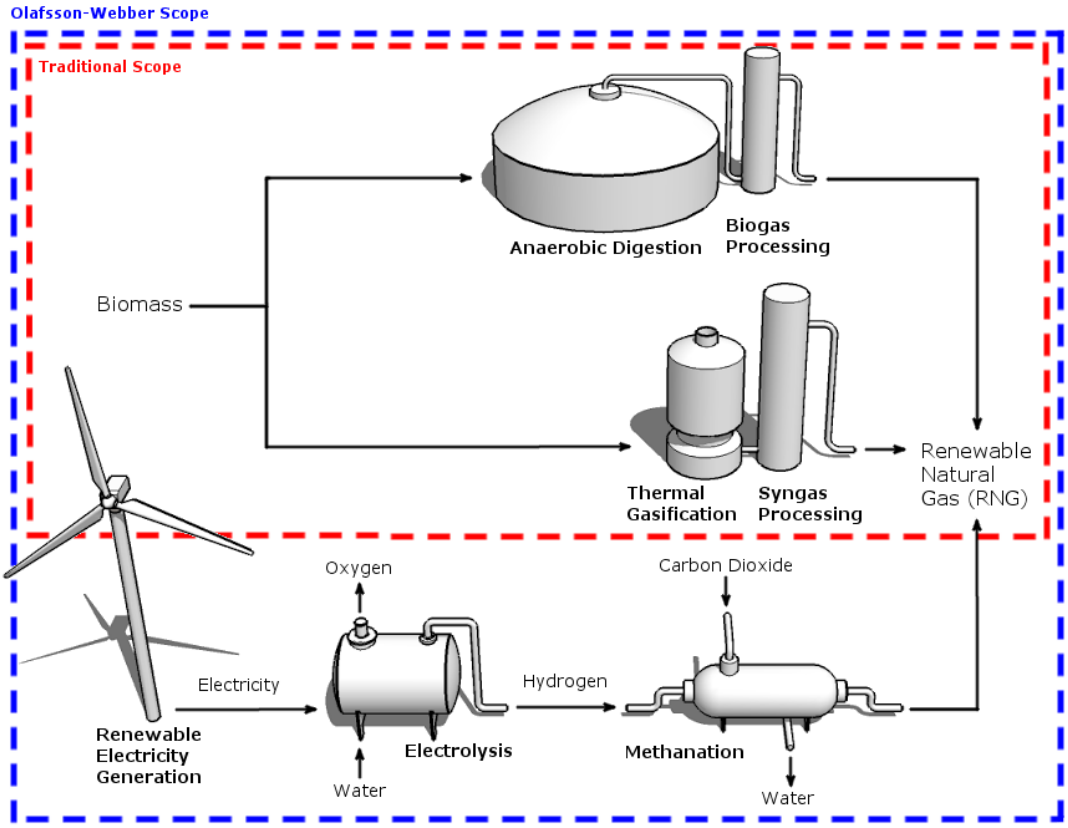

Figure 1.1: Natural gas can be produced renewably, through 1) methanation, using renewable electricity, water and carbon dioxide, or through the 2) anaerobic digestion or 3) thermal gasification of biomass.

The second objective is completely novel, as no attempt has been made to evaluate the economic potential of methanation-derived RNG in Texas, to the author's knowledge. However, the primary value of the second objective is in the analytical framework established in order to reach it. This decision-making framework helps determine, from an economic standpoint, whether to sell renewable electricity directly

to the grid, or use it to produce RNG through electrolysis and methanation, given the availability of the second option. The analysis assumes that all RNG production facilities are integrated with wind power generation facilities, but also considers the potential marginal profit of non-integrated facilities relative to that of integrated ones. Establishing the economic potential of methanation-derived RNG is a two-step process:

1. Establish an economic transition threshold that quantifies the economic and technical conditions that lead to neither production option being preferred over the other.

2. Model the resulting threshold equation in MATLAB to yield the preferred production option on a rolling basis, given fluctuating gas and electricity prices.

This framework is illustrated for the state of Texas by using historical electricity price and power generation data as inputs for the MATLAB model. The choice was made to use Texas wind as the denominator for renewable power generation, due to the disproportionately high amount of installed wind capacity relative to other renewable power sources within the state, and its proximity to a vast natural gas infrastructure. Thus, the Texas economic potential of methanation-derived RNG is quantified. Utilizing the model output also helps establish the potential for hedging against low electricity prices, given the availability of the methanation-derived RNG production option. This assessment is done by considering the total marginal profit from the sales of electricity and RNG, as a function of operating expenses.

While the MATLAB model currently runs using historical data only, the analytical framework is applicable to real-time decision-making. The modifications required to allow the MATLAB model to accommodate for real-time price signals would be trivial.

This thesis consists of 5 chapters. Each chapter (excluding this introductory chapter) consists of a short introduction, followed by a more detailed discussion of the chapter's topic. Chapter 2 reviews the background information relevant to the topic of this thesis, and provides further context for the analysis outlined in this work. Chapter 3 discusses the methodology used to determine the technical potential of RNG in the US. It also describes the derivation of the economic threshold equation, and includes a high-level overview of the MATLAB model used to determine the technical potential of methanation-derived RNG in Texas. At the beginning of Chapter 3, a brief review of literature is conducted, specific to the chapter's main topics. Chapter 4 illustrates the results of the analysis outlined in this work, followed by Chapter 5, which includes a summary of main findings, recommendations, and a discussion of possible future work.

Chapter 2

Background

The first section in this chapter describes the energy landscape of the United States, followed by an analogous discussion specific to the state of Texas. These sections includes a discussion of the energy composition, the energy price, and the role that renewable energy resources play within the aforementioned geographical boundaries. The next section focuses on RNG and the pathways available for the production thereof. This section introduces anaerobic digestion and thermal gasification as the methods for obtaining natural gas from organic material, followed by a discussion of electrolysis and methanation as a way to produce RNG using renewable electricity. The final section in this chapter discusses the merits and drawbacks of using natural gas as an energy storage mechanism.

2.1 General Energy Background

As previously noted, the analysis outlined in this thesis can be divided into two main sections:

1. The technical potential of RNG in the United States.
2. The economic potential of methanation-derived RNG in Texas.

Thus, the energy landscapes of the United States and Texas are discussed separately in the next two sections. The following discussion is primarily focused on

natural gas, wind power generation, and other renewables, as these sources of energy form the foundation of the analysis outlined in this work. The section on Texas also provides relevant background information about the state's electric grid, transmission issues, and the pricing of renewable electricity.

2.1.1 Energy in the United States

The total consumption of primary energy within the United States was 97.3 quadrillion BTU in 2011 [4]. Petroleum consumption was the largest single component, representing 36% of the total, followed by natural gas consumption, which was equal to 24.8 quadrillion BTU, or 26% of the total. The consumption of primary energy from coal was equal to 20% of the total. Finally, renewable energy and nuclear energy represented 9% and 8% of the total consumption of primary energy, respectively. The total amount of renewable primary energy consumed in 2011 was 9.1 quadrillion BTU. These resources can be further divided into hydroelectric power, wood, biofuels, wind, waste, geothermal and solar/PV. Hydroelectric power was the largest renewable energy component, at 35% of the total, followed by wood and biofuels, at 22% and 21% respectively. Figure 2.1 illustrates the actual contribution of these renewable energy resources relative to the total primary energy consumption [4].

The combined contribution of wind and solar was 15% of the total renewable primary energy consumption, or less than 2% of the total primary energy consumption [4]. However, the supply of both wind and solar has increased very rapidly over the last decade, as illustrated in Figure 2.2 [5].

Whenever primary energy is converted to electricity, a part of the energy is lost in the form of heat, light, noise and kinetic energy. The efficiency of a power plant indicates how much of the primary energy is effectively converted into electricity (or another form of useful energy). For renewable resources, efficiencies range

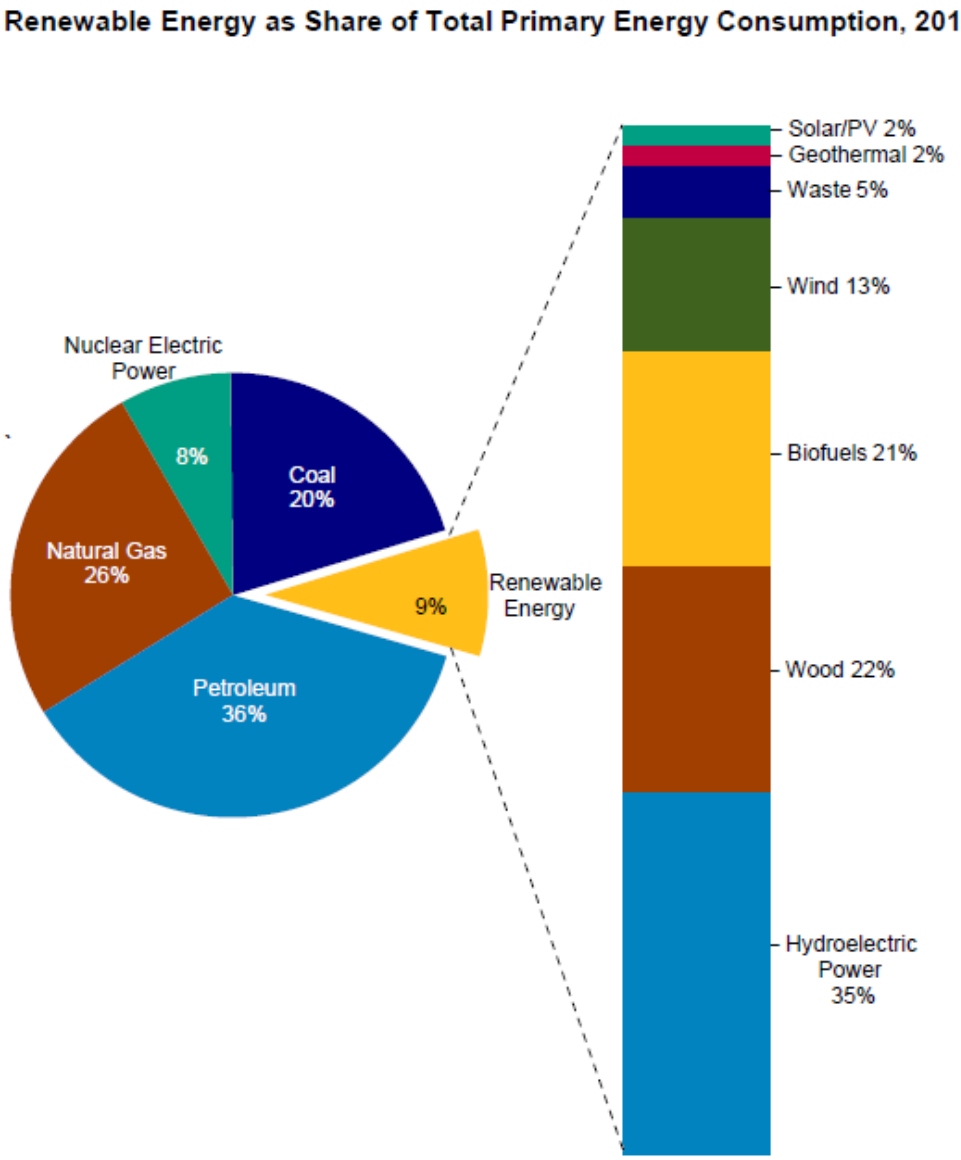

Figure 2.1: Renewable energy represents a significant share of the total primary energy consumption [4].

from around 12% for photovoltaic solar panels, up to above 90% for hydroelectric turbines [21, 22]. As a result, the total amount of electricity generated is less than the primary energy consumed by the electric power sector. In the case of renewables in 2011, 4.9 quadrillion BTU of primary energy were consumed, which yielded 520.1 billion kWh, or 1.78 quadrillion BTU, of electricity [4]. This quantity forms the

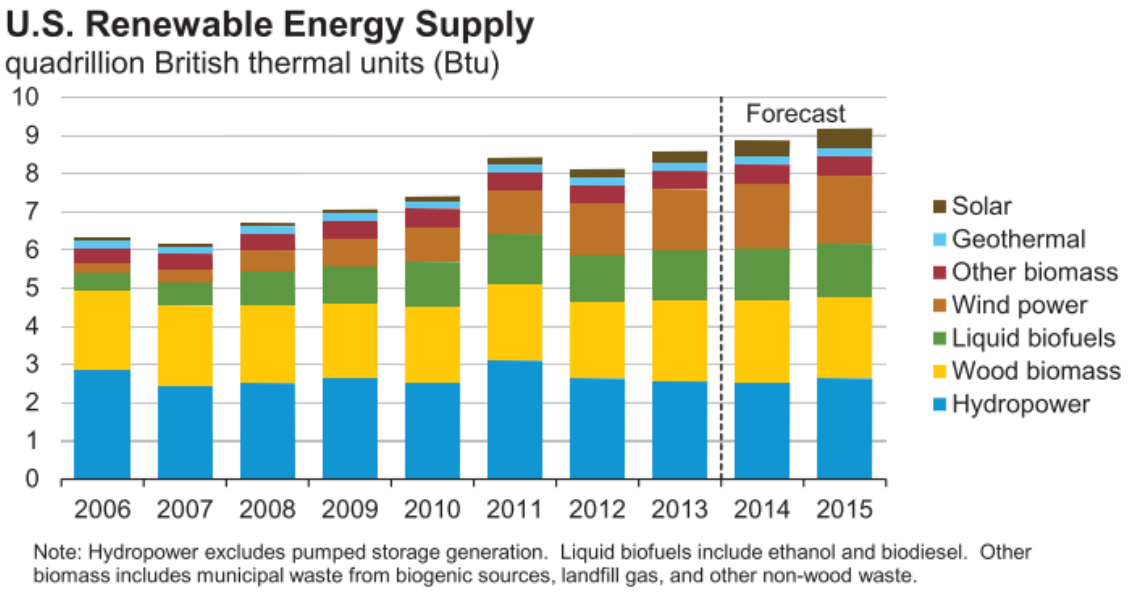

Figure 2.2: Both wind and solar have experienced a rapid growth since 2006, with projections indicating further growth in coming years [5].

foundation used to determine the technical potential of methanation-derived RNG in the United States. As previously stated, the methodology used to determine the US technical potential of RNG is described in detail in Chapter 3.

The economic analysis outlined in this thesis is restricted to Texas. Therefore, a general discussion of energy and electricity prices in the United States is not included.

2.1.2 Energy in Texas

The state of Texas leads the nation in total energy production, most of which is produced in the form of natural gas and crude oil. In addition to being the lead crude oil- and natural gas-producing state, Texas also has the highest wind-powered generation capacity of all 50 states, at more than 12,000 MW [23]. In 2013, Texas generated nearly 36 million MWh of electricity from wind, which was more than one-fifth of the total US wind generation [23]. In addition to wind resources, Texas is very

rich in other renewable resources, such as solar and biomass. Despite projects aimed at expanding the use of biomass for electricity production, most of the biomass is currently used to produce biofuels, and very little is used for electricity generation [23]. Similarly, the vast solar production potential has not been utilized to the same extent as the state's wind resources. In 2012, the cumulative installed solar capacity was 140.3 MW [24].

Through its extensive network of oil and gas wells, the state of Texas has access to a unique geothermal resource. Many of the existing wells connect to geothermal reservoirs, with water reaching temperatures of up to 200°C [23]. Thus far, this resource has been left largely untapped [23]. Finally, despite contributing most to the generation of renewable electricity in the US, the contribution of hydropower to electric generation in Texas is minimal. The lack of hydroelectric power generation is largely due to unfavorable terrain throughout much of the state, as well as generally low levels of precipitation [23]. Thus, wind power accounts for almost all of the renewable electricity generation within the state of Texas [4, 23].

In addition to being the largest energy producer, Texas is also the leading energy consumer, with a total primary energy consumption of 12.3 quadrillion BTU in 2012 [23]. The large industrial sector accounts for most of the state's energy consumption, due to the many power-intensive industries, such as petroleum refining and chemical manufacturing [23]. The size of the state and the number of registered vehicles make the transportation sector the second largest energy consumer [23].

Texas leads the nation in electricity generation and consumption [23]. The state's power grid is largely independent from the interconnected power grids that serve the eastern and western parts of the country. In fact, Texas is the only mainland state that has an independent power grid completely within its boundaries [23]. The

area which the Texas grid covers is known as the Texas Interconnection Region. It covers 75% of the state's surface area, and is shown in Figure 2.3 [6].

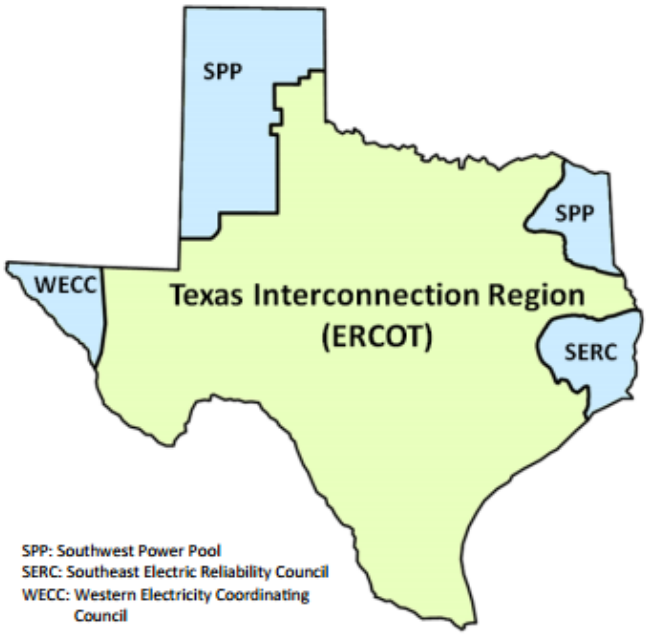

Figure 2.3: The Texas Interconnection Region covers 75% of the state's surface area, and represents 85% of the state's electric load [6].

The Electric Reliability Council of Texas (ERCOT) is the independent system operator (ISO) responsible for operating the electric grid within the Texas Interconnection Region. ERCOT manages 85% of the state's electric load, with 24 million Texas customers receiving electric power through ERCOT's services [25]. ERCOT's electric generation by fuel source is shown in Figure 2.4 [6].

Most of ERCOT's electric generation comes from natural gas and coal fired power plants, with a combined contribution of 78.7% [6]. Nuclear power represents a significant portion at 11.6%, followed by wind at 9.9% [6]. All references to Texas wind power generation in this work are used synonymously with the generation of wind power within ERCOT's boundaries. Other resources contribute less than 1% to

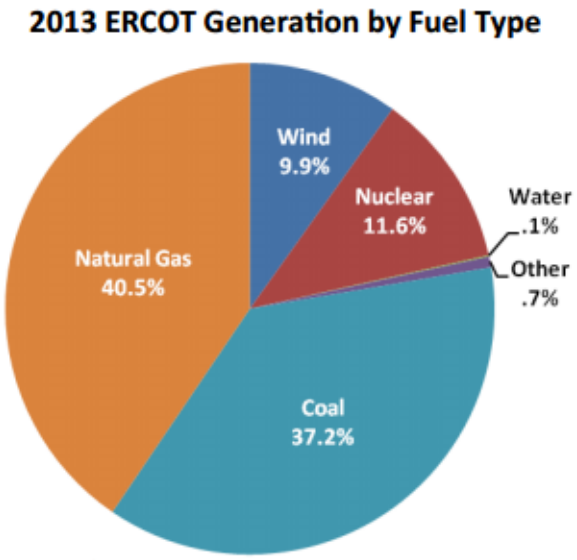

Figure 2.4: Wind represents nearly 10% of ERCOT's total electric power generation [6].

ERCOT's electric power generation [6].

Between the years 2006-09, wind power generation experienced a substantial growth in Texas, with the total generation capacity expanding by more than 7,000 MW [17]. The abundant supply of low cost wind within ERCOT's boundaries, coupled with electricity transmission constraints and the presence of PTC, caused occurrences of negatively priced electricity in West Texas during periods of substantial wind generation [17]. As a response, the Public Utility Commission of Texas (PUCT) authorized a number of transmission expansion projects that would allow 18,500 MW of electricity to be transported from major wind generation sites, denoted as Competitive Renewable Energy Zones (CREZ), to electricity demand areas throughout the state [17]. This expansion resulted in a significant reduction of the number of wind curtailment occurrences, as well as the frequency of negative electricity price occurrences, between the years 2011-14 [17].

The analysis in this work is largely based on 2011 power output and curtailment data. Thus, the economic potential evaluated herein reflects a congested transmission grid, with significant curtailment of power output, and relatively frequent occurrences of negative electricity prices. While that might not be the case in Texas today, it is reflective of other parts of the world where transmission capacity is limited relative to the installed renewable generation capacity. The framework outlined in this analysis can be applied to any scenario, given the appropriate price, power output, and curtailment data. Furthermore, as wind production capacity continues to rise compared to transmission capacity, energy storage based on the methanation of carbon dioxide can be seen as a potential alternative to further grid upgrades. With some modifications to the outlined framework, the incentives for investing in RNG production capabilities could be determined and compared to the incentives for building new transmission lines, as a potential alternative.

2.2 Pathways for RNG Production

This section discusses the pathways available for producing natural gas using renewable resources. The pathways for producing RNG from biomass are considered first, followed by a discussion electrolysis and methanation as a means by which RNG can be produced.

2.2.1 Biomass Pathways

This work considers anaerobic digestion (AD) and thermal gasification (TG) as the two pathways available for converting organic matter to RNG. While both pathways are based on proven technologies, only AD is commercially available at the time of writing. Meanwhile, the TG of biomass is expected to to reach commercial-scale implementation within the next decade [26]. These two technological processes

are discussed in the following two subsections.

2.2.1.1 Anaerobic Digestion

Anaerobic digestion (AD) is the process of converting organic matter into biogas, in an environment bereft of oxygen, through microbial action. This process usually takes place in some sort of tank, referred to as a digester or a reactor, and it can take anywhere from a few days to several weeks, depending the source of the organic materials being digested [3]. Although most organic materials can be anaerobically digested, the process is typically used for wastewater, food waste, animal manure, and other organic feedstocks that have a moisture content of 70% or more [27]. During the digestions process, the microorganisms in the digester break down the organic matter, thus producing a gaseous mixture that consists mostly of methane and carbon dioxide, as well as trace amounts of other gases [3]. The gas is commonly referred to as biogas, or raw biogas, at this stage, and its actual composition depends largely on the materials being digested. The typical composition of AD-derived biogas is shown in Table 2.1 [1].

The temperature at which the AD process takes place also affects the composition of the raw biogas. The process is optimized when it takes place in either the mesophilic (32-35°C) or thermophilic (50-57°C) temperature range. Thus, temperature adjustments are necessary to optimize production in some climates [29].

Raw biogas must be dried, cleaned, and conditioned before it is suitable for injection into the natural gas pipeline network [27]. This process includes the removal water, and of hydrogen sulfide (H_2S), as well as the separation of carbon dioxide from the desired methane [27]. Saber and Takach [1] recently reviewed the methods and processes commonly used to remove these contaminants, and other common impurities, from sub-pipeline quality RNG. An overview of a sample AD production

Table 2.1: Raw biogas generally consists of methane and carbon dioxide as primary constituents, as well as a balance of nitrogen, hydrogen, oxygen, carbon monoxide, and hydrogen sulfide [1].

Compound	Typical Concentration Range (molar %)
Methane (CH_4)	54-70%
Carbon dioxide (CO_2)	27-45%
Nitrogen (N_2)	0.5-3%
Hydrogen (H_2)	1-10%
Carbon monoxide, (CO)	0-0.1%
Oxygen (O_2)	0-0.1%
Hydrogen sulfide (H_2S)	600-7000+ ppm [28]
Trace elements, amines, sulfur compounds, non-methane volatile organic carbons, halocarbons [28]	

and cleaning process is given in Figure 2.5.

In the case of landfill gas (LFG), the AD process takes place as microorganisms break down the organic portion of municipal solid waste (MSW). The landfill itself takes the place of an anaerobic digester, and the raw LFG is collected using a network of perforated pipes. Following collection, the LFG undergoes a cleaning process similar to the process illustrated in Figure 2.5 [27].

2.2.1.2 Thermal Gasification

TG of biomass encompasses a number of processes and reactions that convert solid biomass into synthetic natural gas [27]. TG is generally applicable to biomass that has lower moisture content than the organic matter ideally converted through AD [3]. The thermal breakdown of solid biomass in a gasifier produces a mixture of gases, including hydrogen, carbon monoxide, carbon dioxide, methane, nitrogen, and steam [3]. The composition of the gas mixture depends on the production process

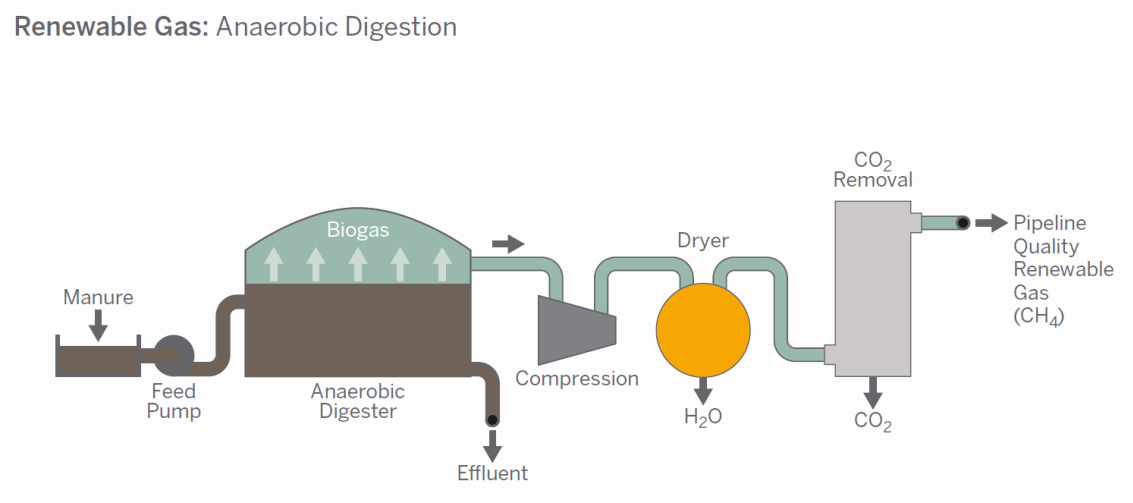

Figure 2.5: Renewable gas can be produced from biomass using AD. To ensure that the gas is of pipeline quality, it must be dried, cleaned and conditioned. The specific energy yield of the AD process is summarized for different feedstocks in Table 3.1. Illustration courtesy of Jeffrey Phillips.

employed, with water vapor and oxygen often being injected into the gasifier to reduce the fraction of nitrogen in the synthesis gas (or syngas), as nitrogen is difficult to extract [3]. The common composition of synthesis gas produced using different production methods is shown in Table 2.2 [2].

TG can be conducted at temperatures ranging from roughly 650°C to 1100°C, and pressure levels ranging from atmospheric pressure to around 70 atm [3]. If pressure levels are low (around or just above 1 atm) when TG takes place, then the product gas must be compressed to be of pipeline quality [3]. Following the actual gasification process, and the potential compression step, the synthesis gas is conditioned and cleaned. During this step, carbon dioxide, particulates, tars, and hydrogen sulfide are removed from the syngas [27]. This conditioning step is followed by the methanation process, where hydrogen and carbon monoxide are converted to methane [27]. This process yields water as a byproduct, so the gas must undergo drying before it is injected into the natural gas pipeline network. An example of the whole TG production

Table 2.2: Using air in the gasification reactions yields a nitrogen-rich synthesis gas mixture. By contrast, using either steam or oxygen significantly reduces the molar percentage of nitrogen in the syntehtic gas [2].

Compound	Typical range (molar percentage)		
	Air-Blown Fixed Bed	Steam-Blown Fluidized Bed	Oxygen-Blown Entrained Bed
Hydrogen (H_2)	11-16%	35-45%	23-28%
Carbon monoxide, (CO)	13-18%	22-25%	45-55%
Carbon dioxide (CO_2)	12-16%	20-23%	10-15%
Methane (CH_4)	2-6%	9-11%	<1%
Nitrogen (N_2)	45-60%	<1%	<5%

process is illustrated in Figure 2.6. Note that while TG only refers to the initial gasification process in the strictest sense, the term is often used to denote the complete process by which biomass is converted into methane, including both the conditioning step and the methanation step. Thus, references to TG in this work are generally used to denote the whole conversion process. Typical conversion efficiencies for this process are between 60-70%, depending on configuration, temperature, pressure, and other conditions [3].

2.2.2 Electric Pathway

The production of RNG using renewable electricity consists of two main processes: electrolysis and methanation. The electrolysis process is stoichiometrically denoted as:

$$2H_2O + e^- \longrightarrow 2H_2 + O_2$$

As the splitting of water into its constituent elements is an endothermic process, a

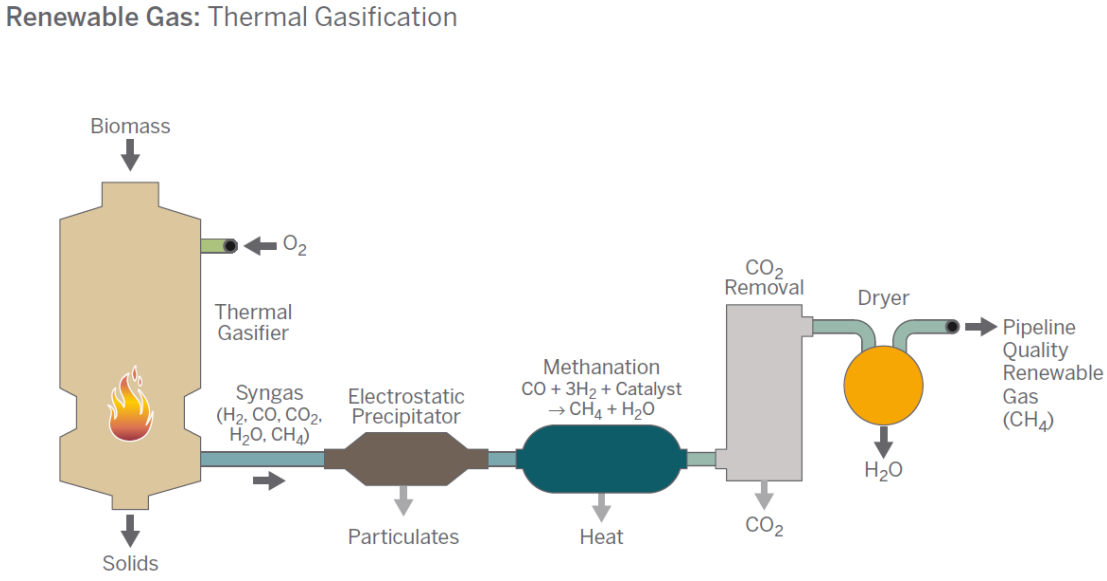

Figure 2.6: TG is an alternative to AD for producing RNG from biomass. The setup illustrated here includes an additional CO_2 removal step, following the methanation of CO. The specific energy yield of the TG process is summarized for different feedstocks in Table 3.1. Illustration courtesy of Jeffrey Phillips.

direct electric current is required for the process to take place. For the practical purposes of hydrogen production through electrolysis, pure water does not conduct electricity [30]. Thus, the electric current is passed through a conductive substance, or electrolyte, in order to facilitate the process. As previously stated, the source of this electric current must be renewable for the output gas to also be considered renewable.

Water quality requirements vary greatly across electrolysers. Some units have a built-in water purifier inside their hydrogen generation units, while others require an external purification process, such as reverse-osmosis, to take place before the water is fed to the cell stacks of the electrolyser [31]. In general, alkaline based electrolyser units don't require the same level of water purity as other commonly used electrolyser systems [31].

The hydrogen product of the electrolysis process is combined with carbon dioxide to form methane. The thermochemical equation of the methanation process is:

$$CO_2 + 4H_2 \longrightarrow CH_4 + 2H_2O, \qquad \Delta H_{600K} = -179 \text{kJ/mol}$$

This reaction is also known as the Sabatier process, named after the French chemist Paul Sabatier, who demonstrated the reaction over a nickel catalyst in 1902 [32]. The Sabatier reaction was recently analyzed in depth by Wang and Gong [10]. Other studies of the methanation process have primarily focused on the types of catalysts used to drive the process, and ways to improve the selectivity and yield of the methane produced using the Sabatier reaction [33]. The National Aeronautics and Space Administration (NASA) is interested in the Sabatier process, as it could enable the conversion of the CO_2-dense atmosphere on Mars into methane for fuel and water for astronaut life-support [34, 35]. The German automobile manufacturer Audi has implemented a practical application of the methanation process in its Werlte power plant. The plant utilizes CO_2 and renewable electricity to generate methane that can be fed directly into the natural gas pipeline network [36].

Opposite to the endothermic electrolysis process, the methanation process is highly exothermic, which means that energy is released in the form of heat during the chemical reaction, even at high process temperatures. Despite the exothermic nature of the Sabatier reaction, a catalyst is required to achieve the selectivities and production rates required for a commercial-scale system [10]. These catalysts are most commonly nickel-based, but the methanation process has also been demonstrated

successfully over a number of nobel metal catalysts [10]. Figure 2.7 illustrates the electric pathway for producing RNG.

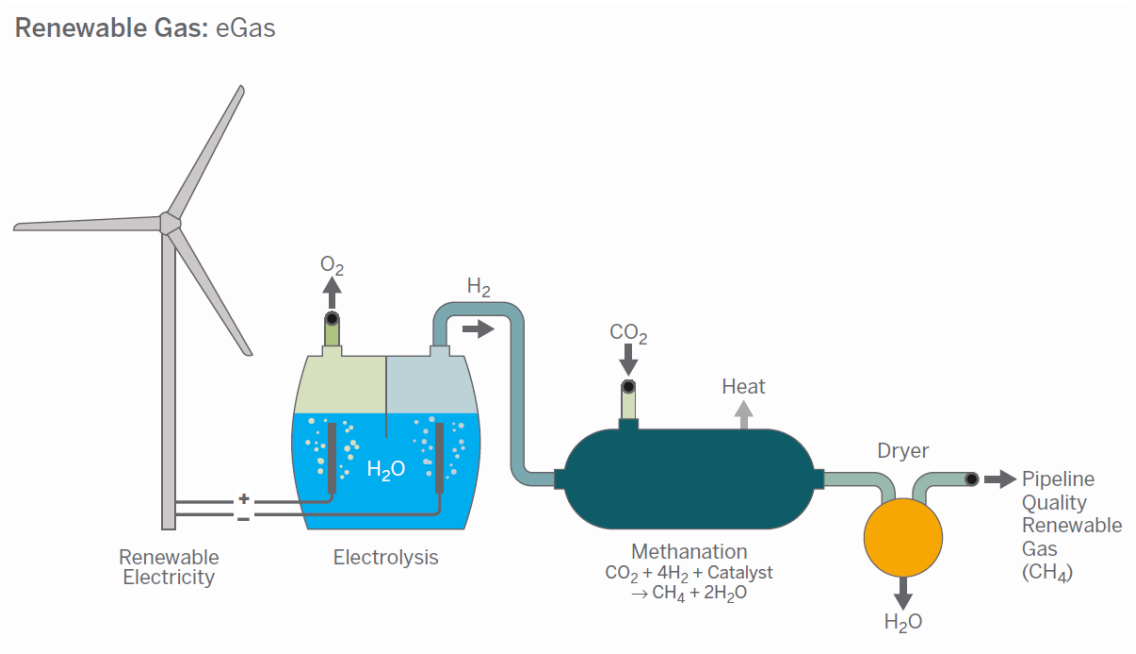

Figure 2.7: Natural gas can be produced renewably, using renewable electricity, water and carbon dioxide. RNG produced this way is often referred to as eGas or synthetic natural gas. The energy yield of this process, along with corresponding input and output values, is shown in Figure 3.2. Illustration courtesy of Jeffrey Phillips.

The CO_2 used for the methanation process would ideally be recycled from a nearby power plant or other industrial operations. Reusing CO_2 as a feedstock for fuels or chemicals can lead to a decreased dependence on fossil fuels, without increasing the overall amount of CO_2 in Earth's atmosphere. Thus, excepting energy losses associated with that capture of CO_2, RNG that is produced through methanation, using surplus renewable electricity, is a carbon-neutral fuel source. Although CO_2 is already being used to some extent as a chemical feedstock, its current use only corresponds to a small fraction of the potential CO_2 that is suitable to be converted into chemicals or fuels [10].

The methanation process can take place at temperatures ranging from room temperature to 500°C, and pressure levels as low as atmospheric pressure [33]. The CH_4 yield of the methanation process depend strongly on the production temperature, pressure, preparation method, catalyst, and feed ratio (H_2:CO_2). Generally, however, operating below 300°C is necessary to ensure a high yield at atmospheric pressure, due to the highly exothermic nature of the methanation process. A more detailed discussion of the production conditions and outputs of the methanation process is deferred to the next chapter.

2.3 RNG as a Storage Mechanism

The stability of the electric grid depends on the delicate balancing of power generation with electric demand. Increasing the generation capacity of weather-dependent power sources, such as wind and solar, leads to an increased need for balancing supply and demand. This balance can be maintained to some extent through the use of flexible electric generators, coupled with energy storage systems.

Energy storage systems vary greatly in their storage capacity, discharge time, and application. High power flywheels and super-capacitors are well adapted to maintain power quality, where the key performance criteria are energy release capacity and cycling capacity, and total storage capacity is not as important [37]. Meanwhile, compressed air energy storage (CAES) and flow batteries are better suited for peak-hour load leveling, where significant storage capacity is required [37]. For decades, however, pumped hydro storage (PHS) has been the storage medium of choice for electric system support and peak-hour load leveling [38]. The Electric Power Research Institute (EPRI) estimates that more than 99% of global installed electricity storage is in the form of PHS [39]. This storage method involves using surplus electricity to pump

water to a higher elevation when electric demand is low, and generating electricity by letting the water flow down through hydroelectric turbines when electric demand is at its peak. Power plants based on PHS generally store anything from a few hours' to a few days' worth of electricity, making this form of storage ideal for peak load coverage, but less so for seasonal balancing of renewable energy sources [38]. Furthermore, PHS is highly dependent on favorable geographical features and weather conditions, and thus the expansion potential for this form of energy storage is often very limited [38].

The process of using renewable electricity to produce SNG through electrolysis and methanation is a relatively new alternative to PHS systems [38]. The power-to-gas (PtG) storage concept is illustrated in Figure 2.8 [7].

The main concept behind PtG is the utilization of excess renewable electricity for the production of methane through the electrolysis of water and the methanation of carbon dioxide, as previously explained. This pathway is illustrated in Figures 2.7 and 2.8. Figure 2.8 furthermore illustrates how the byproducts of the intermediate steps of the PtG process can be utilized to reduce the overall need for water and carbon dioxide as production feedstocks, or to reduce pollution from power generation. The products of the electrolysis process are hydrogen (H_2) and oxygen (O_2). While hydrogen is an essential component of the methanation process, oxygen can be used for the combustion of RNG within a natural gas power plant. Conventional fuel systems based on this technique have reduced NOx emissions by up to 20% relative to the baseline, where air is used for the entire combustion [40]. Conventionally, techniques based on this concept require oxygen to be separated from air, which is not always economical. However, as oxygen is a natural byproduct of the electrolysis process, the cost of oxygen is limited to the cost of transporting it from the electrolysis

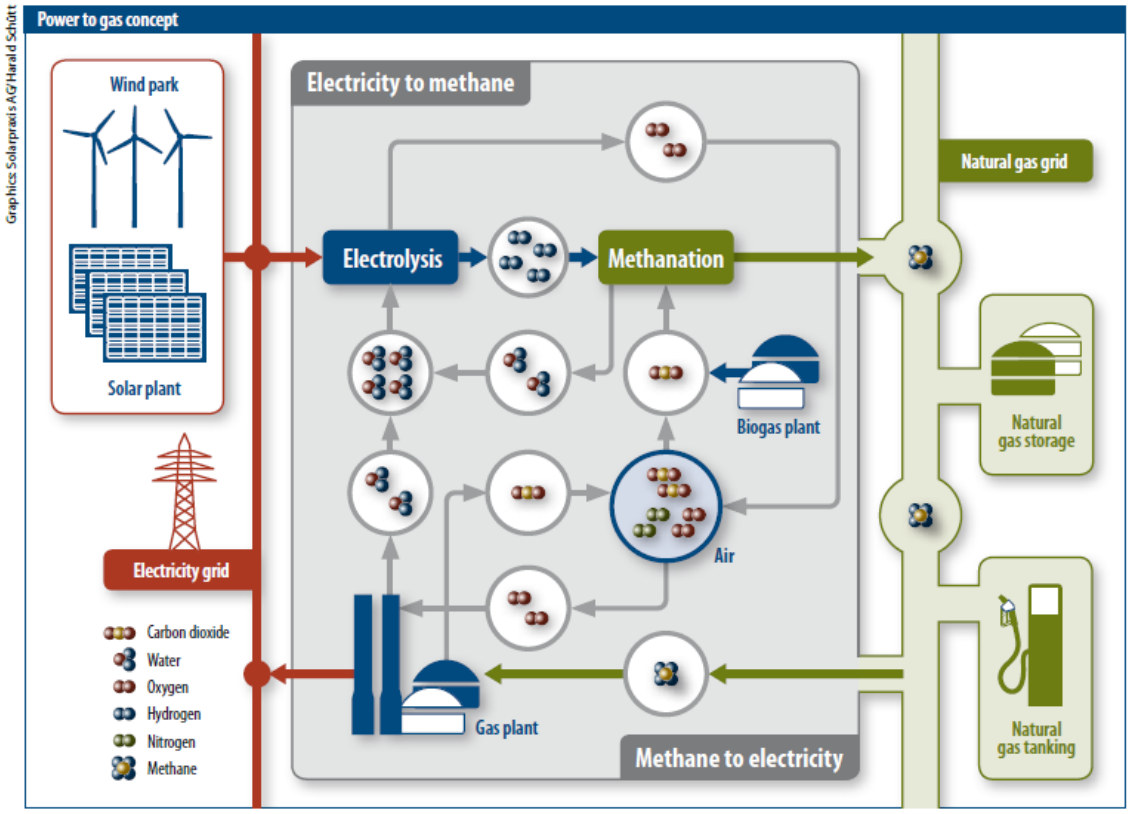

Figure 2.8: Renewable electricity can be converted to natural gas through electrolysis and methanation, thus utilizing existing natural gas infrastructure to balance power generation and electricity demand. Many of the byproducts of the individual conversion processes can be re-used, thus increasing the overall efficiency of the whole system [7].

plant to the natural gas power plant. Thus, the co-location of plants would minimize this cost.

Any industrial-scale production of RNG through electrolysis and methanation would require a significant consumption of pure water for the electrolysis process. However, water is also a byproduct of the methanation process, with two molecules of water being produced for every molecule of methane. The bulk of this water can be collected and re-used for electrolysis, thus reducing the total amount of water consumption required for each molecule of methane produced.

Once the RNG is produced, it is channeled into the natural gas pipeline network, thus utilizing existing natural gas infrastructure. This gas can be compressed and sold as transportation fuel, as illustrated in Figure 2.7, or channeled directly to residential or industrial consumers. If PtG is to be used strictly as a storage mechanism, the gas will be channeled towards a natural gas storage unit, to be used for electric generation when demand is high. Natural gas can be stored in underground caverns, such as depleted gas deposits, salt caverns, and aquifer horizons. These massive storage caverns can generally store between 40 and 100 million m^3 of natural gas each, providing storage capacity that stretches well into the TWh range [7]. The storage capacity of PtG is illustrated relative to that of other storage systems, in Figure 2.9 [8].

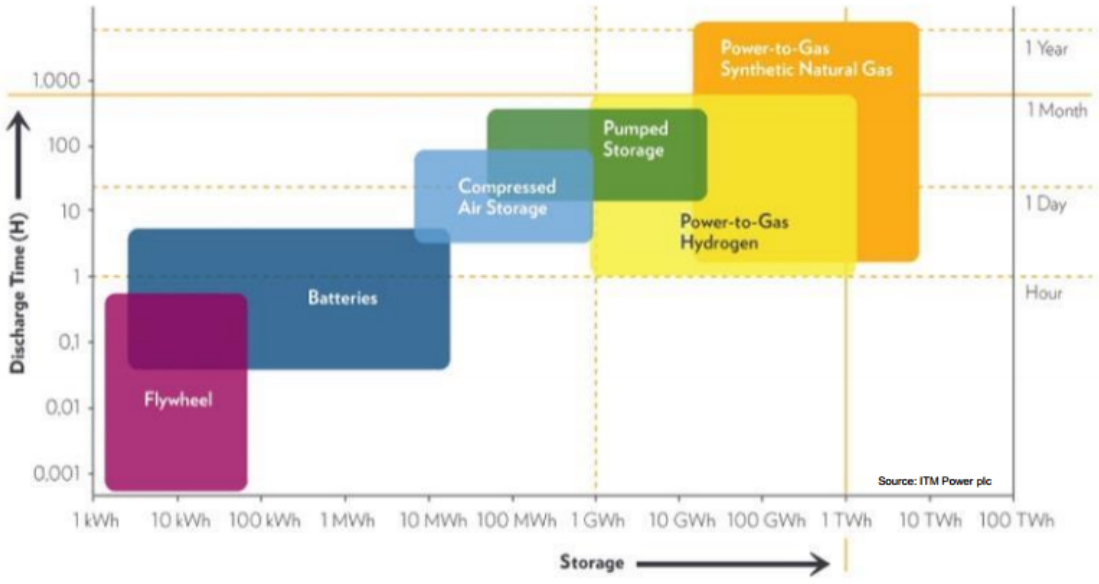

Figure 2.9: Energy storage systems vary greatly in their storage capacity and discharge time. PtG offers storage potential in the high GWh to low TWh range, and a discharge time ranging from a few hours to thousands of hours [8].

The lower range storage capacity of natural gas storage caverns is in the tens of GWh, which is roughly the same as the maximum capacity of PHS. The discharge time

for PtG ranges from hours to more than a year, providing more dispatching flexibility than traditional PHS. Furthermore, the combined withdrawal and conversion capacity of underground gas into electricity can extend well into the range of tens of GW. The massive potential storage capacity of underground natural gas, coupled with its discharging flexibility, makes PtG a reasonable option for seasonally storing and dispatching renewable energy, as well as a potential alternative to PHS for peak-hour load leveling [38].

From an economic standpoint, the US natural gas market makes PtG a potentially attractive storage option for a couple of reasons: Since 2009, the wholesale price of natural gas has been in the range of $2.5 to $5, with only a few exceptions [41]. The abundant (and increasing) production of natural gas in the United States has steadily reduced the net import of natural gas from 3,785 Bcf in 2007 to 1,311 Bcf in 2013 [42]. This trend, coupled with the isolation of the domestic market from foreign markets outside of North America, has increased the market's resistance to fluctuations in the global price of natural gas [42]. The relatively stable price of natural gas means that RNG can be produced using cheap, out-of-demand electricity, and then stored until it is in high demand.

While natural gas prices are relatively stable in the US, these prices also remain much lower than those of foreign markets outside of North America [42]. However, as net imports continue to decrease with increasing overall gas production, the prospect of exporting liquefied natural gas (LNG) to overseas markets becomes more attractive [42]. This development might lead to the increased volatility of the US natural gas market, and the EIA predicts [43, 44] that the average gas price between 2025 and 2035 might be as much as 111% higher than the average price in 2011 was, if gas exports were to increase to 12 Bcf/d, at a rate of 1 Bcf/d per year, from the

year 2014 onwards. While higher gas prices would intuitively make PtG more economically feasible, increasing the total exports of natural gas is a controversial move, as it would likely lead to an increased dependence on coal for electric power generation [43]. Furthermore, consumers could expect to see an increase in their natural gas and electricity expenditures, despite decreased consumption [43]. However, even without increasing natural gas exports, the EIA predicts [43] that natural gas prices will rise by about 57% between the years 2010 and 2035.

One of the main drawbacks of using PtG as an energy storage mechanism is the relatively low conversion efficiency. Jentsch, Trost, and Sterner [45] reported a conversion efficiency of 49-65% for PtG (methane). Charles River Associates (CRA) International [46] reported a weighted average heat rate of 7.08 MMBTU/MWh for 65 combined cycle power plants across the United States. This heat rate corresponds to a conversion efficiency of 48.2%. Thus, converting electric energy to chemical energy (in the form of RNG), and then back to electric energy, can be accomplished at an overall efficiency of 24-31%. Meanwhile, the roundtrip efficiency of a PHS system is about 65-80%, depending on the characteristics of the pump used, as well as other equipment characteristics [37]. Thus, for every MWh released from storage into the electric network, a PHS system requires less electric input than a PtG system. Other large-scale storage systems, such as CAES, have efficiencies comparable to PHS, and significantly greater than PtG [37].

Chapter 3

Methodology

Much prior work has evaluated the technical potential of biomass-derived RNG. A body of prior work exists that evaluates the technical potential of RNG from specific waste streams and energy crops, through AD [3, 16, 29, 47–49]. For example, Cuéllar and Webber [16] evaluated the technical potential of RNG from agricultural manure; Stillwell, Hoppock and Webber [29] evaluated the technical potential of RNG from wastewater; and Zamalloa et al. [47] evaluated the techno-economic potential of RNG through the AD of microalgae. Furthermore, a few country-scale studies have been conducted to determine the total technical potential of RNG through the AD or TG of biomass. Lorenz et al. [48] evaluated the technical potential of organic waste streams for RNG production through AD within the EU-27, and National Grid [49] commissioned a study on the technical potential for RNG in the UK. In 2011, the American Gas Foundation (AGF) published a comprehensive report on RNG [3] that provided an assessment of the potential impact of renewable gas in the United States, and included an evaluation of the total technical potential of biomass-derived RNG. The report included both AD and TG as potential pathways for biomass utilization and conversion to RNG. It did not, however, consider the technical potential of RNG synthesis through electrolysis and methanation. Despite advances in the field, the technical potential of methanation-derived RNG in the United States has yet to be quantified, to the author's knowledge. Thus, the evaluation of the US technical potential of methanation-derived RNG represents a knowledge gap that this work seeks

to bridge. Combining the results of this analysis with the studies that have been conducted on the AD/TG pathways, the total technical potential of RNG in the United States can be obtained. Determining the technical potential of RNG establishes an important theoretical upper limit for the potential availability of RNG. The methodology used to determine this technical potential is described in Section 3.1.

To the author's knowledge, no attempt has been made to establish an analytic framework for evaluating the economic potential of methanation-derived RNG in Texas. The methodology for establishing this framework, determining the economic potential of methanation-derived RNG in Texas, and determining the hedging potential of the methanation-derived RNG production option, is described in Section 3.2.

3.1 Technical Potential of RNG in the United States

To estimate the technical potential of RNG in the United States, we aggregated how much RNG could be obtained through (1) both the thermal gasification and anaerobic digestion of biomass, and (2) the methanation of carbon dioxide. The methanation analysis was based on data from 2011, while the 2011 AGF report was based mostly on 2010 data [3]. In the absence of a comprehensive update between the years 2010 and 2011, the growth of the total biomass potential is assumed to be comparable the growth of electric generation from biomass between the same two years. This increase was equal to less than 4% [50]. Thus, the results of the two analyses are assumed to be comparable. In addition to estimating the total 'current' technical potential, the technical potential of RNG through methanation was also quantified based on EIA renewable electricity generation projections [50] for every year from 2015 until 2040.

In prior work, the technical potential of biomass-derived RNG in the United

States was determined [3]. The organic feedstocks considered for that work were designated for conversion by either AD or TG, depending on which pathway would maximize the impact of the output gas and the associated production process. The potential impact was evaluated in terms of four major components: annual resource availability, annual energy potential, potential greenhouse gas offset, and economic impact [3]. The feedstocks selected for both AD and TG are listed in Table 3.1 [3], along with all major assumptions. The energy density of methane in the prior work is assumed to be equal to 1,000 BTU/cf [3]. To maintain consistency, this energy density value is also assumed for RNG throughout this work.

The study developed three scenarios for examination: *Non-aggressive*, *Aggressive*, and *Maximum*. Each of these scenarios represented the potential of RNG under different levels of feedstock utilization and market penetration [3]. The *Maximum* scenario established the technical potential of biomass-derived RNG in the United States, and is thus of primary interest within the context of this study. The amount of pipeline quality RNG obtainable from each unit of feedstock was determined by four different intermediate processes [3]. These were *Utilization*, *Collection*, *Conversion*, and *Cleanup*. The term *Utilization* indicates the potential application of each given feedstock, and is dependent upon the potential market penetration of the feedstocks considered. *Collection* indicates how efficient the harvesting process is, while *Conversion* refers to how efficiently the feedstock is turned into gas. Finally, *Cleanup* refers to the process of upgrading biogas to pipeline quality natural gas, by removing unwanted contaminants. This cleanup process is required for AD, but conversion through TG produces RNG which is of much higher quality, and thus little to no cleanup is needed [3].

Table 3.1: The feedstocks considered in the AGF report were divided by AD and TG, depending on which conversion method provided a greater environmental, energy and economic impact. The specific energy yield of each source was given in dekatherm (1 dekatherm = 10^6 MMBTU) or cubic feet (cf) of CH_4, per wet-ton, except for wastewater and landfill gas. The specific energy yield of wastewater was defined in dekatherm per million gallons (MG). Landfill gas was assumed to have an average methane content of 60%, with each landfill's production rate being a function of the landfill size, waste-in-place, and climate classification. For further information, see Table 13 in the AGF report [3].

Feedstock	Specific Energy Yield	Other Comments
AD		
Animal waste	766.3 cf CH_4/wet-ton	Includes waste from dairy cows, beef cattle, hogs and pigs, sheep, broiler chickens, turkeys and horses
Wastewater	7.9 dekatherm/MG	Facilities of 17 MG per day, or greater, accepted for RNG production
Landfills	Gas composition: 60% CH_4	Landfill gas production depends on the landfill categorization (small, large, arid, non-arid)
TG		
MSW	8.4 dekatherm/wet-ton	Only considers waste currently directed to landfills, and not that which is usually directed to energy projects
Wood residue	11.2 dekatherm/wet-ton	Includes forest, mill, and urban wood residues
Energy crops	13.8 dekatherm/wet-ton	Includes switch grass, willow and hybrid poplar
Agricultural residues	11.2 dekatherm/wet-ton	Includes the residues of corn, wheat, soybeans, barley, oats, rice, rye canola, beans, peas, peanuts, potatoes, safflower, sunflower, sugarcane, and flaxseed

The efficiency of each of the aforementioned processes was set to 100% in the *Maximum* scenario, with the exception of the conversion efficiency of TG, which was set at 65% [3]. This efficiency estimate is conventionally used for the thermal gasification process. The conversion efficiency of AD remained at 100%, because the real losses in the process were implicitly contained in the data obtained by AGF [3]. While the implicitly reported losses of the AD process simplify calculations, they also skew the apparent specific energy yield of the AD process relative to the TG process, as reported in Table 3.1. The TG technology is newer, but the specific energy yield of the AD process seems unreasonably low by comparison. This disparity stems from the fact that the conversion losses of the TG process have yet to be accounted for.

Determining the US technical potential of methanation-derived RNG is a three-step process, that consists of (1) determining the total amount of renewable electricity theoretically available for electrolysis, (2) determining how much hydrogen can be produced using that electricity, and (3) determining how much methane could be produced by utilizing the available hydrogen for the methanation of carbon dioxide. This process is illustrated in Figure 3.1.

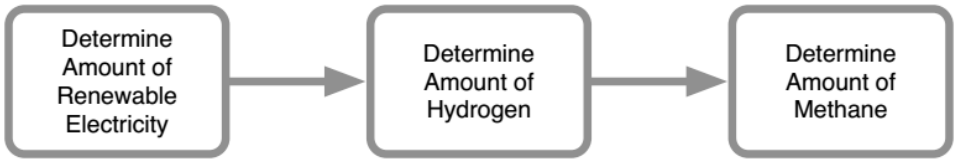

Figure 3.1: The number of kWh of renewable electricity must be determined to ascertain how many Quads of hydrogen are available for methanation, given a fixed electrolyser efficiency. This amount of hydrogen establishes the upper limit of RNG (in Quads) obtainable through methanation.

The total amount of renewable electricity was determined by the actual 2011 generation of renewable electricity in the United States, as reported by the EIA's 2011 Annual Energy Review [4]. The sources of renewable electricity in the EIA's

data are *Conventional Hydropower*, *Geothermal*, *Municipal Waste*, *Wood and Other Biomass*, *Wind*, and *Solar*. As noted previously, the AGF report does not consider municipal waste that is currently being used for energy projects, or electricity generation, as a feedstock for its technical potential of biomass-derived natural gas [3]. It does, however, consider all available wood and other types of biomass [3]. Thus, the electricity generation corresponding to *Wood and Other Biomass* in the EIA data is omitted from the total generation of renewable electricity that would theoretically be available for RNG production through electrolysis and methanation. However, the electricity generation corresponding to *Municipal Waste* in the EIA data [4] is considered to be available for electrolysis. There is no further intersect between the sources of actual renewable electricity generation and the organic feedstocks considered in the AGF report.

Next, we determined how much hydrogen can be produced for every unit of renewable electricity supplied to the electrolysis process. For the purpose of this analysis, the electrolysis reaction is assumed to be complete, and pure water is assumed to be available in abundance. The RNG potential is assumed to be limited by the supply of renewable energy available for electrolysis. The balanced chemical equation of the electrolysis process is:

$$2H_2O + e^- \longrightarrow 2H_2 + O_2$$

The standard enthalpy of formation of water ($\Delta_f H^\circ$) is -285.8 kJ/mol [51]. Thus, 285.8 kJ of energy in the form of electricity is required to dissociate 1 mole of water into its constituent elements at standard conditions. The molar mass of water is 18.0153 g/mol [52]. The energy required to dissociate each gram of water through

electrolysis is obtained by dividing the enthalpy, or heat of formation, by the molar mass. Thus, the energy required for the decomposition of water into its elements is 15.86 kJ/g_{H_2O}.

During the electrolysis process, a single molecule of H_2 is produced for every molecule of water dissociated. Carrying out a mass balance for the electrolysis reaction, and noting that the molar mass of H_2 is 2.0159 g/mol [53], we observe that 8.9366 kg of water need to be dissociated to produce 1 kg of hydrogen. Recalling that 15.86 MJ/kg_{H_2O} of electricity are required to split water into its elements, the electricity required for electrolysis at 100% efficiency, is 141.8 MJ/kg_{H_2}. This value is equal to the higher heating value of hydrogen [54]. Following the same methodology, but assuming 80% efficiency, the electricity required becomes 19.83 MJ/kg_{H_2O}. Thus, 177.3 MJ/kg_{H_2} of electricity are required at an electrolyser efficiency of 80%. This methodology applies generally, but if standard conditions are assumed the energy required to produce 1 kg of hydrogen through electrolysis can be obtained by simply dividing the HHV of hydrogen by the electrolyser efficiency, as is shown in Equation 3.1.

$$\alpha = \frac{e_{H_2}}{\eta_{el}} = \frac{141.8 \frac{MJ}{kg_{H_2}}}{\eta_{el}} \tag{3.1}$$

The variable α represents the electric energy required to produce 1 kg of hydrogen at standard conditions. The variable e_{H_2} stands for the specific energy, or HHV, of hydrogen, while the electrolyser efficiency is denoted by η_{el}. The amount of hydrogen produced per unit of electricity is obtained by inverting the equation above to form Equation 3.2.

$$\frac{1}{\alpha} = \frac{\eta_{el}}{e_{H_2}} = \frac{\eta_{el}}{141.8 \frac{MJ}{kg_{H_2}}} \tag{3.2}$$

Once the hydrogen is produced, it can be combined with carbon dioxide through methanation to produce methane. The methanation process is highly exothermic (ΔH_{600K} = -179 kJ/mol), so unlike electrolysis, no additional energy source is required to drive the reaction [55]. The balanced chemical equation of the methanation process is:

$$CO_2 + 4H_2 \longrightarrow CH_4 + 2H_2O$$

By using the Gibbs free energy minimization method at 1 atm, with the feed gas containing H_2 and CO_2 at a stoichiometric molar ratio of 4:1, the CH_4 yield is optimized at a relatively low temperature (between 200-250°C) [56].

In practice, the reduction of CO_2 to CH_4 is an eight-electron process with significant kinetic limitations [10]. A catalyst is required to achieve the production rates and selectivities necessary in a commercial-scale system [10]. A number of catalysts have been shown to give CH_4 selectivities in the range of 90-100%, at various temperatures, and employing different preparation methods [57–60]. As an example, Rh/γ-Al_2O_3 has been demonstrated as a catalyst for the methanation of CO_2, producing CH_4 at room temperature and atmospheric pressure, with selectivity between 99.9-100%, and without the need for photoexcitation [61]. For the purpose of this analysis, it is assumed that the potential supply of hydrogen can be converted completely, with 100% CH_4 selectivity. Furthermore, the CO_2 feedstock is assumed to be available in abundance.

The molar mass of methane is 16.0425 g/mol [62]. By balancing the mass of the reactants to that of the products in the methanation process, a methane-to-hydrogen mass ratio of 1.990 is obtained. In other words, every kilogram of input hydrogen

yields approximately 1.990 kilograms of methane. The specific energy of methane, assumed to be equal to its HHV, is 55.53 MJ/kg [54]. Multiplying the methane-to-hydrogen mass ratio by the specific energy of methane yields Equation 3.3.

$$\beta = MR \times e_{CH_4} = 1.990 \frac{kg_{CH_4}}{kg_{H_2}} \times 55.53 \frac{MJ}{kg_{CH_4}} = 110.5 \frac{MJ}{kg_{H_2}} \tag{3.3}$$

The variable MR is the methane-to-hydrogen mass ratio, and e_{CH_4} represents the specific energy of methane. The product β is the amount of chemical energy, in the form of RNG, which is produced when 1 kg of H_2 reacts completely with CO_2 through the Sabatier process. Under the given assumptions, the value of β is fixed at 110.5 MJ/kg_{H_2}. Multiplying this quantity by Equation 3.2, or kg of hydrogen produced per unit of electricity, gives the overall efficiency of the combined electrolysis and methanation process. This overall end-to-end system efficiency is given as a function of electrolyser efficiency in Equation 3.4.

$$\eta = \beta \times \frac{1}{\alpha} = \frac{MR \times e_{CH_4} \times \eta_{el}}{e_{H_2}} = \frac{110.5 \frac{MJ}{kg_{H_2}}}{141.8 \frac{MJ}{kg_{H_2}}} \times \eta_{el} = 0.779 \times \eta_{el} \tag{3.4}$$

This equation defines, for a given electrolyser efficiency, the quantity of chemical energy (in the form of RNG) per unit of input electric energy. Note again that this relationship applies given the assumption of standard atmospheric pressure and a temperature of 25°C.

In practice, the reported efficiency of commonly used alkaline electrolysers exceeds 80% (HHV) [63]. An electrolyser efficiency of 80%, which corresponds to an overall efficiency of 62.3%, is used as a reference in calculating the technical potential of RNG through electrolysis and methanation. Under these assumptions, 1 Quad of renewable electricity will yield 0.8 Quads of H_2 through electrolysis, which will

produce a total of 0.623 Quads of CH_4 through methanation. Out of the initial 1 Quad of electricity, 0.2 Quads are lost due to electrolyser inefficiencies, and a further 0.177 Quads are lost as heat during the exothermic methanation process. This specific energy yield and the associated losses are illustrated in Figure 3.2.

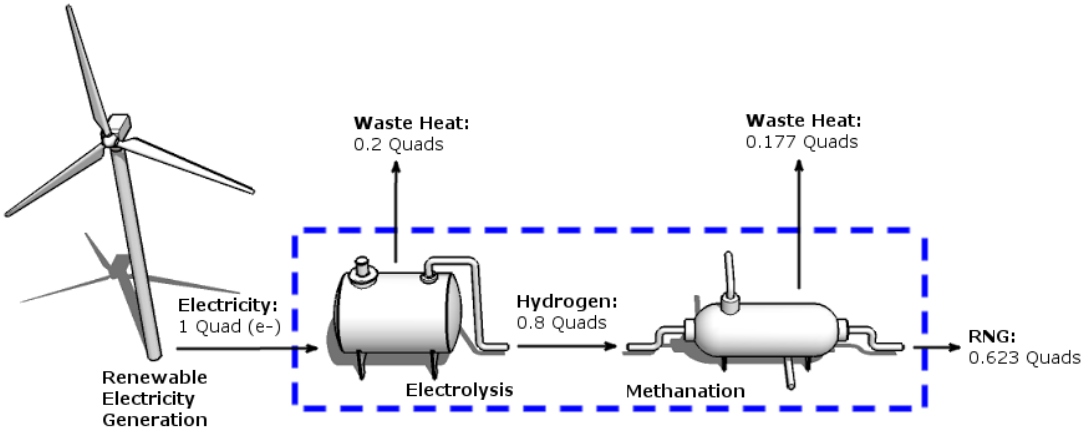

Figure 3.2: The specific energy yield of an RNG production system with an electrolyser efficiency of 80% is 0.623 [$Quad(RNG)/Quad(e^-)$], or 62.3%. Inefficiencies stem primarily from the resistance between the electrodes in the electrolysis chamber, and the heat lost due to the exothermic nature of the methanation process.

Using the overall efficiency, the technical potential of RNG through electrolysis and methanation can be calculated by multiplying the overall efficiency by the total annual generation of renewable electricity in the United States. The data used for this purpose are obtained from the EIA's 2011 Annual Energy Review [4]. Once the 2011 technical potential of methanation-derived RNG has been obtained, it is aggregated with the technical potential of biomass-derived natural gas, as reported by AGF. This sum represents the total technical potential of RNG in the United States, shown in Chapter 4.

This work also considers the feedstocks necessary for the electrolysis and methanation processes, and the secondary outputs of these processes. Water re-

quirements and the carbon dioxide recycling potential are of special interest in this context. As previously derived, 8.9366 kg of water are required to produce 1 kg of hydrogen through electrolysis. Thus, the mass of the water consumption required is discovered by multiplying the mass of the technical potential of hydrogen by a coefficient of 8.9366. The corresponding volume is obtained by assuming a water density of 1 kg/L. This analysis only considers the raw water consumption and not other water needs, such as the cooling water required for the hydrogen generation unit. The carbon dioxide recycling potential is determined by carrying out an analogous mass balance analysis of the methanation process.

To determine the future technical potential of methanation-derived RNG in the United States, the aforementioned steps are applied to EIA's future projections for renewable electricity generation [50], for every year between 2015 and 2040. Three different scenarios are considered: (1) *Constant Efficiency*, (2) *Slow Efficiency Growth*, and (3) *Rapid Efficiency Growth*. The *Constant Efficiency* scenario assumes a constant electrolyser efficiency of 80% until the year 2040. The *Slow Efficiency Growth* scenario assumes a nominal electrolyser efficiency increase of 0.25% every year, until the year 2040. Thus, an electrolyser efficiency of 86.25% is assumed for the year 2040 within this scenario. The *Rapid Efficiency Growth* scenario is analogous to the *Slow Efficiency Growth* scheme, except the yearly efficiency increase equals 0.5% instead of 0.25%. This scenario therefore assumes a steady increase in electrolyser efficiency, until it reaches 92.5% in the year 2040. The incremental efficiency improvements represent potential advances in electrolyser technology over the next 25 years. The actual values of the increments for the *Slow Efficiency Growth* and the *Rapid Efficiency Growth* scenarios were chosen arbitrarily.

3.2 Economic Potential of Methanation-derived RNG in Texas

The first step of establishing the desired maximization framework is to derive the so-called threshold equation. The threshold equation describes the underlying conditions that render the marginal profit from selling renewable electricity directly to the electricity grid, equal to the marginal profit from using the same amount of electricity to produce RNG, and selling it directly to the natural gas grid. This analysis does not consider the capital expenses, or fixed costs, associated with the construction of power generation, electrolysis, or methanation facilities. The following derivations do, however, accommodate for the inclusion of all the operating expenses associated with the production of electricity from wind, and the production of RNG through electrolysis and methanation, assuming that the infrastructure is already in place. Thus, the use of the words 'marginal profit' in this work refers to the operational profit of production, or the difference between the total revenue and the operating expenses associated with RNG production and wind generation. Unless otherwise stated, the use of the word 'profit', by itself, denotes the marginal profit of production rather than the total profit. The derivation of the threshold equation is detailed in Section 3.2.1.

The threshold equation serves as a foundation for a model, written in MATLAB, that illustrates the practical application of the decision-making framework. The code structure is explained, along with any necessary deviations from the threshold equation, in Section 3.2.2.

Finally, the methodology for establishing the financial hedging potential of each scenario is considered in Section 3.2.3.

3.2.1 Economic Threshold of RNG Production through Electrolysis and Methanation

The function of the threshold equation is to determine, given a supply of renewable electricity, whether it is beneficial to sell the electricity directly, or use it to produce RNG. The first step of the derivation is to define the economic transition threshold, or in other words, the condition for which the marginal economic benefit of selling electricity is equal to that of producing and selling RNG. This relationship is then expanded to reflect the dependence of the result on the price of electricity, the price of natural gas, electrolyser efficiency, and the operating expenses associated with the energy conversion processes. Unless otherwise stated, the analysis and modeling in this work assumes integrated wind generation and RNG production facilities. In this case, the price of electricity required for the electrolysis process is not included in the total operating expenses associated with the RNG production process. The operating expenses associated with wind power generation, however, are considered as expenditures. The marginal profit of an integrated wind and methanation facility is shown as a control volume in Figure 3.3, and the derivation of the associated threshold equation is shown in Section 3.2.1.1. By contrast to integrated RNG production facilities, it is assumed that non-integrated facilities must pay at least the wholesale price for the electricity required for the electrolysis process, as shown in Figure 3.4. Furthermore, non-integrated facilities do not include the marginal cost of wind production in their operating expenses. The derivation of the economic threshold equation for non-integrated facilities is shown in Section 3.2.1.2.

3.2.1.1 Economic Threshold Equation for Integrated Facilities

At the economic transition threshold for integrated facilities, the marginal profit from selling a MWh of renewable electricity, π_e, is equal to the marginal profit

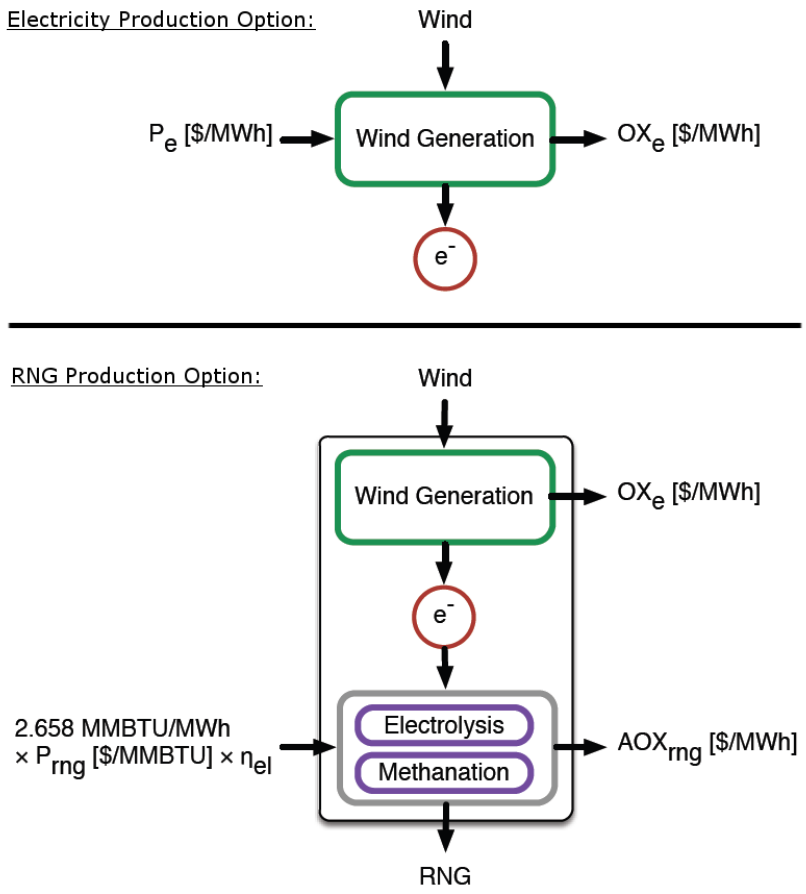

Figure 3.3: An integrated methanation facility has two production options: 1) Producing and selling electricity directly to the grid (top), or 2) using that same amount of electricity to produce RNG (bottom). This illustration shows the flow of energy through the facility from top to bottom (for both production options), and the flow of money from left to right, with the revenue stream on the left-hand side, and the operating expenses on the right-hand side. When electricity is sold directly to the grid, the marginal profit is equal to the price of electricity, P_e, minus the operating expenses associated with wind power generation, OX_e. When RNG is produced and sold, the marginal profit is equal to the revenue from selling RNG, or $2.658\,MMBTU/MWh \times P_{rng} \times \eta_{el}$, minus the wind power operating expenses, OX_e, and the operating expenses associated with the electrolysis and methanation processes, AOX_{rng}. Note that the variable AOX_{rng} does not include the price of the electricity required for the electrolysis process, due to the integration of facilities. The derivation of the threshold equation associated with this scenario is detailed in Section 3.2.1.1. Illustration courtesy of Jeffrey Phillips.

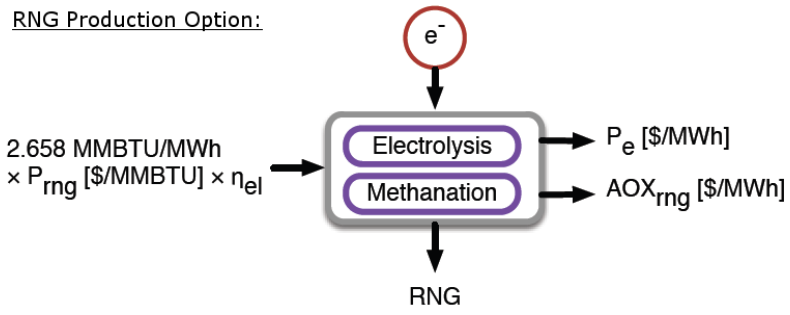

Figure 3.4: A non-integrated methanation facility has the option of producing and selling RNG, with the option of ceasing RNG production as the only alternative. The marginal profit of a non-integrated facility equals the revenue from selling RNG, or $2.658 MMBTU/MWh \times P_{rng} \times \eta_{el}$*, minus the cost of electricity required for electrolysis process,* P_e*, and any additional operating expenses associated with the electrolysis and methanation processes,* AOX_{rng}*. Note that a non-integrated facility will be wholly unconcerned with the operating expenses associated with wind power generation,* OX_e*. The derivation of the threshold equation associated with this scenario is detailed in Section 3.2.1.2. Illustration courtesy of Jeffrey Phillips.*

from selling the amount of RNG that can be produced using the same amount of electricity, π_{rng}:

$$\pi_e \left[\frac{\$}{MWh}\right] = \pi_{rng} \left[\frac{\$}{MWh}\right] \tag{3.5}$$

Note that when the left-hand side of Equation 3.5 is greater than the right-hand side, or $\pi_e > \pi_{rng}$, it is economically preferable to sell the renewable electricity directly to the electric grid. However, when the opposite is true, or $\pi_{rng} < \pi_e$, it is economically preferable to use the electricity to produce RNG that will then be sold directly to the gas grid. Throughout this section, and unless otherwise stated, the left-hand side (LHS) of the threshold equation denotes the marginal profit of the electricity production option, while the right-hand side (RHS) denotes the marginal profit of the RNG production option. As stated previously, the capital costs associated with

the power generation and industrial processes discussed herein, are not considered in this analysis.

The threshold equation, or Equation 3.5, can be rewritten to show both the revenue stream and the operating expenses associated with each production option. The marginal profit of the electricity production option (LHS of Equation 3.5) equals the selling price of electricity, P_e, minus the operating expenses associated with the generation of renewable electricity from wind, OX_e. The marginal profit of the electricity production option is shown in Equation 3.6.

$$\pi_e \left[\frac{\$}{MWh}\right] = P_e \left[\frac{\$}{MWh}\right] - OX_e \left[\frac{\$}{MWh}\right] \tag{3.6}$$

The marginal profit of the RNG production option (RHS of Equation 3.5) equals the selling price of natural gas, PR_{ng}, minus the operating expenses associated with production of RNG through electrolysis and methanation, OX_{rng}, and the operating expenses associated with the generation of renewable electricity, OX_e. The marginal profit of the RNG production option is shown in Equation 3.7.

$$\pi_{rng} \left[\frac{\$}{MWh}\right] = PR_{ng} \left[\frac{\$}{MWh}\right] - OX_{rng} \left[\frac{\$}{MWh}\right] - OX_e \left[\frac{\$}{MWh}\right] \tag{3.7}$$

Substituting Equations 3.6 and 3.7 into Equation 3.5, we obtain:

$$P_e \left[\frac{\$}{MWh}\right] - OX_e \left[\frac{\$}{MWh}\right] = PR_{ng} \left[\frac{\$}{MWh}\right] - OX_{rng} \left[\frac{\$}{MWh}\right] - OX_e \left[\frac{\$}{MWh}\right] \tag{3.8}$$

The OX_e terms on both sides of Equation 3.5 are algebraically redundant. This is intuitive, since the operating expenses associated with the generation of renewable electricity do not affect the economic feasibility of each production option relative to the other. However, the terms are included in Equation 3.5 so that each side of the equation can still be interpreted as the marginal profit of its respective production option. Note that the variable OX_e is given in dollars per MWh of electricity produced, while OX_{rng} is given in terms of the dollars required to convert a single MWh of electricity to RNG. The operating expenses associated with each of the energy conversion processes are addressed in more detail later in this section.

The selling price of natural gas, PR_{ng}, in Equation 3.8, is given in terms of dollars per MWh of electricity required for the production thereof. To align the threshold equation with US pricing conventions for natural gas (dollars per MMBTU), a new natural gas selling price variable, P_{ng}, is introduced. This variable is multiplied by a conversion constant of 3.412 MMBTU/MWh, as well as an efficiency variable, η. Thus, Equation 3.8 becomes:

$$P_e\left[\frac{\$}{MWh}\right] - OX_e\left[\frac{\$}{MWh}\right] = P_{ng}\left[\frac{\$}{MMBTU}\right] \times 3.412\frac{MMBTU}{MWh} \times \eta - OX_{rng}\left[\frac{\$}{MWh}\right] - OX_e\left[\frac{\$}{MWh}\right] \quad (3.9)$$

The efficiency variable, η, in Equation 3.9 was defined as a linear function of the electrolyser efficiency in Equation 3.4 in Section 3.1. A simplified version of Equation 3.4 is given here as Equation 3.10:

$$\eta = 0.779 \times \eta_{el} \quad (3.10)$$

The coefficient in Equation 3.10 stems from the exothermic nature of the methanation process. In a complete reaction, the energy content of RNG produced through methanation equals 77.9% of the energy content of the hydrogen input. The remaining 22.1% are lost as heat during the methanation process. Substituting Equation 3.10 into Equation 3.9, the threshold equation becomes:

$$P_e \left[\frac{\$}{MWh}\right] - OX_e \left[\frac{\$}{MWh}\right] = P_{ng} \left[\frac{\$}{MMBTU}\right] \times 2.658 \, \frac{MMBTU}{MWh} \times \eta_{el} - OX_{rng} \left[\frac{\$}{MWh}\right] - OX_e \left[\frac{\$}{MWh}\right] \quad (3.11)$$

In general, the operating expenses of running the electrolysis process are assumed to be at least equal to the price of electricity utilized, P_e. Any additional operating expenses associated with either the electrolysis process or the methanation are summed up in the variable AOX_{rng}, which has the same units as the variable OX_{rng}. As previously stated, however, it is assumed that integrated methanation facilities do not pay directly for the electricity used in the electrolysis process. Thus, we can write:

$$OX_{rng} \left[\frac{\$}{MWh}\right] = AOX_{rng} \left[\frac{\$}{MWh}\right] \quad (3.12)$$

The variable AOX_{rng} is used in lieu of OX_{rng} to maintain consistency with the derivation of the threshold equation for non-integrated facilities, as detailed in Section 3.2.1.2. Substituting Equation 3.12 into the threshold equation, we obtain:

$$P_e \left[\frac{\$}{MWh}\right] - OX_e \left[\frac{\$}{MWh}\right] = P_{ng} \left[\frac{\$}{MMBTU}\right] \times 2.658 \, \frac{MMBTU}{MWh} \times \eta_{el} - AOX_{rng} \left[\frac{\$}{MWh}\right] - OX_e \left[\frac{\$}{MWh}\right] \quad (3.13)$$

Equation 3.13 describes the economic transition threshold as a function of the price of electricity, the price of natural gas, electrolyser efficiency, and the operating expenses associated with the energy conversion processes. Recall that if the LHS of Equation 3.13 is greater than the RHS, it is economically preferable to sell the available electricity directly instead of using it to produce RNG. The reverse is true when the RHS is greater than the LHS.

Up to this point, no major assumptions have been made about the operating expenses of the different production options. Unless otherwise stated, however, the following analysis assumes a 'best case scenario', where the operating expenses of the two production processes are limited to their respective fuel costs. Thus, the value of the variable OX_e is \$0/MWh, as the wind used for electricity production is free. Similarly, the price of the electricity required for the electrolysis process is a nonfactor due to the integration of production facilities, and the value of the variable AOX_{rng} is \$0/MWh. Thus, Equation 3.13 becomes:

$$P_e = 2.658 \frac{MMBTU}{MWh} \times P_{ng} \times \eta_{el} \quad (3.14)$$

A decision-making representation of the threshold equation is obtained by dividing Equation 3.14 by the LHS of itself, and substituting the number 1 on the LHS with the dimensionless variable ν. Carrying out this manipulation, we obtain the following:

$$\nu = 2.658 \frac{MMBTU}{MWh} \times \eta_{el} \times \frac{P_{ng}}{P_e} \tag{3.15}$$

If $\nu > 1$, producing and selling RNG is economically preferable, but if $\nu < 1$, selling electricity directly to the grid is the economically preferred decision. If $\nu = 1$, both options yield an equal marginal profit.

The marginal profit of an integrated facility for a given time period is either the marginal profit from selling electricity, or the marginal profit from producing and selling RNG, depending on which value is higher. Thus, we can write the marginal profit, MP [$/MWh], as:

$$MP = \begin{cases} P_e, & \text{if } P_e \geq 2.658 \ \frac{MMBTU}{MWh} \times P_{ng} \times \eta_{el} \\ 2.658 \ \frac{MMBTU}{MWh} \times P_{ng} \times \eta_{el}, & \text{otherwise} \end{cases} \tag{3.16}$$

Note that Equation 3.16 is derived directly from Equation 3.14, which denotes a scenario where any operating expenses are considered to be negligible. A more general marginal profit equation can be derived in a similar way from Equation 3.13.

3.2.1.2 Economic Threshold Equation for Non-Integrated Facilities

At the economic transition threshold for non-integrated facilities, the marginal profit from producing and selling RNG is $0/MWh. Thus, the economic transition threshold is defined as:

$$\pi_{rng} \left[\frac{\$}{MWh} \right] = 0 \ \frac{\$}{MWh} \tag{3.17}$$

Note that the marginal profit of the RNG production option is on the LHS of Equation 3.17, and not the RHS as before. If the LHS of the equation is greater than 0,

producing and selling RNG is marginally profitable. Otherwise, no RNG production takes place. The derivation of the threshold equation for non-integrated facilities is analogous to the derivation for integrated facilities, discussed in the previous section. Thus, we can write:

$$2.658\ \frac{MMBTU}{MWh} \times P_{ng} \left[\frac{\$}{MMBTU}\right] \times \eta_{el} - OX_{rng}\ \left[\frac{\$}{MWh}\right] = 0\ \frac{\$}{MWh} \tag{3.18}$$

The LHS of Equation 3.18 is identical to the RHS of Equation 3.11, except the OX_e term is missing. This omission stems from the fact that the non-integrated methanation facilities would be unconcerned with the operating expenses of the wind farms from whence they obtain their electricity. Conversely, the operating expenses of the non-integrated methanation facilities are assumed to be at least equal to the price of electricity required for the electrolysis process. Thus, OX_{rng} becomes:

$$OX_{rng}\ \left[\frac{\$}{MWh}\right] = P_e\ \left[\frac{\$}{MWh}\right] + AOX_{rng}\ \left[\frac{\$}{MWh}\right] \tag{3.19}$$

The variables P_e and AOX_{rng} are defined in the same way as before. Substituting Equation 3.19 into Equation 3.18, we obtain:

$$2.658\ \frac{MMBTU}{MWh} \times P_{ng} \left[\frac{\$}{MMBTU}\right] \times \eta_{el} - P_e\ \left[\frac{\$}{MWh}\right] - AOX_{rng}\ \left[\frac{\$}{MWh}\right] = 0\ \frac{\$}{MWh} \tag{3.20}$$

Equation 3.20 is algebraically equivalent to Equation 3.13. Thus, assuming that wind power is generated regardless of wholesale electricity prices, the decision to produce and sell RNG is the same, regardless of whether the methanation facilities are integrated with wind power generation facilities or not.

As in the previous section, the operating expenses of the RNG production process are limited to the fuel costs required for the production of hydrogen. These fuel costs correspond to the cost of electricity required for electrolysis process, which is implicitly defined in Equation 3.20. As before, the value of AOX_{rng} is assumed to be \$0/MWh. Thus, Equation 3.20 can be rewritten as:

$$2.658\ \frac{MMBTU}{MWh} \times P_{ng}\left[\frac{\$}{MMBTU}\right] \times \eta_{el} - P_e\ \left[\frac{\$}{MWh}\right] = 0\ \frac{\$}{MWh} \tag{3.21}$$

The marginal profit of a non-integrated facility for a given time period is equal to the marginal profit from producing and selling RNG, if RNG is produced, or \$0/MWh otherwise. Thus, we can write the marginal profit, MP [\$/MWh], as:

$$MP = \begin{cases} 2.658\ \frac{MMBTU}{MWh} \times P_{ng} \times \eta_{el} - P_e, & \text{if } 2.658\ \frac{MMBTU}{MWh} \times P_{ng} \times \eta_{el} - P_e > 0\ \frac{\$}{MWh} \\ 0\ \frac{\$}{MWh}, & \text{otherwise} \end{cases} \tag{3.22}$$

Equation 3.22 is derived directly from Equation 3.21. As before, a more general equation can be derived by choosing an earlier version of the threshold equation, such as Equation 3.20, as the foundation for the marginal profit equation.

3.2.2 Modeling the Threshold Equation

This section considers three separate cases for modeling the threshold equation: A base case scenario, a high gas-price scenario, and a curtailment option scenario. The nature of these scenarios, along with the nuances of the model code associated therewith, are detailed in Sections 3.2.2.1, 3.2.2.2, and 3.2.2.3, respectively. The model described in these sections corresponds to integrated wind and methanation

facilities. Section 3.2.2.4 addresses the major differences between modeling a non-integrated methanation facility and an integrated one.

A decision model was written for integrated facilities, primarily based on Equation 3.13, and by extension, Equation 3.16, in the previous section. The model, which was written in MATLAB, accepts two price vectors as inputs, one of which corresponds to the variable P_e, or the price of electricity, and the other corresponds to the price of natural gas, P_{ng}. These vectors store the historical prices of both natural gas and electricity for every 15 minute time interval over the course of a single year. The model steps through each of these time intervals, comparing the potential marginal profit from selling electricity to that of selling RNG, and storing the value and index of the more profitable option in each case. By default, the model gathers the aforementioned data for 6 different electrolyser efficiency scenarios, corresponding to the variable η_{el}, ranging from 50% to 100% at increments of 10%. The model also gathers data for different values of the variable AOX_{rng}, ranging from \$0/MWh to \$100/MWh at increments of \$5/MWh. This setup yields data for 126 possible operating expense/efficiency permutations for 35,040 time steps, constituting a single year, each instance the model is executed.

The 'best case scenario' analysed in this work is represented by one of the aforementioned modeling permutations, where the electrolyser efficiency is set at 80.0%, continuing the efficiency assumptions from Section 3.1. This electrolyser efficiency corresponds to an overall end-to-end system efficiency of 62.3%. Similarly, the 'best case scenario' operating expenses associated with the production of RNG are limited to the price paid for the electricity required for the electrolysis process. These expenses are captured in the variable P_e on the LHS of Equation 3.21, for non-integrated facilities. As previously discussed, this electricity cost is a nonfactor for integrated

facilities. Additional operating expenses are assumed to be negligible, and thus, the value of AOX_{rng} is assumed to be \$0/MWh throughout the bulk of this analysis, and the value of OX_e is \$0/MWh throughout. In other words, the water required for the electrolysis, the carbon dioxide required for the methanation, and other necessary feedstocks (other than the renewable electricity) are assumed to be freely and abundantly available on location. Similarly, the maintenance cost associated with keeping the wind turbines up and running is assumed to be negligible. Section 3.2.3 is an exception, as it includes an analysis of the total marginal profit of each scenario, as a function of additional operating expenses (AOX_{rng}). This particular analysis still assumes a negligible wind turbine operating cost.

At its core, each of the three scenarios discussed later in this section function as described in the previous paragraph. The particular section of code that carries out the comparison of potential profits is shown in Figure 3.5. The complete code of the MATLAB model corresponding to the *Curtailment Option Scenario*, which is detailed in Section 3.2.2.2, is included in Appendix A.

The threshold equation gives the option of either consuming electricity to produce and sell RNG, or selling electricity directly to the grid. In reality, the option of ceasing production of renewable electricity also exists, as production curtailment is not an uncommon option. Thus, in its basic format, the 'compmatrix' array contains three vectors. These vectors correspond to the options of selling electricity directly, producing and selling RNG, and ceasing electricity production. The actual profit values are based on Equation 3.16, with slight variations to accommodate for the option of ceasing electricity production. The threshold for ceasing electricity production is determined by the PTC for wind. The PTC is assumed to be \$23/MWh, which is equivalent to about \$35/MWh in pre-tax income [64]. In other words, the

```
for k = 1:length(erev)
%Loops through all the time periods
    maxval = compmatrix(1,k);
    index = 1;
    for m = 2:length(compmatrix(:,1))
    %Loops through all the consumption options
        if compmatrix(m,k) > maxval
        %Finds the maximum profit value, and its index
            index = m;
            maxval = compmatrix(m,k);
        end
    end
    ...
end
```

Figure 3.5: The 'compmatrix' array consists of 3 or 4 vectors, which store the potential marginal profit of their corresponding production option for every 15 minute interval of the year. This segment of code steps through all the time periods, compares the marginal profit of each potential option, and stores the highest values along with their index.

wind power projects included in this analysis are assumed to be revenue-positive if the power market prices are higher than -$35/MWh. These PTCs are not included in the derivation of the threshold equation in Sections 3.2.1.1 and 3.2.1.2. However, the MATLAB model considers PTCs as a revenue stream, and a component of the total marginal profit, across all modeling scenarios. It is assumed that PTCs are awarded for every MWh of renewable electricity generated, and not simply the portion that is sold directly to the electric grid. Chapter 4 includes a brief analysis of the difference between maximizing the marginal profit of given modeling scenario that considers PTCs, and one that doesn't.

Once the preferred option for each time period has been determined, the marginal profit value per MWh can be multiplied by the production capacity, which yields the total marginal profit for each 15 minute interval. In the MATLAB model, this multiplication actually takes place prior to the comparison conducted in Fig-

ure 3.5. Both methods yield the same results in terms of the model output. The definition of the production capacity varies slightly by scenario, as is explained in the following subsections.

As the model steps through each time period, the following data points are gathered: The index of the option yielding the highest marginal profit, the corresponding marginal profit value, the amount of electricity and RNG produced and sold, and the total marginal profit from selling electricity and RNG respectively. The model also gathers information on how much of the production capacity goes unutilized, given the stated assumptions. In addition to the previously stated assumptions, it is assumed that choosing one option over the other does not affect the market prices of natural gas or electricity. It is also assumed that each production decision can be implemented instantaneously, which will be unlikely in practice.

The primary focus of this analysis is to establish how much RNG would have been produced during the year 2011 if methanation facilities had been in place, and the most economically profitable production option had been chosen for every 15 minute period of the year. Thus, the total amount of electricity directed towards the production of RNG is aggregated for each of the three modeling scenarios, and then multiplied by the overall conversion efficiency to give the total energy value of the output RNG. These findings are summarized in Chapter 4. Other model results, such as the predominant RNG production times, are also highlighted as appropriate.

3.2.2.1 Base Case Scenario

The *Base Case Scenario* is based on the Henry Hub natural gas spot prices [65], and the West Texas Hub Real-Time Market (RTM) electricity prices [66] for the year 2011, as reported by the US Energy Information Administration (EIA) and ERCOT, respectively. The year 2011 was chosen for modeling due to the availability

of consistently reported power output data, as well as production curtailment data, which serve as the foundation for the comparison between the *Base Case Scenario* and the following two scenarios. This production curtailment data set is explained in the *Curtailment Option Scenario* section.

The availability of high quality data makes the year 2011 a good candidate for modeling the *Base Case Scenario*. In addition, it should also be noted that it was an unusual year for Texas in terms of electricity prices. Rolling blackouts throughout the state caused a temporary price spike in February 2011 [67], and the average price of electricity over the summer months was unusually high as a result of extended periods of hot weather [68]. Meanwhile, negative electricity prices were quite common, as previously discussed, especially during the months of spring and autumn. By contrast, the average Henry Hub natural gas spot price has remained relatively low and stable since 2009, when it dropped to \$3.94/MMBTU, from \$8.86/MMBTU the previous year [44]. In 2011, the average Henry Hub gas price was \$4.00/MMBTU [44]. Thus, the *Base Case Scenario* essentially represents a 'high electricity price, low gas price' scenario, that provides a conservative estimate for the economic potential of methanation-derived RNG in Texas.

The electricity prices in the ERCOT data set are reported on a 15 minute basis. The natural gas prices, however, are only reported on a daily basis. To ensure that the two data sets are comparable, and for the model to accurately reflect the rapid fluctuations of electricity prices in West Texas, the natural gas price data set is divided into 15 minute intervals as well. It is assumed that the price is constant over the course of each day. In the case of missing data points for either data set, the price reported for the previous time interval applies. Unless explicitly stated, the aforementioned methods also apply to the *High Gas Price Scenario* and the

Curtailment Option Scenario.

The generation capacity of the *Base Case Scenario* is determined by the aggregated wind plant power output data for the year 2011, as reported in the ERCOT monthly wind power forecast (WFP) report [69]. The power output data in the WFP report are given on an hourly basis, but as before, each hour is divided into four 15 minute intervals, during which the power output value is assumed to be constant. As before, missing data points assume the output values of the previous time interval.

3.2.2.2 Curtailment Option Scenario

In addition to the actual power output of ERCOT wind resources, the WFP report also publishes the High Sustained Limit (HSL) for Texas wind. In this context, HSL is the upper limit established by the Qualified Scheduling Entity (QSE) for the sustained electricity production capability of ERCOT wind plants [70]. In many cases there is a difference between the actual production output and this listed capacity, with the actual output most often being slightly lower than the HSL. This discrepancy stems from the constraints associated with transmitting electricity from its production sites in West Texas to consumers across the state. When the grid is highly congested, ERCOT has historically curtailed the production of electricity temporarily to alleviate some of the stress. This behavior is reflected in the 2011 WFP data. The *Curtailment Option Scenario* adds the option of utilizing curtailed capacity to produce RNG, as the potential production of RNG would not be affected by electric grid transmission constraints, assuming the co-location of wind and methanation plants.

The HSL, like the actual power output, is reported on an hourly basis. Fundamentally, the two data sets are curated in the same way to ensure consistency and comparability. Referring back to Figure 3.5, the *Curtailment Option Scenario* introduces a fourth vector, corresponding to a fourth production option, to the 'comp-

matrix' array. This option is essentially the same as the option of selling electricity directly to the electric grid, in the *Base Case Scenario*. However, the marginal profit from selling electricity is supplemented by the marginal profit (or loss) associated with the use of curtailed capacity to produce RNG. Furthermore, the vector corresponding to the option of producing and selling RNG is also updated within this scenario. Instead of multiplying the overall efficiency by the power output values, the HSL values are used. The HSL values are chosen, again, due to the fact that the potential production of RNG is independent of any constraints on the electric grid. It is assumed that when the actual power output is greater than the HSL, the production capacity is equal to the power output, and not the HSL. The resource utilization options of the *Curtailment Option Scenario* are contrasted against those of the *Base Case Scenario* in Figure 3.6.

While determining the technical potential of methanation-derived RNG for Texas was not a primary objective of this work, the introduction of the HSL allows for an accurate estimation thereof. The HSL vector, when multiplied by the time it spans, yields the maximum electric generation capacity for each hour of that time period. By summing up the components of the resulting vector, the total generation capacity of that time period is obtained. This generation capacity can then be used to determine the technical potential of methanation-derived RNG in Texas, using the methodology described in Section 3.1.

3.2.2.3 High Gas Price Scenario

The *High Gas Price Scenario* is analogous to the *Curtailment Option Scenario*, with only one modification: Instead of using Henry Hub gas prices from 2011, the gas prices from 2008 are used. The average price of natural gas in 2008 was more than 2.2 times higher than in 2011 [44]. Thus, a theoretical 'high electricity price, high gas

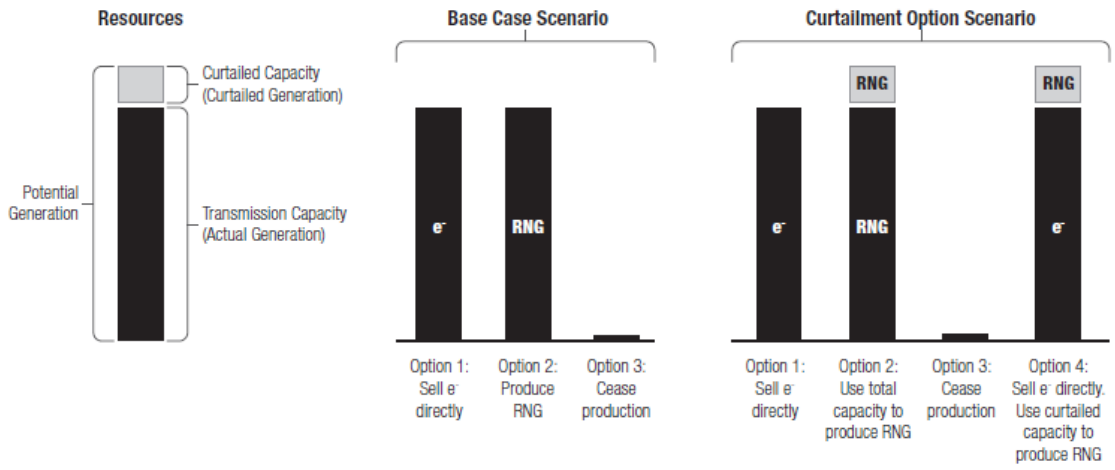

Figure 3.6: The production capacity of the Base Case Scenario is limited by the electric grid's transmission capacity. By contrast, the production capacity of the Curtailment Option Scenario is limited by the total potential generation capacity, or HSL. However, the additional curtailed capacity can only be used to produce RNG. Thus, Option 2 is expanded within Curtailment Option Scenario to include the increased RNG production capacity, and Option 4 is introduced as the option of selling electricity directly to the grid, while using curtailed production capacity to produce and sell RNG. Option 1 and Option 3 remain unchanged between scenarios. Illustration courtesy of Jeffrey Phillips.

price' scenario is established by using the Henry Hub gas prices from 2008 alongside the ERCOT production and electricity price data from 2011. This scenario is more reasonable than a 'low electrcity price, high gas price' scenario, as Texas' dependence on natural gas for electric generation results in a positive correlation between the price of natural gas and the price of electricity [71]. By comparison to the previous two scenarios, however, the *High Gas Price Scenario* yields a more optimistic estimate for the economic potential of methanation-derived RNG in Texas.

3.2.2.4 Difference between Modeling Integrated and Non-Integrated Methanation Facilities

As explained in Section 3.2.1.2, the decision to produce and sell RNG is the same for integrated and non-integrated methanation facilities, assuming that wind power is generated regardless of prevailing wholesale electricity prices. This assumption does not hold, however, when PTCs are counted towards the total marginal profit of integrated facilities. The effects of PTCs are addressed briefly in this section, along with significant variations between the two types of models, and other important considerations.

Integrated production facilities will benefit from utilizing wind power for RNG production in at least a couple of ways that non-integrated facilities will not. First of all, having a secondary revenue stream hedges against fluctuating and negative electricity prices, as well as variable demand. Furthermore, assuming that PTCs are dependent upon the actual production of wind power, and not the amount of electricity sold to the grid, integrated facilities can claim the PTCs associated with wind production without selling electricity to the grid at a diminishing marginal profit. As previously stated, the MATLAB model for integrated facilities considers PTCs as a revenue stream and a component of the total marginal profit. By contrast, non-integrated methanation facilities do not generate any renewable electricity, and as a result, can not claim any PTCs. Thus, the MATLAB model for non-integrated facilities does not include PTCs in the marginal profit calculations.

A fundamental assumption associated with both types of models is that of marginal profitability. It is assumed that each facility will seek to make the most economically preferable decision for every given time period. Furthermore, unless a facility is marginally profitable, it will cease production. This assumption applies to both wind generation and RNG production, as integrated facilities, and as

separate, non-integrated facilities. Thus, when the marginal profit from wind production (including a PTC of $35/MWh) goes below $0/MWh, wind production for non-integrated facilities ceases. As a result, no RNG production can take place, regardless of the potential marginal profit of the methanation facility. This requirement does not apply in the case of the integrated facilities. In other words, wind production will take place within an integrated facility as long as the marginal profit of either electricity or RNG production (including PTCs) exceeds $0/MWh. This condition was implemented with a simple if-sentence in the non-integrated version of the MATLAB model.

Another significant difference stems from the way curtailed capacity is utilized by integrated facilities relative to non-integrated ones. Integrated facilities will use curtailed wind capacity to produce RNG as long as the production is marginally profitable, regardless of how high the wholesale price of electricity is. By contrast, co-located, yet non-integrated methanation facilities will only utilize the full production capacity when the wholesale price of electricity is low relative to the wholesale price of natural gas. Referring back to Figure 3.6, non-integrated facilities will never exclusively use curtailed capacity for RNG production, while allowing the rest of the potential production capacity to go unused, because the entire production capacity hinges on favorable electricity prices. Thus, option 4 in Figure 3.6 was effectively removed from the non-integrated version of the MATLAB model. The rest of the model was also modified to more accurately reflect the profit-comparison of non-integrated methanation facilities. The vectors composing the 'compmatrix' array in Figure 3.5 were modified to reflect Equation 3.22 rather than Equation 3.16, and Option 1 from Figure 3.6 was removed altogether, since non-integrated facilities are not immediately concerned with the marginal profit of their vendors.

3.2.3 Hedging Potential

The annual marginal profit of each scenario is stored as a variable within the MATLAB model. This variable equals the sum of the highest marginal profit values for each of the 15 minute intervals of the modeling period. The hedging potential of a given scenario is defined as the difference between the total marginal profit of that scenario, and the marginal profit of a production scenario that offers no RNG production option.

The total marginal profit is a function of the additional operating expenses, AOX_{rng}, associated with the RNG production process. These additional expenses, such as potential water and CO_2 costs, salaries, and maintenance, should be included in the AOX_{rng} variable when modeling a real-life production scenario. The AOX_{rng} variable, however, does not include operating expenses purely associated with the generation of wind power, which are still assumed to be \$0/MWh. While determining reasonable AOX_{rng} values is outside the scope of this work, plotting the hedging potential of each scenario as a function of AOX_{rng} illustrates the rate at which the marginal profit decreases with increasing operating expenses, and shows the potential increase in marginal profit if the RNG production option did exist. The hedging potential is plotted using model output for integrated facilities, with and without including the contribution of wind PTCs. For further comparison, the marginal profit of a non-integrated methanation facility is also plotted. These results are shown in Chapter 4.

Chapter 4

Results

The results from this analysis are divided into two sections. Section 4.1 presents the results relating to the technical potential of RNG in the United States, while Section 4.2 presents the results of the economic analysis, specific to Texas. The latter includes an analysis of the economic threshold equation, modeling results, and the results of the hedging potential analysis.

4.1 Technical Potential

The overall efficiency of RNG production through electrolysis and methanation, as a function of electrolyser efficiency, is given in Equation 4.1:

$$\eta = 0.779 \times \eta_{el} \tag{4.1}$$

The production process is thus has a maximum overall efficiency of 77.9%, even if an electrolyser efficiency of 100% could be achieved. Figure 4.1 shows the linear relationship between the overall efficiency and the electrolyser efficiency, for electrolyser efficiencies in the range of 50-100%.

The total US generation of renewable electricity in 2011 was 520.1 billion kWh, with 36.9 billion kWh from wood and other biomass [4]. Thus, the total amount of electricity available for electrolysis is 483.2 billion kWh. At an overall conversion efficiency of 62.3%, the technical potential of RNG through methanation in the United

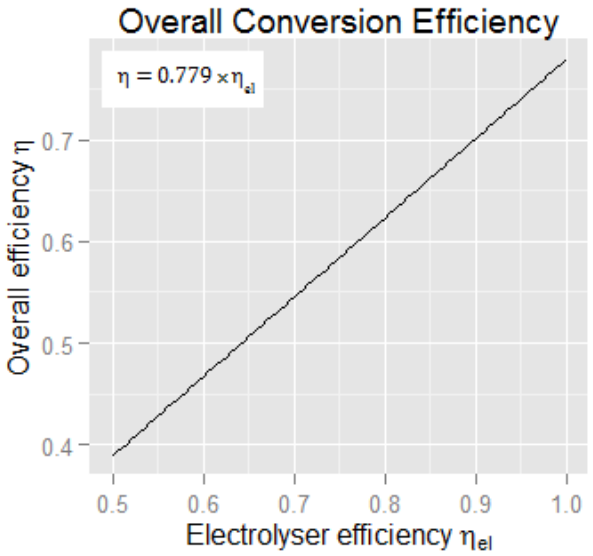

Figure 4.1: The overall conversion efficiency of the production process is a linear function of the electrolyser efficiency.

States is equal to 1.03 quadrillion BTU/year. This represents 4.2% of the total US consumption of natural gas in 2011 (24.37 quadrillion BTU) [72]. At 1,000 BTU/cf, the technical potential of RNG through methanation equals 1.03 trillion cf, or slightly less than the total annual consumption of natural gas in the state of New York (1.20 trillion cf) [73].

The water consumption required to produce 1.03 Quads of RNG annually through electrolysis and methanation is 23.2 billion gallons/year. However, the amount of water produced through methanation equals up to half of the initial water consumption required for the electrolysis process, or 11.6 billion gallons/year. Furthermore, 53.6 million metric tons of carbon dioxide would be recycled in the technical potential production scenario. Finally, 77.9 million metric tons of oxygen would be produced through electrolysis. This byproduct of the electrolysis process could be used for the combustion of RNG in traditional natural gas power plants, thus re-

ducing NOx emissions as described in Section 2.3. The flow of energy and materials corresponding to the US technical potential of methanation-derived RNG is detailed in Figure 4.2.

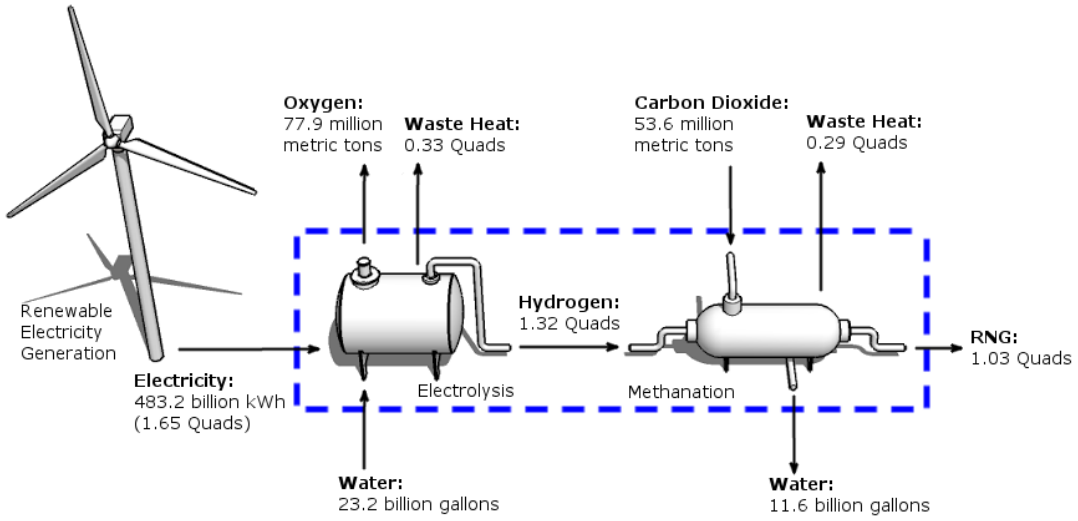

Figure 4.2: The total technical potential of methanation-derived RNG in the United States is 1.03 Quads. Producing 1.03 Quads of RNG would require a consumption of at least 23.2 billion gallons of water for the electrolysis process, up to half of which could be recovered as a byproduct of the methanation process. The CO_2 recycling potential corresponding to the technical potential is 53.6 million metric tons, and up to 77.9 million metric tons of oxygen could be produced through the electrolysis process.

The 2011 US technical potential of RNG from biomass is 9.5 quadrillion BTU/year [3]. Thus, the total combined technical potential of RNG is 10.5 quadrillion BTU/year, or 43.1% of the total consumption of natural gas in the United States [72]. A detailed overview of the annual energy flow, feedstock inputs, and material outputs considered in this work is shown in Figure 4.3. The data points corresponding to the biomass pathways in Figure 4.3 are based on the assumptions and results of the AGF report [3].

The technical potential of methanation-derived RNG until the year 2040 was

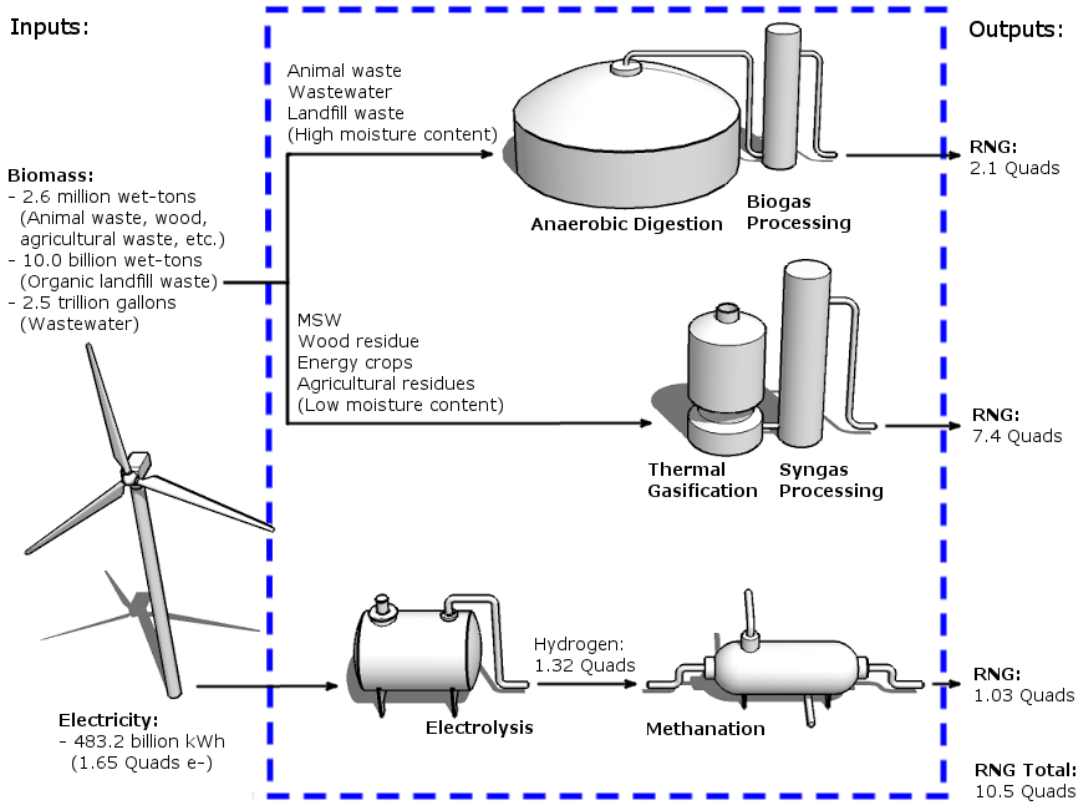

Figure 4.3: The total technical potential of RNG in the United States is 10.5 Quads, with 9.5 Quads corresponding to the biomass pathways, and 1.03 Quads corresponding to the electric pathway.

determined based on EIA's renewable electricity generation projections. Assuming a constant electrolyser efficiency of 80%, the 2040 technical potential of methanation-derived RNG will be 1.54 Quads. Assuming a yearly electrolyser efficiency increase of 0.25% (*Slow Growth*), the 2040 technical potential will be 1.66 Quads. Assuming a yearly electrolyser efficiency increase of 0.5% (*Rapid Growth*), the 2040 technical potential of methanation will be 1.78 Quads. The average growth rate of the technical potential for each of the aforementioned scenarios is shown in Table 4.1, while the actual potential growth curves of the three scenarios are illustrated in Figure 4.4.

Table 4.1: The technical potential of methanation-derived RNG is expected to grow at an average growth rate of 1.4% per year between 2015 and 2040, given a constant electrolyser efficiency of 80%. Incremental increases in electrolyser efficiency would result in a higher annual growth rate.

Average annual growth rate of the technical potential	
Scenario	Average annual growth rate
Constant Efficiency	1.4%
Slow Efficiency Growth	1.7%
Rapid Efficiency Growth	2.0%

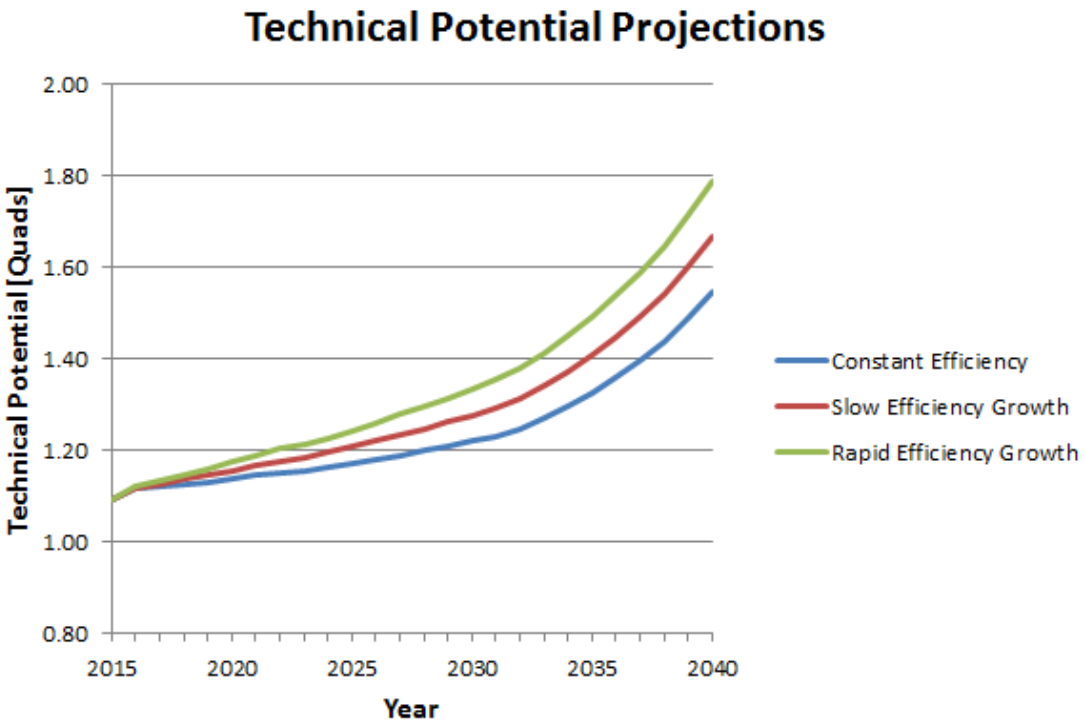

Figure 4.4: The technical potential of methanation-derived RNG grows faster given incremental increases in electrolyser efficiency, than under the assumption of constant electrolyser efficiency.

The technical potential of methanation-derived RNG in Texas was determined by denoting the HSL for wind, rather than the actual generation of electricity, as the renewable electric generation capacity available for electrolysis. Using the HSL yields a slightly higher estimation of the technical potential of methanation-derived RNG than using the actual generation does. The difference stems from the fact that the HSL represents the actual, real-time generation capacity, regardless of production curtailments. The 2011 technical potential of methanation-derived RNG in Texas was 1.06 $\times 10^8$ MMBTU, or 10.2% of the 2011 technical potential of methanation-derived RNG in the United States.

4.2 Economic Potential

The economic feasibility of producing RNG at the expense of selling electricity directly to the grid can be determined by employing the threshold equation. The fully derived threshold equation for an integrated wind and methanation facility is shown below as Equation 4.2:

$$P_e - OX_e = 2.658 \, \frac{MMBTU}{MWh} \times P_{ng} \times \eta_{el} - AOX_{rng} - OX_e \tag{4.2}$$

The variable P_e is the wholesale price of electricity [$/MWh], OX_e denotes the operating expenses associated with wind power generation [$/MWh], P_{ng} is the wholesale price of natural gas [$/MMBTU], η_{el} is the electrolyser efficiency, and AOX_{rng} denotes the operating expenses associated with RNG production, not including the potential cost of electricity required for the electrolysis process [$/MWh].

By substituting actual electricity and natural gas prices, operating expenses, and electrolyser efficiencies into Equation 4.2, the economically preferred production option in a theoretical decision-making scenario can be obtained. If the RHS of Equa-

tion 4.2 is greater than the LHS, producing and selling RNG is preferred, but if the LHS is greater than the RHS, selling the available electricity directly is the economically preferred decision. The decision to produce RNG is the same for integrated and non-integrated facilities, given only the options of producing and selling RNG, or selling electricity directly to the grid (or an RNG production facility), and not the option of ceasing wind power generation. However, the total profit of each scenario is different, as shown by Equations 3.16 and 3.22, in Sections 3.2.1.1 and 3.2.1.2, respectively. The results presented in this section assume integrated facilities, unless otherwise stated.

Figure 4.5 illustrates the economic transition threshold for the parameters used throughout this analysis ($\eta_{el} = 80\%$ and $AOX_{rng} = \$0/MWh$). Note that Figure 4.5 only illustrates when one production option is economically preferable to the other. It does not, however, illustrate how large the profit margin is, or when the different production options have a positive marginal profit. Thus, the value of OX_e is trivial in this context.

As the electrolyser efficiency increases, the economic transition threshold is raised, making RNG the economically preferred product at higher and higher electricity prices. The opposite is true as the electrolyser efficiency decreases. The positive correlation between the electrolyser efficiency and the economic transition threshold is illustrated in Figure 4.6.

The application of the threshold equation is illustrated in Figure 4.7, where the production decisions of 1 April 2011 are contrasted against the price of electricity that same day. The *Base Case Scenario* assumptions were used to create this illustration. The lowest electricity price reported during the course of the day was -$17.94/MWh, while the maximum value was $32.68/MWh. The Henry Hub natural gas price for

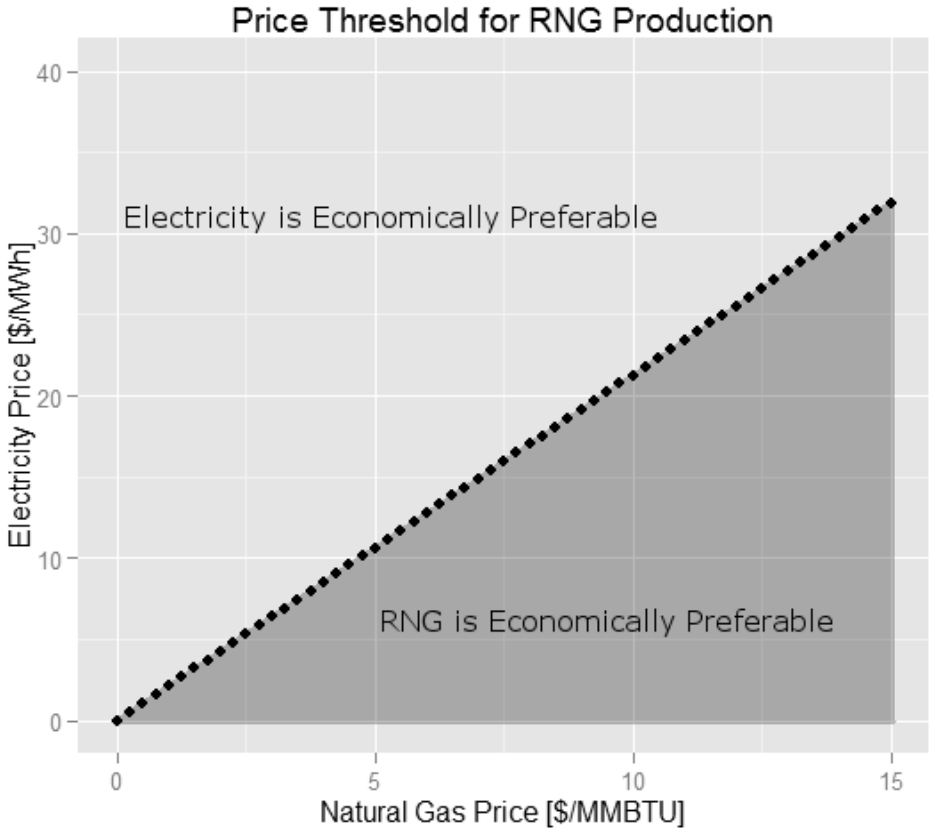

Figure 4.5: The dotted line marks the economic transition threshold given an electrolyser efficiency of 80%. For any given price combination in the shaded area below the line, the option of producing and selling RNG is more profitable than selling electricity directly to the grid. The price combinations above the line denote scenarios where the option of selling electricity directly to the grid is most profitable. Given only these two options, and not accounting for the influence of PTCs on the production decision for integrated facilities, the transition threshold is the same for both integrated and non-integrated methanation facilities.

that same day was \$4.32/MMBTU. Using the actual natural gas price, and solving for P_e from Equation 3.14, the transition threshold for that day is revealed to be at an electricity price of \$9.18/MWh. Thus, when the electricity price exceeds transition threshold of \$9.18/MWh, it is economically preferable to sell electricity directly to the grid. However, when the electricity drops below the transition threshold, pro-

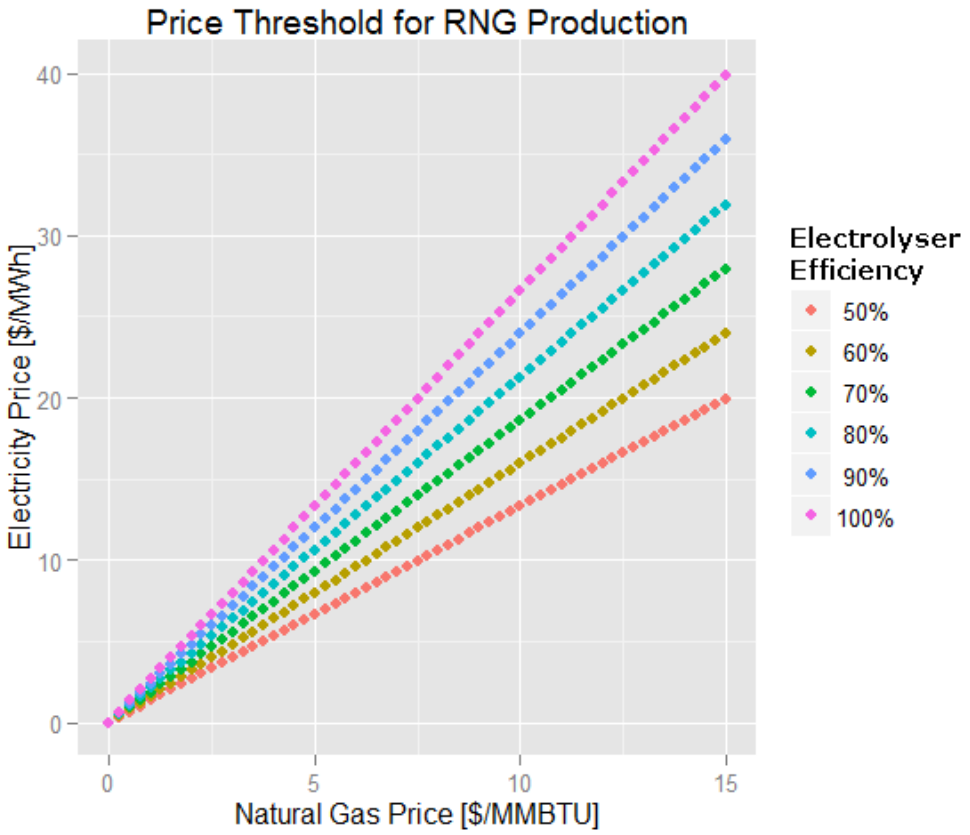

Figure 4.6: At low electrolyser efficiencies, the area beneath the transition threshold, denoting the price conditions where the option of producing and selling RNG is economically preferable, is relatively small. Raising the electrolyser efficiency essentially increases the slope of the economic transition threshold, thus expanding that area.

ducing and selling RNG becomes the economically preferred option. This behavior is consistent with the production decisions illustrated in Figure 4.7.

The amount of RNG produced within the *Base Case Scenario*, at an overall conversion efficiency of 62.3%, is 2.06×10^7 MMBTU/year, an order of magnitude below the technical potential. At 1,000 BTU/cf, this amount of RNG is greater than the average natural gas consumption of the state of Texas over the course of two days (1.79×10^7 MMBTU/year) [73]. Given the high price of electricity, the relatively low price of natural gas, and the fact that the electricity available for electrolysis

was limited by the actual wind power output (as opposed to the HSL), this number sets the lower boundary for the desired economic potential of methanation-derived RNG. Figure 4.8 is a stacked bar chart that shows the total energy output of the *Base Case Scenario* for every month of the year 2011. The relatively low electricity prices in the spring make RNG production more economically preferable than in the summer months, when electricity prices are consistently high, and the option of selling electricity to the grid is all the more attractive as a result. Figure B.1 in Appendix B illustrates the same data, as divided into daily intervals rather than monthly ones.

The amount of RNG produced within the *Curtailment Option Scenario*, at the same overall conversion efficiency as before, is 2.62×10^7 MMBTU/year. The difference between this amount, and the total amount from the *Base Case Scenario* is 5.61×10^6 MMBTU/year. Recall that both scenarios utilized the same electricity and natural gas price data, so this difference is all due to the theoretical utilization of otherwise curtailed wind capacity. The effects of this additional RNG production capacity are illustrated in Figure 4.9. Figure B.2 in Appendix B illustrates the model production decisions made on a daily basis, rather than a monthly one.

Finally, the amount of RNG produced within the *High Gas Price Scenario* is 3.19×10^7 MMBTU/year, out of which 2.64×10^6 MMBTU/year are produced using power that would otherwise have been curtailed. Given the previous assumptions on the energy density of natural gas, this total amount of RNG is slightly below the average consumption of natural gas in the state of Texas, over a four day period (3.57×10^7 MMBTU/year) [73]. This number marks the upper boundary of the desired economic potential. Thus, the full economic potential of wind- and methanation-derived RNG in Texas is between 2.06×10^7 MMBTU and 3.19×10^7 MMBTU annually, or between 19.4% and 30.1% of the technical potential.

The total energy output of the *High Gas Price Scenario* are illustrated in Figure 4.10. Despite the high gas prices, the electricity prices during the late summer months are still too high to make RNG production the economically preferred option. Thus, the increase in RNG production, compared to the previous scenario, mostly takes place during the spring and fall months. As with previous modeling scenarios, the daily model production decisions for this scenario are illustrated in Appendix B, as Figure B.3.

The annual marginal profit of integrated facilities within the *Base Case Scenario* is $1.82 billion when the additional production operating expenses are assumed to be negligible. The corresponding marginal profit of the *Curtailment Option Scenario* is $1.94 billion, and that of the *High Gas Price Scenario* is $2.09 billion. These numbers are the raw marginal profit values yielded by the MATLAB model, considering wind PTCs as part of the total marginal profit for each scenario. When the PTCs are not considered, the marginal profit values decrease by about $1 billion across all scenarios. These results are summarized alongside the annual RNG output of each of the three modeling scenarios in Table 4.2. For further comparison, Table 4.3 summarizes the results of the analysis for non-integrated facilities. Note that Table 4.3 has no PTC column, as the PTCs associated with wind power generation would not be awarded to a non-integrated methanation facility. Furthermore, the total marginal profit values in Table 4.3 reflect the marginal profit from the production and sale of RNG only, and are thus comparable to the marginal RNG profit values reported in parentheses in Table 4.2. By contrast, the total marginal profit values in Table 4.2 reflect the combined marginal profit from the production and sales of both electricity and RNG.

The total marginal profit of a production scenario involving no production of

Table 4.2: More than half the annual marginal profit of integrated facilities would come from wind PTCs, across all scenarios. The marginal profit associated with RNG production (shown in parentheses) would range from roughly 10-30% of the total, when PTCs are not included, and 23-40% when they are included.

Modeling Scenario (Integrated)	Annual RNG Output [MMBTU]	Annual Marginal Profit [Million $]	Annual Marginal Profit, including PTCs [Million $]
Base Case Scenario:	2.06×10^7	831 (82.0 from RNG)	1,824 (421 from RNG)
Curtailment Option Scenario:	2.62×10^7	854 (104 from RNG)	1,949 (536 from RNG)
High Gas Price Scenario:	3.19×10^7	1,003 (300 from RNG)	2,088 (825 from RNG)

RNG is $1.72 billion, assuming marginally profitable production only. This value denotes the baseline used to calculate the hedging potential of the different scenarios. Recall that the hedging potential is defined as the difference between the total marginal profit of a given scenario, and the marginal profit of a production scenario that offers no RNG production option. Based on the values in the fourth column of Table 4.2, the marginal profit gap between the three modeling scenarios (for integrated facilities) and the baseline is considerable. The *High Gas Price Scenario* yields the highest annual hedging potential at around $366 million.

When the PTCs are not considered as part of the marginal profit, the annual marginal profit of a production scenario involving no production of RNG is $731 million. This value denotes the baseline used to calculate the 'no-PTC' hedging potential. Here, the *High Gas Price Scenario* again yields the highest hedging potential, equal to around $272 million.

As previously stated, the hedging potential results described in the previous two paragraphs are obtained under the assumption of negligible operating expenses.

Table 4.3: The annual marginal profit of non-integrated facilities is generally higher than the marginal RNG profit of integrated ones, if PTCs are not considered. These results stem from the fact that non-integrated facilities can occasionally purchase electricity at negative wholesale prices. When gas prices are high, however, actual RNG production values outweigh the impact of negative electricity prices, and the integrated facilities become more profitable. Finally, the marginal RNG profit of integrated facilities is much higher than that of non-integrated ones if PTCs are considered. However, a significant portion of those PTCs would still be awarded for wind generation, even if no RNG production took place.

Modeling Scenario (Non-Integrated)	Annual RNG Output [MMBTU]	Annual Marginal Profit [Million $]
Base Case Scenario:	2.05×10^7	111
Curtailment Option Scenario:	2.49×10^7	144
High Gas Price Scenario:	3.09×10^7	287

However, as the operating expenses of electrolysis and methanation (AOX_{rng}) increase from \$0/MWh, all three scenarios eventually converge towards the baseline. When PTCs are considered as part of the total marginal profit, the *Base Case Scenario* converges to the baseline between \$40/MWh and \$45/MWh, while the *Curtailment Option Scenario* does so between \$45/MWh and \$50/MWh. The *High Gas Price Scenario* is noticably more profitable than the other two scenarios, converging to the baseline between \$60/MWh and \$65/MWh. These results are shown in Figure 4.11. The marginal profit increase of each scenario relative to the baseline, and as a function of the additional operating expenses (AOX_{rng}), is shown as Figure B.4 in Appendix B.

The hedging potential of each modeling scenario where PTCs are not included in the marginal profit is illustrated in Figure 4.12. The trends converge towards the baseline at the same additional operating expenses as the trends illustrated in

Figure 4.11, as they represent the same modeling results. However, before reaching equilibrium, the model production decisions of the *Curtailment Option* and *High Gas Price Scenarios* drive the 'no-PTC' hedging potential to negative values. These trends are the direct results of the modeling decision to include wind PTCs in the total marginal profit of each scenario. In the aforementioned scenarios, the model will utilize curtailed wind to produce RNG, even at a raw marginal loss, to collect the PTCs associated with that power generation. These decisions are made as long as the awarded PTCs outweigh the raw marginal loss associated with the actual RNG production. In light of this behavior, it is straightforward to conclude that maximizing the 'no-PTC' marginal profit will in most cases not result in a maximized total marginal profit.

Opposed to its integrated counterpart, a non-integrated methanation facility does not have any production options other than producing and selling RNG. Thus, non-integrated facilities do not have a hedging potential according to the definition in this work. The marginal profit of non-integrated facilities is plotted as a function of additional operating expenses (AOX_{rng}) in Figure 4.13. The trends illustrated in Figure 4.13 are similar to the trends in Figure 4.11, except the marginal profit of non-integrated methanation facilities reaches relative equilibrium at lower operating expenses than the hedging potential of integrated facilities.

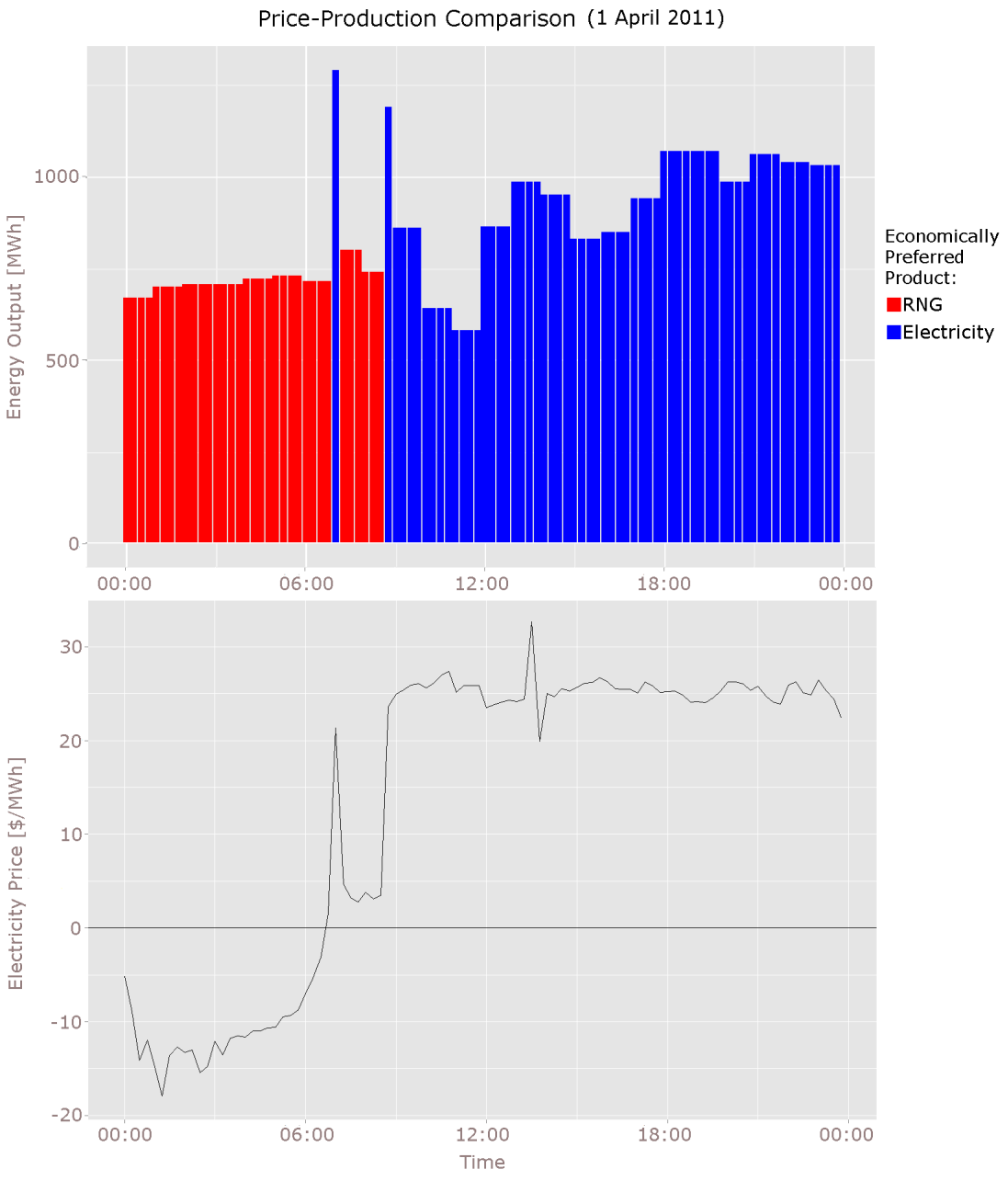

Figure 4.7: Using renewable electricity to produce RNG is more economically feasible than selling the electricity directly to the grid only when the wholesale price of electricity is low compared to the wholesale price of natural gas. The energy output for RNG is given in MWh_{th}, rather than MWh_{e^-} required to produce the RNG. The same applies to Figures 4.8 - 4.10.

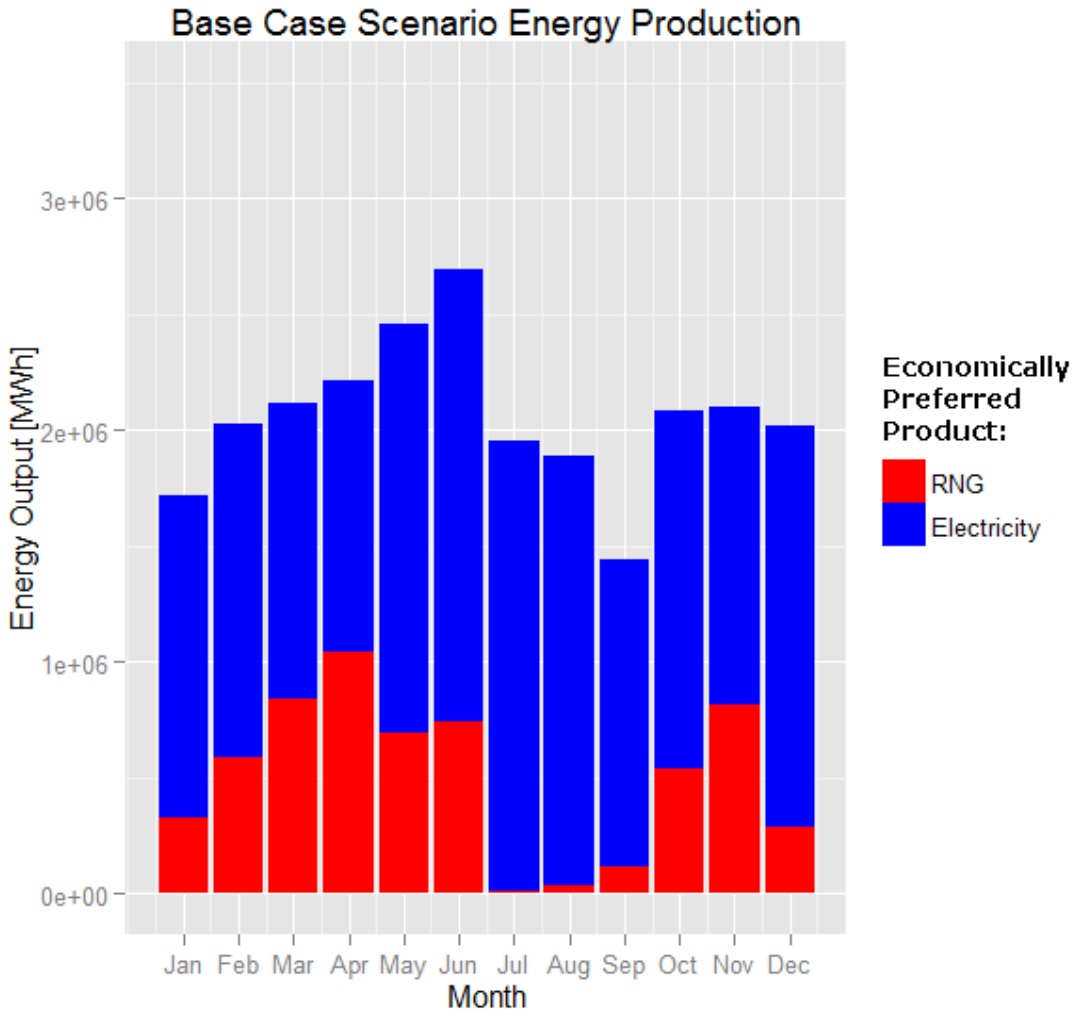

Figure 4.8: The height of each bar represents the total amount of energy produced and sold within the Base Case Scenario, either as RNG (MWh_{th}, red bars) or as electricity (MWh_{e^-}, blue bars), during each month of the year 2011. In summer months, when electricity prices are high, electricity is almost exclusively the economically preferred product.

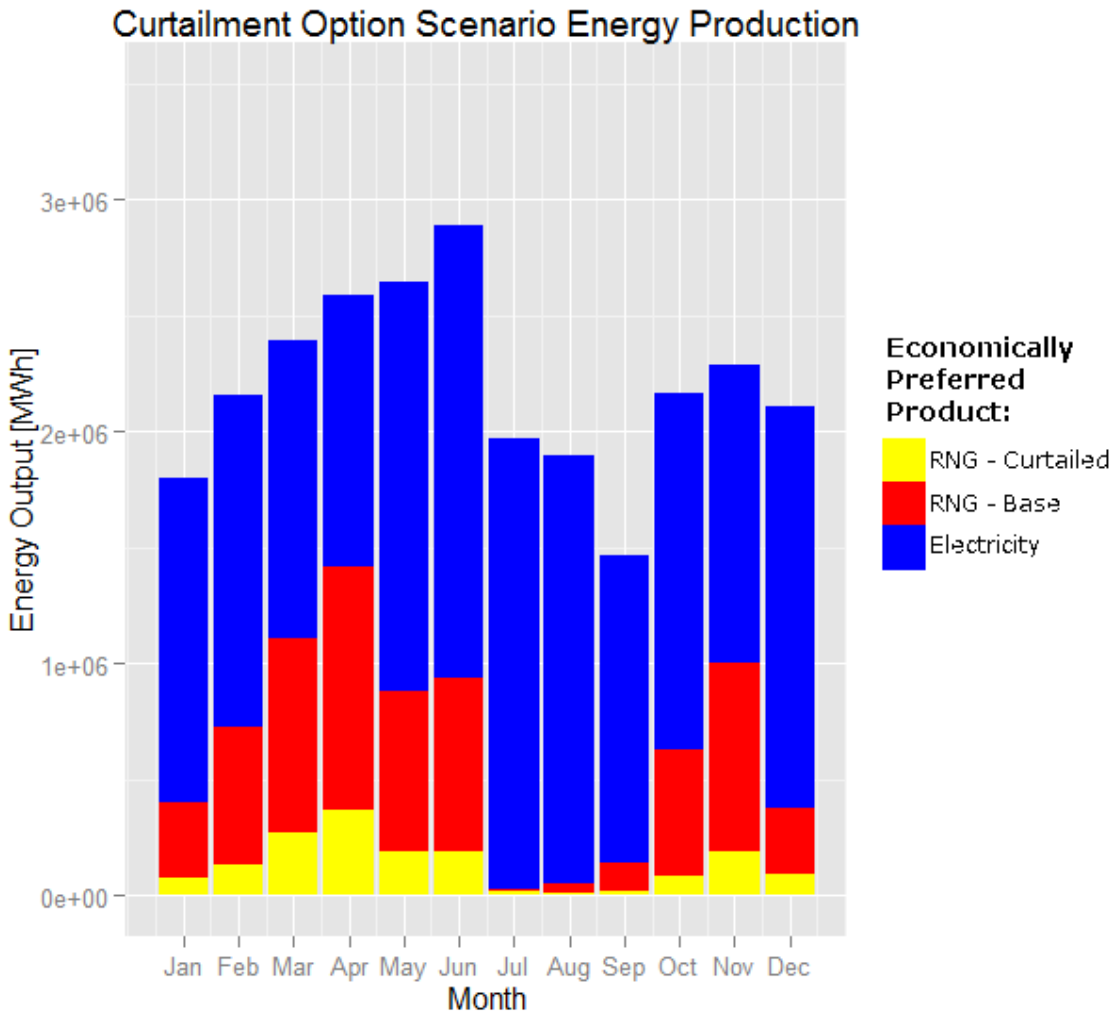

Figure 4.9: The energy output of the Curtailment Option Scenario. The yellow bars represent the RNG produced using otherwise curtailed wind capacity, while the red bars represent RNG product from actual recorded wind power output. As before, the blue bars represent electricity produced and sold directly to the electric grid. The utilization of curtailed production capacity leads to a considerable increase in RNG production, especially during the months of March and April.

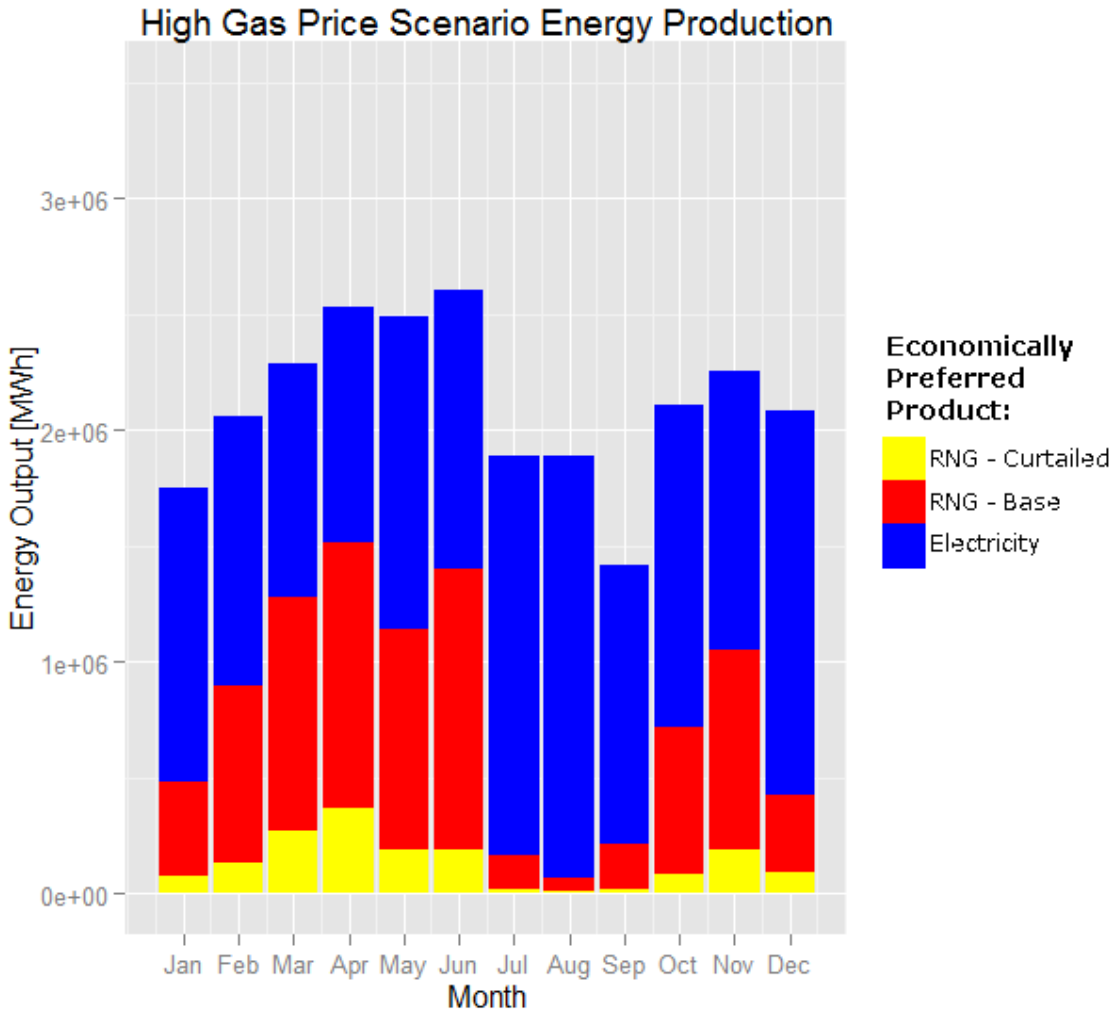

Figure 4.10: The energy output of the High Gas Price Scenario. The high gas price leads to a significant increase in overall RNG production relative to the Curtailment Option Scenario, and at the expense of the amount of electricity sold directly to the grid. This increase is most noticeable during the months of May and June.

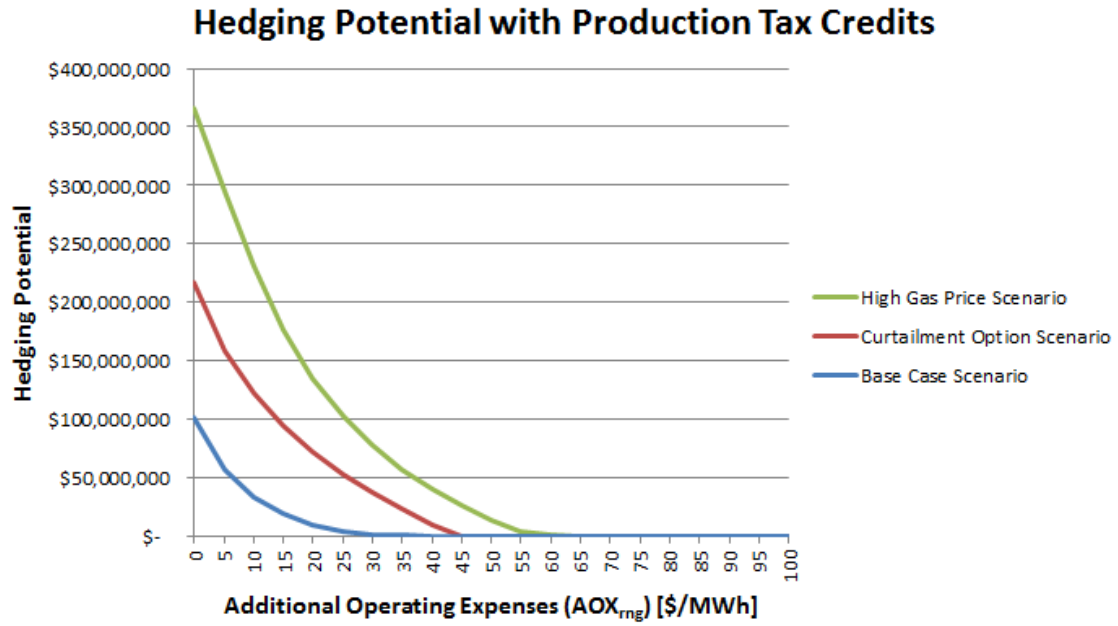

Figure 4.11: The hedging potential of each modeling scenario is a function of additional operating expenses (AOX_{rng}). As the additional operating expenses increse, the marginal profit decreases, resulting in a diminished hedging potential.

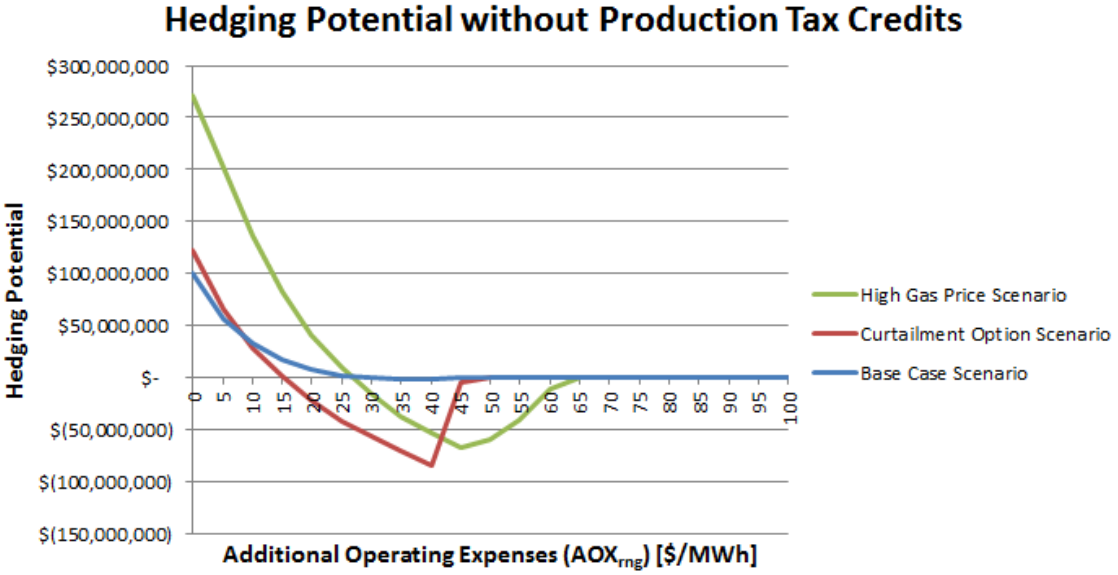

Figure 4.12: The model utilizes curtailed wind for RNG production, even at a raw marginal loss, to maximize the total marginal profit when PTCs are considered.

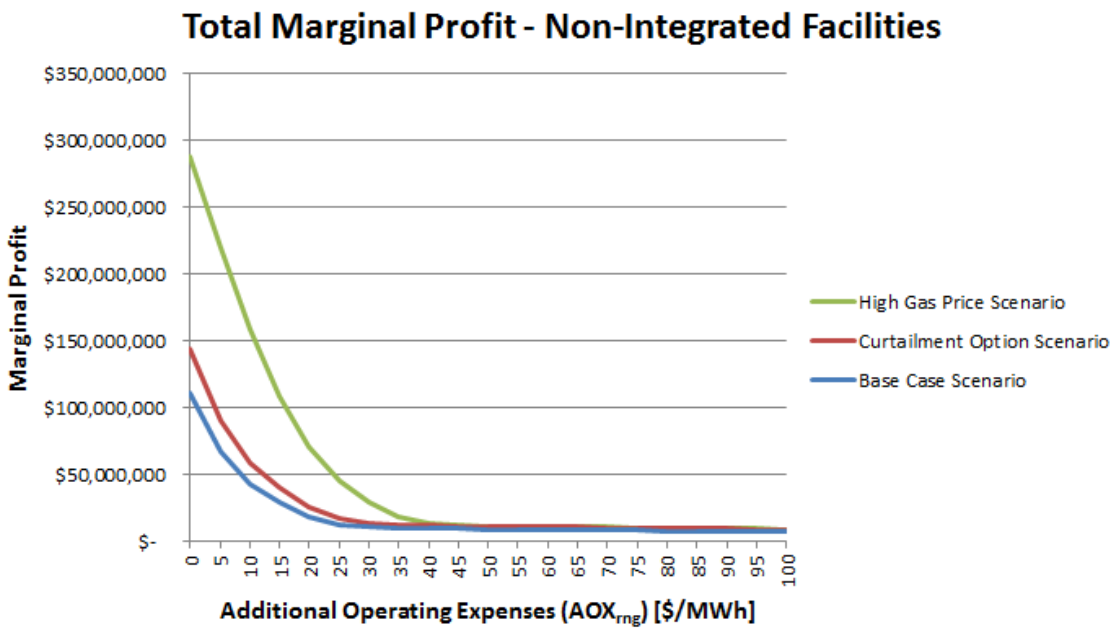

Figure 4.13: The total annual marginal profit of all three non-integrated modeling scenarios has mostly tapered off at AOX_{rng} = \$45/MWh. However, due to the powerful incentive of negative electricity prices, the marginal profit does not converge toward \$0/MWh within the AOX_{rng}-range considered.

Chapter 5

Conclusions

This thesis had the following primary objectives:

1. Quantifying the total annual technical potential of biomass- and methanation-derived RNG in the United States.

2. Quantifying the annual economic potential of methanation-derived RNG in Texas.

Section 5.1 summarizes the main conclusions pertaining to these objectives, and the lessons learned from the analysis described in this work. Section 5.2 then discusses the future steps for improving upon the work in this thesis.

5.1 Summary of Findings

Section 3.1 presented analysis that quantifies the technical potential of RNG in the United States. This analysis is novel due to its inclusion of the technical potential of methanation-derived RNG in the total technical potential of RNG. The results of this analysis set the theoretical upper limit for the potential availability of RNG at 10.5 Quads, or 43.1% of the total annual consumption of natural gas in 2011, with the technical potential of methanation-derived RNG representing 1.03 Quads, or 4.2% of the total. The technical potential of methanation-derived RNG is expected to grow at an average rate of 1.4-2.0% per year, over the next 25 years. The American

Gas Foundation estimates that between 10-25% of the technical potential of biomass-derived RNG can realistically be obtained [3]. Assuming a similar potential yield for methanation-derived RNG results in a realistic energy potential of 0.4-1.1% of the total annual natural gas consumption.

Section 3.2 established a decision-making framework for determining under which conditions the option of producing and selling methanation-derived RNG is economically preferable to the option of selling renewable electricity directly to the grid. This analysis resulted in the derivation of a threshold equation, that returns a production decision as a function of electrolyser efficiency, electricity and gas prices, and the operating expenses associated with the electrolysis and methanation processes. The complete derivation of the threshold equation is described in Section 3.2.1. Low operating expenses, high electrolyser efficiencies, and high gas prices, relative to the price of electricity, all indicate that the production of methanation-derived RNG is economically preferable to selling electricity directly to the grid. Continued advancements in decreasing the cost of hydrogen production through electrolysis would therefore make the production of methanation-derived RNG more economically feasible.

The aforementioned framework was utilized as a foundation for a decision-making computer model, as described in Section 3.2.2. This model has the following key features:

1. The model uses real natural gas and electricity prices to determine the economically preferred production option on a rolling basis, and over an extended period of time.

2. Inputting real renewable electricity production data, the model aggregates the amount of RNG produced over a single year, for a few different price and electric

generation capacity scenarios. Thus, the model helps establish a range for the economic potential of RNG within a specific geographical area.

3. For each price/capacity scenario, the model collects output for 126 operating expense/efficiency permutations. This setup allows for a very detailed analysis of the effects of operating expenses and electrolyser efficiencies on the economic potential and feasibility of RNG production through electrolysis and methanation.

The model output, given an electrolyser efficiency of 80% and minimal operating expenses, suggests that the 2011 economic potential of methanation-derived RNG in Texas was between 19.4-30.1% of the annual technical potential for the state. These numbers should be used cautiously, as they represent an energy landscape suffering from electric transmission constraints, frequent occurrences of generation curtailment, and many instances of negative electricity prices. While these conditions do not describe the current energy landscape of the state, due in part to massive transmission expansion projects, they do reflect other parts of the world where renewable generation capacity is limited by transmission capacity. Furthermore, it is recommended that this framework be used as a foundation for evaluating the economic feasibility of employing methanation-derived RNG as an alternative to future grid expansions, given the rapid and continual growth of renewable generation capacity within the state of Texas.

The operational profit increase obtainable by introducing the option of producing RNG through methanation is between $102 and $366 million per year for the state of Texas, with the inclusion of PTCs and assuming minimal operating expenses. The marginal profit of non-integrated methanation facilities ranges between $100 and $272 million per year, given the same assumptions of minimal operating

expenses. The profit margin for both integrated and non-integrated facilities gradually disappears across all modeling scenarios as operating expenses increase. While capital expenditures are not included in this analysis, the hedging potential analysis described in this work can help determine the potential payback period associated with the construction of RNG production plants and infrastructure.

5.2 Future Work

The work in this thesis generally represents a best case scenario. This work can be augmented by introducing further constraints that would affect or limit a realistic RNG production scenario. These constraints would primarily be economic, geographic, and technical. Thus, future analyses should include a consideration of the capital expenditures associated with wind power generation, as well as those of constructing the facilities necessary for industrial-scale methanation-derived RNG production.

Furthermore, future work should include a more detailed analysis of the effects of non-negligible operating expenses on the economic feasibility of producing RNG through methanation. The operating expenses that were not considered specifically in this work include: The cost of water required for the electrolysis, the cost of obtaining CO_2 for the methanation process, the cost of catalysts needed to maintain required methane production rates and selectivities, and so forth. Accounting for these expenses is necessary in anything but a 'best case scenario' analysis, and the economic model developed in this work can be easily modified to account for their effect. By doing so, the model output would become more applicable to real-life production and decision making scenarios.

Long term aspirations for this work would be to alter the model to account for

production location. In reality, the potential of RNG production through methanation is limited by accessibility to all the feedstocks required for the production, and not only the availability of renewable electricity. For example, this work assumes that CO_2 and water are available both freely and in abundance. Determining the limiting effects of CO_2 and water availability would be of interest, specifically in terms of transportation and logistics, but also in terms of additional energy requirements and implications. In a similar way, the lack of natural gas infrastructure or the lack of access to the natural gas pipeline network can also affect the feasibility of RNG production. Thus, quantifying both the technical and economic potential of RNG production by location would be a worthwhile venture.

Another technical consideration that should be included in future work is that of start-up times and production rates. The analysis in this work assumes that the entire amount of available, low-price electricity can be used for RNG production before electricity prices rise again. Thus, the production window can theoretically be as short as 15 minutes. In reality, production would be limited by the time it takes to start up the production equipment, and the rate at which methane can be produced through the methanation process.

Finally, the environmental and economic benefits of using curtailed wind to produce RNG are relatively clear. However, if renewable electric supply to the grid is dialed back expressly to produce RNG and maximize profits, the environmental benefits become less obvious. Thus, possible future work would also include an analysis of the environmental and economic impact of producing RNG through electrolysis and methanation, a study of the trade-offs between the two, and an environmental-economic optimization of the production decision.

Appendices

Appendix A

MATLAB Model Code

A.1 Curtailment Option Run File

```
clc;
clear;

%Price of electricity in [$/MWh]
ep = xlsread('WindProductionHSLInstCapHHGPandEP.xlsx',
     'Sheet1','E2:E35041');
%Gas price in [$/MMBTU]
rngp = xlsread('WindProductionHSLInstCapHHGPandEP.xlsx','Sheet1',
     'F2:F35041');
%Production capacity [MW]
prodcap = xlsread('WindProductionHSLInstCapHHGPandEP.xlsx',
     'Sheet1','D2:D35041');
%Actual production after curtailment [MW]
production = xlsread('WindProductionHSLInstCapHHGPandEP.xlsx','Sheet1',
     'C2:C35041');

%Production capacity for every 15 minute period [MWh]
adjprodcap = prodcap * 0.25;

%Actual production sustained over every 15 minute period [MWh]
adjproduction = production * 0.25;

%Different OPEX scenarios - Variable H2price corresponds to variable AOX
%in analysis
%Operational expenses associated with the production of RNG [$/MWh]
H2price = [0 5 10 15 20 25 30 35 40 45 50 55 60 65 70 75 80 85 90 95
     100];

%Overall conversion efficiency with electrolyser efficiency set to 100%,
%90%, 80%, 70%, 60%, and 50%, respectively

%               100%    90%    80%    70%    60%    50%
overalleff = [0.7787 0.7008 0.6230 0.5451 0.4672 0.3894];
efficiency = [1 0.9 0.8 0.7 0.6 0.5];

```

```
MJ2MWhcoeff = 2.778 * 10.^(-4);

%Electricity needed (in MJ) to produce a kg of hydrogen
energyneedMJ = [141.797 157.552 177.246 202.567 236.328 283.797];
%Electricity needed (in MWh) to produce a kg of hydrogen
energyneedMWh = energyneedMJ * MJ2MWhcoeff;
le1 = length(overalleff);
le2 = length(H2price);

%Loops through the efficiency vector and the hydrogen cost vector,
%initializing structures for each scenario - Line refers to efficiency,
%column refers to hydrogen cost
for i = 1:le1
    for j = 1:le2
        mod_scenario(i,j).overalleff = overalleff(i);
        mod_scenario(i,j).eleff = efficiency(i);
        mod_scenario(i,j).eneedMJ = energyneedMJ(i);
        mod_scenario(i,j).eneedMWh = energyneedMWh(i);
    end
end

mod_scenario = actprodandcurt(mod_scenario, le1, le2, rngp, ep,
    adjprodcap, adjproduction, H2price);
```

A.2 Curtailment Option Model File

```
function mod_scenario = actprodandcurt(mod_scenario, le1, le2, rngp, ep,
    adjprodcap, adjproduction, H2price)

%Conversion coefficient (WolframAlpha) -> 1 MMBTU = 0.2931 MWh
MMBTU2MWhcoeff = 0.293071;

%Difference between HSL/e- production capacity and actual production
%[MWh]
capgap = adjprodcap - adjproduction;

%Loops through each electrolyser efficiency scenario
for i = 1:le1
    %Loops through all electrolysis/methanation cost scenarios
    for j = 1:le2
        %Operational expenses associated with the production of RNG
        %[$/MWh]
        mod_scenario(i,j).H2pricespec = H2price(j);

        %Potential revenue per 15 min from selling electricity directly
        %to the consumer - limited by transmission capacity [$]
        erev = adjproduction .* ep;
        %Given the assumption that the marginal cost of electricity from
        %wind is $0, the potential revenue from selling electricity
        %directly (erev) is equal to the potential profit. This is not
        %the case with RNG. The marginal cost associated with the
        %electrolysis process is equal to the price of the electricity
        %required to perform the process. This cost, along with the
        %OPEX, is implemented below.

        %Potential revenue per 15 min from using electricity to produce
        %RNG for selling - limited by production capacity [$]
        rngrev = ((rngp./MMBTU2MWhcoeff)
            .* (mod_scenario(i,j).overalleff)) .* adjprodcap;
        %Potential profit per 15 min from using electricity to produce
        %RNG for selling [$]
        rngprofit = rngrev - (mod_scenario(i,j).H2pricespec
            .* adjprodcap);

        %The same RNG revenue/profit calculations as above, except only
        %using the surplus electric generation capacity
        surprngrev = ((rngp./MMBTU2MWhcoeff)
            .* (mod_scenario(i,j).overalleff)) .* capgap;
        surprngprofit = surprngrev - (mod_scenario(i,j).H2pricespec
            .* capgap);

        %Construction of a comparison matrix, comparing the potential
```

```
47          %profits of the two pathways, and the option of ceasing
48          %electricity production
49
50          %The following row represents the option of selling electricity
51          %only, and directly, at a given time interval (assuming a ptc
52          %of 2.3 cents/kWh for wind)
53          compmatrix(1,:) = erev + 35 .* adjproduction;
54          %The following row represents the option of producing and
55          %selling RNG at a given time interval (assuming a ptc of 2.3
56          %cents/kWh for wind)
57          compmatrix(2,:) = rngprofit + 35 .* adjprodcap;
58          %The following row represents the option of selling electricity
59          %directly, and using surplus capacity (due to curtailment) to
60          %produce and sell RNG (assuming a ptc of 2.3 cents/kWh
61          %for wind)
62          compmatrix(3,:) = erev + surprngprofit + 35 .* adjprodcap;
63          %The following row represents the option of ceasing electricity
64          %production
65          compmatrix(4,:) = 0;
66
67          %Records how much of the time electricity is being sold directly
68          %[hours]
69          mod_scenario(i,j).timeel = 0;
70          %Records how much of the time RNG is being produced [hours]
71          mod_scenario(i,j).timerng = 0;
72          %Records how much of the time no electricity is being produced
73          %[hours]
74          mod_scenario(i,j).timezero = 0;
75
76          %Loops through all the time periods
77          for k = 1:length(erev)
78              maxval = compmatrix(1,k);
79              index = 1;
80              %Loops through all the consumption options
81              for m = 2:length(compmatrix(:,1))
82                 %Finds the maximum profit value, and the index of that
83                 %value
84                  if compmatrix(m,k) > maxval
85                      index = m;
86                      maxval = compmatrix(m,k);
87                  end
88              end
89
90              %Assigns the index of the highest value to the first line
91              %of the result matrix
92              mod_scenario(i,j).resmat(1,k) = index;
93              %Assigns the highest value to the second line of the result
94              %matrix
95              mod_scenario(i,j).resmat(2,k) = maxval;
96              %The same as the line above - however, this number will be
```

```
97              %updated to not include profit from using surplus capacity
98              %to produce RNG
99              mod_scenario(i,j).resmat(3,k) = maxval;
100
101             if index == 1
102                 %Time electricity is being sold updated
103                 mod_scenario(i,j).timeel = mod_scenario(i,j).timeel
104                     + 0.25;
105                 %Amount of e- sold at time period k stored [MWh]
106                 mod_scenario(i,j).resmat(4,k) = adjproduction(k);
107                 %Actual profit from selling electricity directly at time
108                 %period k (not including PTCs) [$]
109                 mod_scenario(i,j).resmat(6,k) = erev(k);
110                 %Unused capacity at time period k [MWh]
111                 mod_scenario(i,j).resmat(8,k) = capgap(k);
112             elseif index == 2
113                 %Time RNG is being produced and sold updated
114                 mod_scenario(i,j).timerng = mod_scenario(i,j).timerng
115                     + 0.25;
116                 %Amount of RNG produced at time period k stored [MMBTU]
117                 mod_scenario(i,j).resmat(5,k) = adjprodcap(k)
118                     * mod_scenario(i,j).overalleff / MMBTU2MWhcoeff;
119                 %Actual profit from producing and selling RNG at time
120                 %period k (not including PTCs) [$]
121                 mod_scenario(i,j).resmat(7,k) = rngprofit(k);
122                 %No unused capacity
123                 mod_scenario(i,j).resmat(8,k) = 0;
124                 %Actual amount of RNG produced at time period k using
125                 %solely surplus capacity updated [MMBTU]
126                 mod_scenario(i,j).resmat(10,k) = capgap(k)
127                    * mod_scenario(i,j).overalleff / MMBTU2MWhcoeff;
128             elseif index == 3
129                 %Time electricity is being sold updated
130                 mod_scenario(i,j).timeel = mod_scenario(i,j).timeel
131                     + 0.25;
132                 %Time RNG is being produced and sold updated
133                 mod_scenario(i,j).timerng = mod_scenario(i,j).timerng
134                     + 0.25;
135                 %Profit w/o utilizing surplus capacity to produce and
136                 %sell RNG updated
137                 mod_scenario(i,j).resmat(3,k) =
138                     mod_scenario(i,j).resmat(3,k) - surprngprofit(k);
139                 %Amount of e- sold at time period k stored [MWh]
140                 mod_scenario(i,j).resmat(4,k) = adjproduction(k);
141                 %Amount of RNG produced at time period k stored [MMBTU]
142                 mod_scenario(i,j).resmat(5,k) = capgap(k)
143                     * mod_scenario(i,j).overalleff / MMBTU2MWhcoeff;
144                 %Actual profit from selling electricity directly at time
145                 %period k (not including PTCs) [$]
146                 mod_scenario(i,j).resmat(6,k) = erev(k);
```

```
147                 %Actual profit from producing and selling RNG using
148                 %surplus capacity at time period k (not including
149                 %PTCs) [$]
150                 mod_scenario(i,j).resmat(7,k) = surprngprofit(k);
151                 %No unused capacity
152                 mod_scenario(i,j).resmat(8,k) = 0;
153                 %Actual amount of RNG produced at time period k using
154                 %solely surplus capacity updated [MMBTU]
155                 mod_scenario(i,j).resmat(10,k) = capgap(k)
156                    * mod_scenario(i,j).overalleff / MMBTU2MWhcoeff;
157                %Actual amount of RNG produced alongside electricity
158                 %at time period k [MMBTU]
159                 mod_scenario(i,j).resmat(11,k) = capgap(k)
160                    * mod_scenario(i,j).overalleff / MMBTU2MWhcoeff;
161             else
162                 %Time wind turbines are stationary updated
163                 mod_scenario(i,j).timezero = mod_scenario(i,j).timezero
164                      + 0.25;
165                 %Unused capacity at time period k [MWh]
166                 mod_scenario(i,j).resmat(8,k) = adjprodcap(k);
167             end
168         end
169
170         mod_scenario(i,j).erev = erev;
171         mod_scenario(i,j).grev = rngrev;
172         mod_scenario(i,j).gprofit = rngprofit;
173
174         %Summaries:
175         %Total potential revenue/profit from electricity only scenario
176         %(not including PTCs) [$]
177         mod_scenario(i,j).potrevel = sum(erev);
178         %Total potential revenue from RNG only scenario
179         %(not including PTCs) [$]
180         mod_scenario(i,j).potrevrng = sum(rngrev);
181         %Total potential profit from RNG only scenario
182         %(not including PTCs) [$]
183         mod_scenario(i,j).potprofitrng = sum(rngprofit);
184         %Total profit in dollars (with PTCs) w/o using surplus
185         %capacity to produce RNG [$]
186         mod_scenario(i,j).totprofitwosprng =
187              sum(mod_scenario(i,j).resmat(3,:));
188         %Actual total profit from electricity (not including PTCs) [$]
189         mod_scenario(i,j).totprofitel =
190              sum(mod_scenario(i,j).resmat(6,:));
191         %Actual total profit from RNG (not including PTCs) [$]
192         mod_scenario(i,j).totprofitrng =
193              sum(mod_scenario(i,j).resmat(7,:));
194          %Total electricity sold directly [MWh]
195         mod_scenario(i,j).totel = sum(mod_scenario(i,j).resmat(4,:));
196         %Total RNG produced and sold [MMBTU]
```

```
197         mod_scenario(i,j).totrng = sum(mod_scenario(i,j).resmat(5,:));
198         %Total unused capacity [MWh]
199         mod_scenario(i,j).totunused =
200              sum(mod_scenario(i,j).resmat(8,:));
201         %Total PTC profit from RNG production [$]
202         mod_scenario(i,j).totptcrng = mod_scenario(i,j).totrng
203              * MMBTU2MWhcoeff / mod_scenario(i,j).overalleff * 35;
204         %Total PTC profit from electricity production [$]
205         mod_scenario(i,j).totptcel = mod_scenario(i,j).totel * 35;
206         %Total profit (pre-tax) without production tax credits [$]
207         mod_scenario(i,j).totprofitwoptc = mod_scenario(i,j).totprofitel
208            + mod_scenario(i,j).totprofitrng;
209         %Total amount of RNG produced using solely surplus capacity
210         %[MMBTU]
211         mod_scenario(i,j).surpcaprng
212            = sum(mod_scenario(i,j).resmat(10,:));
213         %Actual amount of RNG produced alongside electricity at time
214         %period k [MMBTU]
215         mod_scenario(i,j).rngwelec
216            = sum(mod_scenario(i,j).resmat(11,:));
217         %Total profit (pre-tax) including production tax credits [$]
218         mod_scenario(i,j).totprofitptc =
219            sum(mod_scenario(i,j).resmat(2,:));
220
221     end
222 end
```

Appendix B

Additional Graphs and Plots

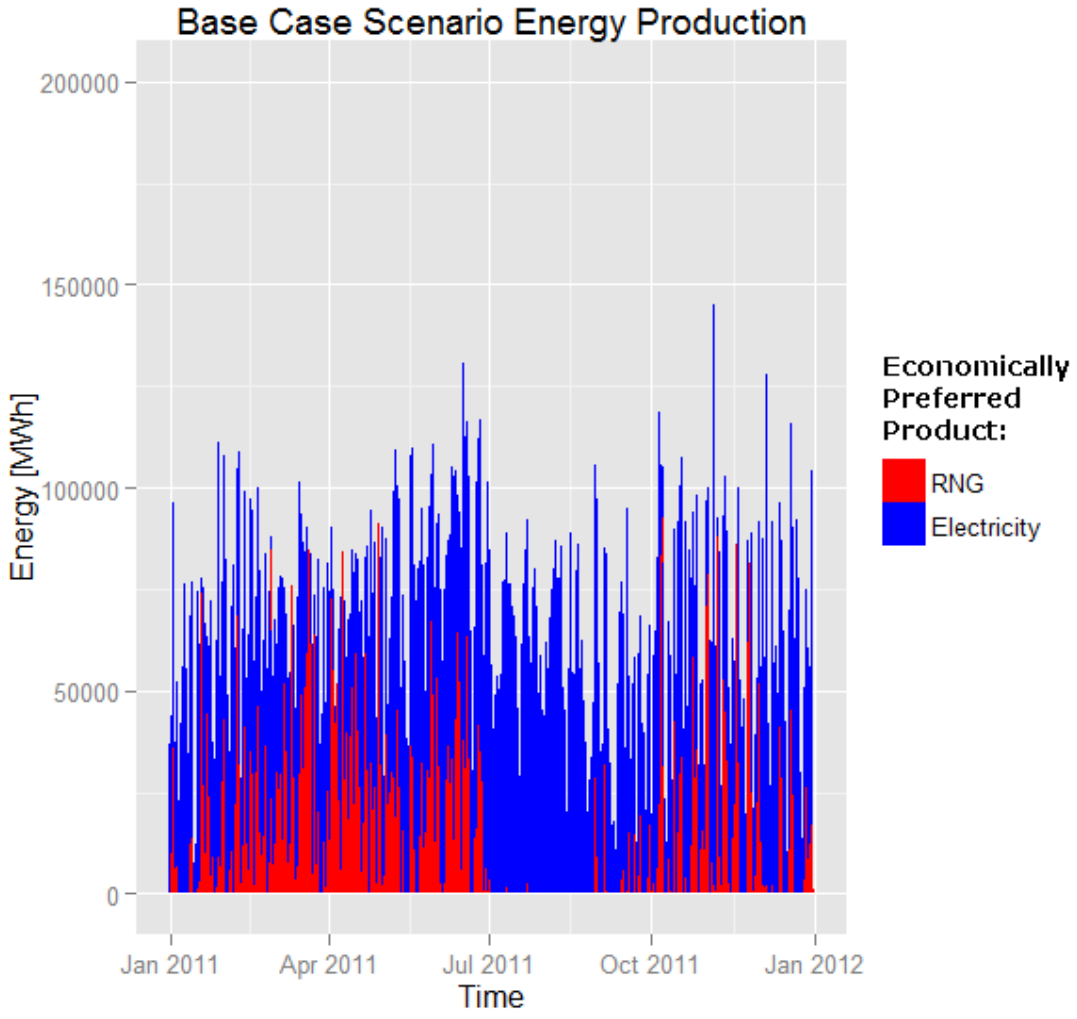

Figure B.1: Each bar represents the total amount of energy produced and sold in a single day within the Base Case Scenario. The red bars represent RNG produced and sold (MWh_{th}), while the blue bars represent electricity sold directly to the grid (MWh_{e^-}).

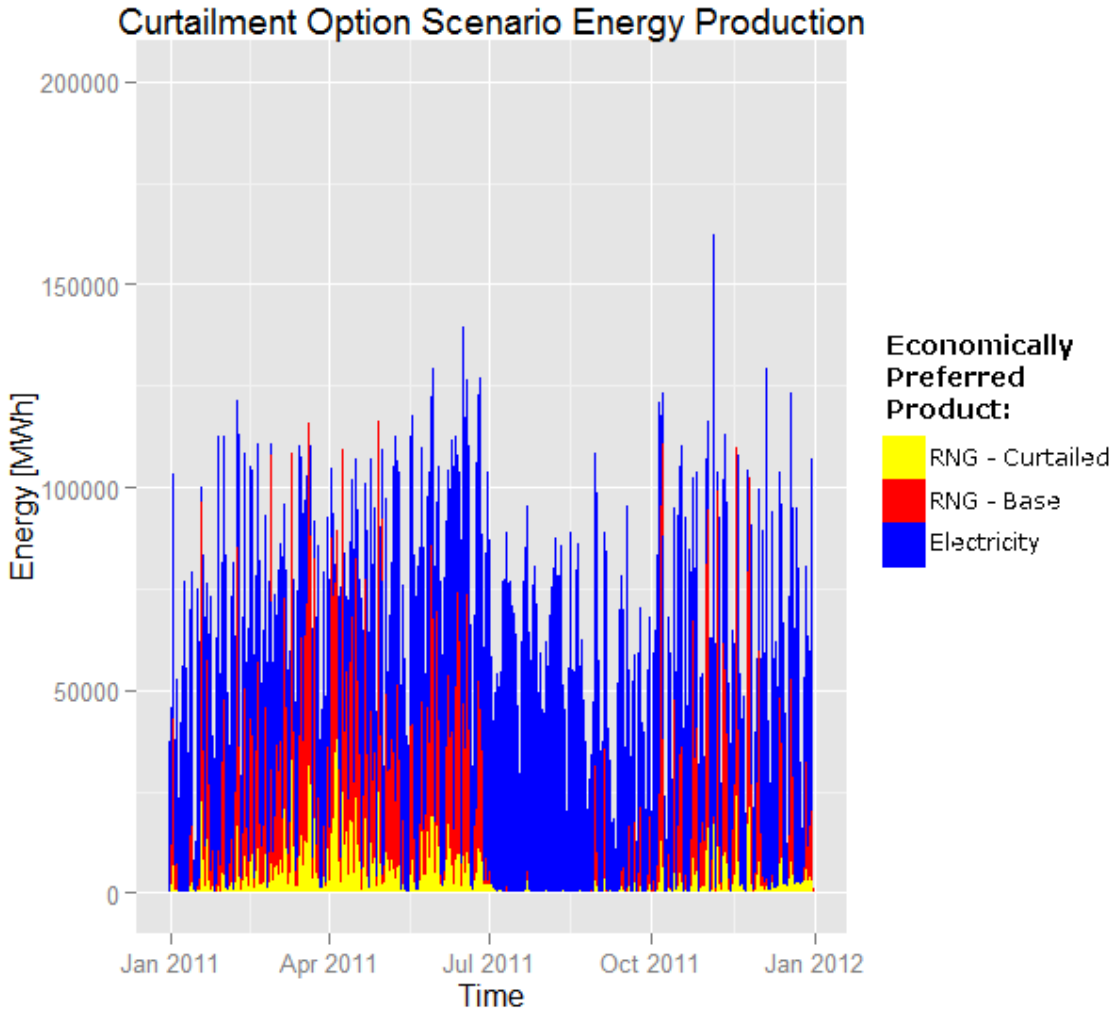

Figure B.2: Each bar represents the total amount of energy produced and sold in a single day within the Curtailment Option Scenario. The yellow bars represent RNG produced using otherwise curtailed wind capacity (MWh_{th}), the red bars represent RNG produced using baseline generation capacity (MWh_{th}), and the blue bars represent electricity sold directly to the grid (MWh_{e^-}).

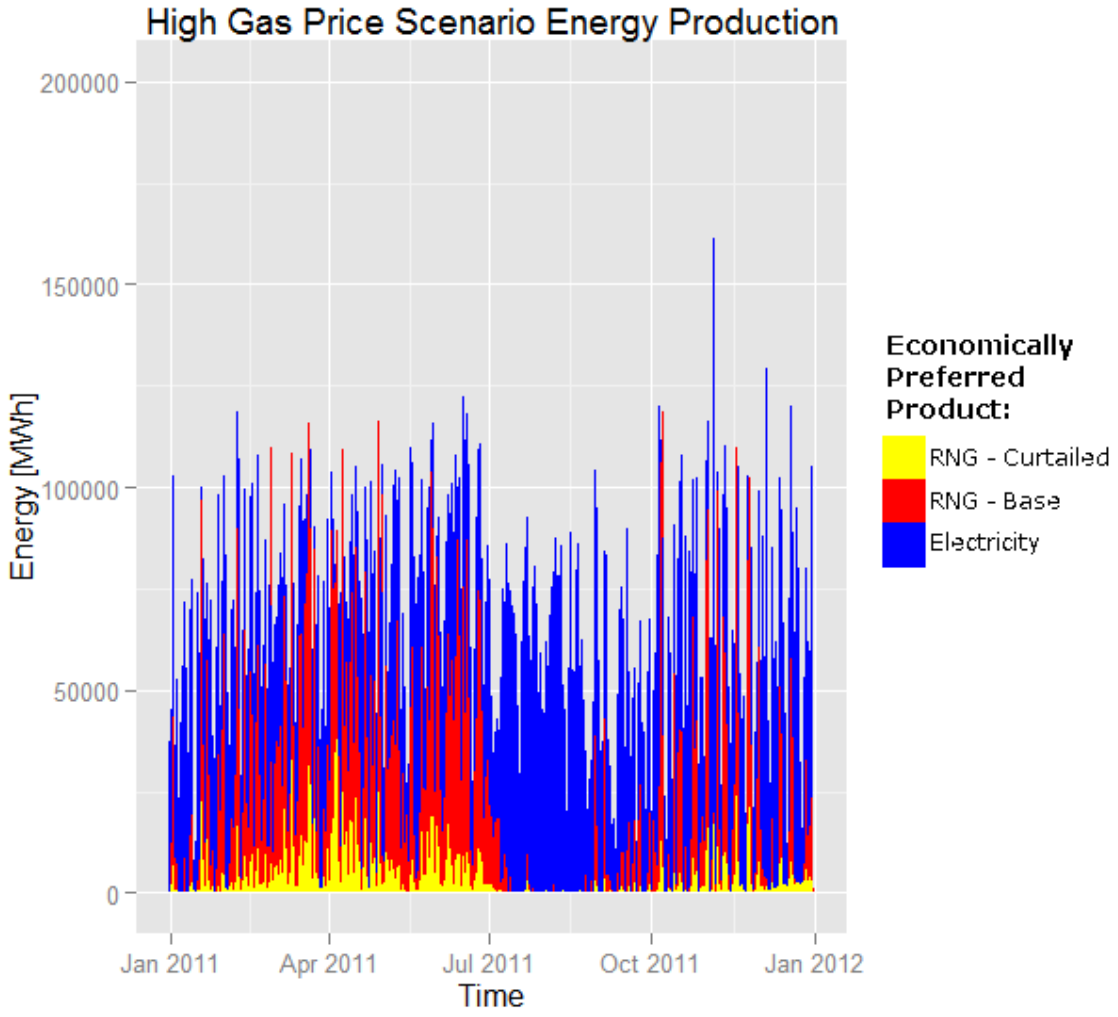

Figure B.3: Each bar represents the total amount of energy produced and sold in a single day within the High Gas Price Scenario. The yellow bars represent RNG produced using otherwise curtailed wind capacity (MWh_{th}), the red bars represent RNG produced using baseline generation capacity (MWh_{th}), and the blue bars represent electricity sold directly to the grid (MWh_{e^-}).

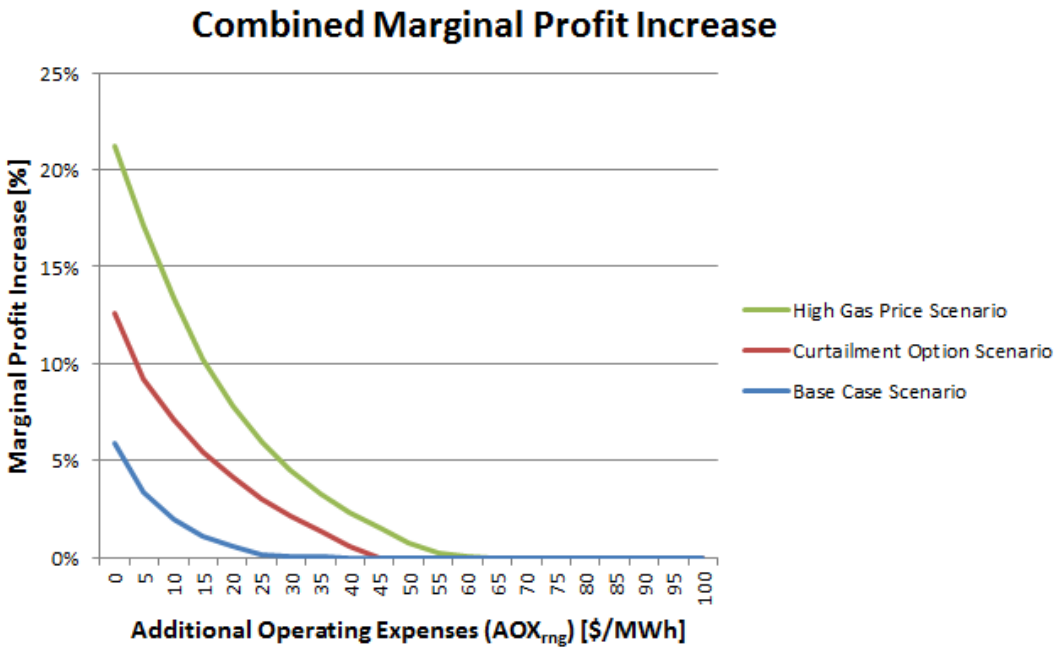

Figure B.4: The marginal profit increase (considering PTCs) of each modeling scenario as a function of additional operating expenses (AOX_{rng}), relative to the baseline.

Bibliography

[1] D. L. Saber and S. F. Takach, "Task 1 Final Report: Technology Investigation, Assessment, and Analysis," Tech. Rep. 20614, Gas Technology Institute, Des Plaines, Il, 2009.

[2] H. Hofbauer, "Indirect (Allothermal) Gasification," in *International seminar on gasification and methanation*, (Göteborg, Sweden), 2007.

[3] American Gas Foundation, "The Potential for Renewable Gas : Biogas Derived from Biomass Feedstocks and," Tech. Rep. September, Washington, D.C., 2011.

[4] US Energy Information Administration, "Annual Energy Review 2011," tech. rep., Washington, D.C., 2012.

[5] US Energy Information Administration, "Short-Term Energy Outlook (STEO)," tech. rep., Washington, D.C., 2014.

[6] Economic Development and Tourism Business Research Department, "The Texas Renewable Energy Industry," tech. rep., Office of the Governor, Austin, TX, 2014.

[7] S. Ali-Oettinger, "Sun power to gas," *pv magazine*, pp. 92–95.

[8] ITM Power, "Power-to-Gas: Storing Renewable Energy in the Gas Grid," in *The Royal Academy of Engineering*, 2014.

[9] C. B. Field, V. R. Barros, D. J. Dokken, K. J. Mach, M. D. Mastrandrea, T. Bilir, M. Chatterjee, K. Ebi, Y. Estrada, R. Genova, B. Girma, E. Kissel, A. Levy,

S. MacCracken, P. Mastrandrea, and L. White, "2014: Summary for policymakers," in *Climate Change 2014: Impacts, Adaptation, and Vulnerability. Part A: Global and Sectoral Aspects. Contribution of Working Group II to the Fifth Assessment Report of the Intergovernmental Panel on Climate Change*, (Cambridge, United Kingdom and New York, NY, USA), pp. 1–32, IPCC, Cambridge University Press, 2014.

[10] W. Wang and J. Gong, "Methanation of carbon dioxide: an overview," *Frontiers of Chemical Science and Engineering*, vol. 5, pp. 2–10, Dec. 2011.

[11] E. Dlugokencky, "No Title," tech. rep., NOAA Earth System Research Laboratory, 2014.

[12] R. Alley, T. Berntsen, N. L. Bindoff, Z. Chen, A. Chidthaisong, P. Friedlingstein, J. Gregory, G. Hegerl, M. Heimann, B. Hewitson, B. Hoskins, F. Joos, J. Jouzel, V. Kattsov, U. Lohmann, M. Manning, T. Matsuno, M. Molina, N. Nicholls, J. Overpeck, D. Qin, G. Raga, V. Ramaswamy, J. Ren, M. Rusticucci, S. Solomon, R. Somerville, T. F. Stocker, P. Stott, R. J. Stouffer, P. Whetton, R. A. Wood, and D. Wratt, "2007: Summary for Policymakers," in *Climate Change 2007: The Physical Science Basis. Contribution of Working Group I to the Fourth Assessment Report of the Intergovernmental Panel on Climate Change*, (Geneva, Switzerland), pp. 1–18, 2007.

[13] US Environmental Protection Agency, "Inventory of U.S. Greenhouse Gas Emissions and Sinks: 1990-2012," tech. rep., Washington, D.C., 2014.

[14] M. Albadi and E. El-Saadany, "Overview of wind power intermittency impacts on power systems," *Electric Power Systems Research*, vol. 80, pp. 627–632, June 2010.

[15] US Environmental Protection Agency, "Overview of Greenhouse Gases - Methane Emissions."

[16] A. D. Cuéllar and M. E. Webber, "Cow power: the energy and emissions benefits of converting manure to biogas," *Environmental Research Letters*, vol. 3, p. 034002, July 2008.

[17] US Energy Information Administration, "Fewer wind curtailments and negative power prices seen in Texas after major grid expansion," 2014.

[18] M. Goggin, "NREL Releases Wind Curtailment Case Studies," 2009.

[19] E. Drury, P. Denholm, and R. Sioshansi, "The value of compressed air energy storage in energy and reserve markets," *Energy*, vol. 36, pp. 4959–4973, Aug. 2011.

[20] D. Lew, L. Bird, M. Milligan, B. Speer, X. Wang, E. M. Carlini, A. Estanqueiro, D. Flynn, E. Gomez-lazaro, N. Menemenlis, A. Orths, I. Pineda, J. C. Smith, L. Soder, P. Sorensen, A. Altiparmakis, and Y. Yoh, "Wind and Solar Curtailment," in *International Workshop on Large-Scale Integration of Wind Power Into Power Systems as Well as on Transmission Networks for Offshore Wind Power Plants*, no. September, (London), NREL, 2013.

[21] E. Skoplaki and J. Palyvos, "On the temperature dependence of photovoltaic module electrical performance: A review of efficiency/power correlations," *Solar Energy*, vol. 83, pp. 614–624, May 2009.

[22] US Department of the Interior, "Reclamation: Managing Water in the West," tech. rep., 2005.

[23] US Energy Information Administration, "Texas State Energy Profile," 2014.

[24] L. Sherwood, "U.S. Solar Market Trends 2012," Tech. Rep. JuLy, 2013.

[25] Electric Reliability Council of Texas, "About ERCOT."

[26] American Gas Association, "Securing a Role for Renewable Gas," tech. rep., Washington, D.C., 2011.

[27] National Grid, "Renewable Gas — Vision for a Sustainable Gas Network," tech. rep., Waltham, MA, 2010.

[28] N. R. Scott, S. Zicari, K. Saikkonen, and K. Bothi, "Characterization of Dairy-Derived Biogas and Biogas Processing," in *ASABE Annual International Meeting*, (Portland, OR), 2006.

[29] A. S. Stillwell, D. C. Hoppock, and M. E. Webber, "Energy Recovery from Wastewater Treatment Plants in the United States: A Case Study of the Energy-Water Nexus," *Sustainability*, vol. 2, pp. 945–962, Apr. 2010.

[30] Fuel Cell Today, "Water Electrolysis & Renewable Energy Systems," tech. rep., Royston, UK, 2013.

[31] National Renewable Energy Laboratory, "Current (2009) State-of-the-Art Hydrogen Production Cost Estimate Using Water Electrolysis," Tech. Rep. September, 2009.

[32] S. Califano, *Pathways to Modern Chemical Physics*. Springer Science & Business Media, 2012 ed., 2012.

[33] D. J. Goodman, "Methanation of Carbon Dioxide," 2013.

[34] P. J. Lunde and F. L. Kester, "Carbon Dioxide Methanation on a Ruthenium Catalyst," *Industrial & Engineering Chemistry Process Design and Development*, vol. 13, no. 1, pp. 27–33, 1974.

[35] D. P. Vanderwiel, Y. Wang, A. Y. Tonkovich, R. S. Wegeng, P. O. Box, and M. K, "Carbon Dioxide Conversions in Microreactors," in *IMRET 4: Proceedings of the 4th International Conference on Microreaction Technology, Topical Conference Proceedings, AIChE Spring National Meeting, March 5-9, 2000 Atlanta, GA*, no. 2, (New York NY), pp. 187–193, American Institute of Chemical Engineers.

[36] P. F. Tropschuh and E. Pham, "Audi Future Energies: Balancing Business and Environmental Concerns," in *Sustainable Automotive Technologies 2013* (J. Wellnitz, A. Subic, and R. Trufin, eds.), pp. 185–190, Springer International Publishing, 2014.

[37] H. Ibrahim, a. Ilinca, and J. Perron, "Energy storage systems—Characteristics and comparisons," *Renewable and Sustainable Energy Reviews*, vol. 12, pp. 1221–1250, June 2008.

[38] M. Specht, F. Baumgart, B. Feigl, V. Frick, B. Stürmer, U. Zuberbühler, M. Sterner, and G. Waldstein, "Storing bioenergy and renewable electricity in the natural gas grid," *FVEE AEE Topics*, pp. 69–78, 2009.

[39] Electric Power Research Institute, "Bulk Energy Storage Impact and Value Analysis," tech. rep., 2012.

[40] US Environmental Protection Agency, "Nitrogen Oxides (NOx), Why and How They Are Controlled," Tech. Rep. November, Research Triangle Park, NC, 1999.

[41] US Energy Information Administration, "Natural Gas Weekly Update (August 27, 2014)," 2014.

[42] US Energy Information Administration, "U.S. Natural Gas Imports & Exports 2013," 2014.

[43] US Energy Information Administration, "Effect of Increased Natural Gas Exports on Domestic Energy Markets," Tech. Rep. January, Washington, D.C., 2012.

[44] US Energy Information Administration, "Henry Hub Natural Gas Spot Price (Annual)," 2014.

[45] M. Jentsch, T. Trost, and M. Sterner, "Optimal Use of Power-to-Gas Energy Storage Systems in an 85% Renewable Energy Scenario," *Energy Procedia*, vol. 46, pp. 254–261, 2014.

[46] M. Sapozhnikov, A. Rudkevich, R. Tabors, J. McMahon, J. Goldis, and B. Tsuchida, "Historical performance of combined cycle generation in the U.S.," tech. rep., 2008.

[47] C. Zamalloa, E. Vulsteke, J. Albrecht, and W. Verstraete, "The techno-economic potential of renewable energy through the anaerobic digestion of microalgae.," *Bioresource technology*, vol. 102, pp. 1149–58, Jan. 2011.

[48] H. Lorenz, P. Fischer, B. Schumacher, and P. Adler, "Current EU-27 technical potential of organic waste streams for biogas and energy production.," *Waste management (New York, N.Y.)*, vol. 33, pp. 2434–48, Nov. 2013.

[49] National Grid, "The potential for Renewable Gas in the UK," Tech. Rep. January, National Grid, 2009.

[50] US Energy Information Administration, "Annual Energy Outlook 2013 - Renewable Energy," 2013.

[51] D. Kondepudi and I. Prigogine, *Modern Thermodynamics: From Heat Engines to Dissipative Structures*. John Wiley & Sons, 1st ed., 1998.

[52] National Institute of Standards and Technology, "Water."

[53] National Institute of Standards and Technology, "Hydrogen."

[54] The Engineering Toolbox, "Fuels - Higher Calorific Values."

[55] F. D. Doty, L. Holte, and S. Shevgoor, "Securing Our Transportation Future by Using Off-Peak Wind Energy to Recycle CO2 into Fuels," in *ASME 2009 3rd International Conference of Energy Sustainability*, (San Francisco), pp. 1–8, 2009.

[56] J. Gao, Y. Wang, Y. Ping, D. Hu, G. Xu, F. Gu, and F. Su, "A thermodynamic analysis of methanation reactions of carbon oxides for the production of synthetic natural gas," *RSC Advances*, vol. 2, no. 6, p. 2358, 2012.

[57] T. Yoshida, K. Nishizawa, M. Tabata, H. Abe, T. Kodama, M. Tsuji, and Y. Tamaura, "Methanation of CO2 with H2-reduced magnetite," *Journal of Materials Science*, vol. 28, pp. 1220–1226, 1993.

[58] T. Abe, M. Tanizawa, K. Watanabe, and A. Taguchi, "CO2 methanation property of Ru nanoparticle-loaded TiO2 prepared by a polygonal barrel-sputtering method," *Energy & Environmental Science*, vol. 2, no. 3, p. 315, 2009.

[59] S. Abelló, C. Berrueco, and D. Montané, "High-loaded nickel–alumina catalyst for direct CO2 hydrogenation into synthetic natural gas (SNG)," *Fuel*, vol. 113, pp. 598–609, Nov. 2013.

[60] A. E. Aksoylu and Z. I. Önsan, "Hydrogenation of carbon oxides using coprecipitated and impregnated Ni/Al2O3 catalysts," *Applied Actalysis A: General*, vol. 164, pp. 1–11, 1997.

[61] P. Ruiz, M. Jacquemin, and N. Blangenois, "Catalytic co2 methanation process," 2010.

[62] National Institute of Standards and Technology, "Methane."

[63] B. r. Kruse, S. Grinna, and C. Buch, "Hydrogen: Status og Muligheter," Tech. Rep. 6, Bellona, 2002.

[64] M. Giberson, "Assessing Wind Power Cost Estimates," tech. rep., Institute for Energy Research, Washington, D.C., 2013.

[65] US Energy Information Administration, "Henry Hub Natural Gas Spot Price (Daily)," 2014.

[66] Electric Reliability Council of Texas, "Historical RTM Load Zone and Hub Prices 2010-2013," 2013.

[67] US Energy Information Administration, "New Texas wholesale power market weathers extreme cold," 2011.

[68] US Energy Information Administration, "Texas Heat Wave, August 2011: Nature and Effects of an Electricity Supply Shortage," 2011.

[69] Electric Reliability Council of Texas, "Nodal Monthly Aggregate WPF Report," tech. rep., Taylor, TX, 2011.

[70] Electric Reliability Council of Texas, "Glossary - H," 2005.

[71] R. J. Dyer, "Deregulated Electricity in Texas: A History of Retail Competition," Tech. Rep. December, Texas Coalition for Affordable Power, 2012.

[72] US Energy Information Administration, "Annual Energy Outlook 20013 - Liquids and Natural Gas Supply and Prices," 2013.

[73] The California Energy Commission, "Average Per Capita Natural Gas Consumption by State 2011."